Mixing of Diluted Bitumen and Conventional Crude Oil in Fresh and Marine Environments

by

Hena Farooqi

A thesis submitted in partial fulfillment of the requirements for the degree of

Master of Science

in
Chemical Engineering

Department of Chemical and Materials Engineering
University of Alberta

Abstract

With public concern over potential impacts to water environments that could result from a spill of diluted bitumen during transportation, a study is being conducted to determine the mixing characteristics of diluted bitumen and conventional crude in fresh and salt water. The conventional crude (CC) and diluted bitumen (DB1) oils chosen for this study were selected because of their extensive transportation via pipelines, railways, and over water and, because of their relative differences in chemical and physical properties. The mixing behaviour between water and oil depends on the environment, oil composition and types of water and sediment. To study the relative effects of the different variables, mixing tests in a rotary agitator were conducted varying the oil (fresh conventional crude versus fresh diluted bitumen), water (salt versus fresh), temperature (ambient versus 30^{o}C), sediment (sand versus diatomaceous earth), and mixing speed (38.7 versus 55.4 RPM, where both speeds were turbulent mixing regime).

To sequentially examine the effects of all of variables, a total of 288 runs would be needed. However, factorial experimental design with five variables (oil, water, sediment, temperature and mixing speed) with two levels reduced the number of tests from 288 to 32, the minimum needed to obtain the key information about the effects of all variables (i.e. 5 factors at 2 levels each). This design allowed the study of 5 main effects, 10 two-factor interactions, 10 three-factor interactions, 5 four-factor interactions and 1 six-factor interaction. The data collected for the tests included emulsion formation, and water and oil mass balances. As well, floating oil was distilled to remove water. The boiling point

(b.p.) >204°C fraction was separated into maltene and asphaltene fractions. Oil was isolated from the water and sediment phases by carbon disulfide and methylene chloride extraction. The maltenes and asphaltenes fractions and were then analyzed by high temperature simulated distillation, and elemental (CHNSO) analyses.

The focus of this work comprised of two objectives; the first objective was to identify the significant variables in oil-water mixing and, the second objective was to identify the chemical reasons for the siginicant physical effects identified in the first study. It was seen that mixing behaviours in salt and fresh water were different, resulting in interesting patterns for oil loss and sediment interactions for both oils. From the initial variable screening study, it was found that salt water had the greatest impact on floating oil recovery with greater recovery of DB1 than CC in salt water; DB1 dispersed more in fresh water than CC; CC interacted more with sediment than DB1; and, thicker emulsions were formed when mixing with DB1. Analyses of the oil samples after mixing revealed the physical properties of each oil along with the presence of bioactivity and effects of interaction with sediment were causes for the changes that were observed during the mixing tests. From further analyses of the floating oil and sub fractions of the oil, it was found that the changes in the boiling point distributions were most significant when mixing with CC than DB1. There was also greater increase in the asphaltenes content after mixing with CC along with a greater increase in oxygen content in the asphaltenes fraction for CC.

Further analyses of the metals content in the asphaltenes fraction, along with analysis of nuclear magnetic resonance (NMR) and Fourier transform infrared spectroscopy (FTIR) data would provide insight to the source of oxygen.

Preface

This research was supervised by Dr. Suzanne M. Kresta, Dean of the College of Engineering, University of Saskatchewan (former Professor with Department of Chemical and Materials Engineering, University of Alberta) and Dr. Heather D. Dettman, Natural Resources Canada (NRCan), CanmetENERGY Devon, Alberta.

The funding for this study was provided by NRCan Program of Energy Research and Development (PERD) and the Interdepartmental Tanker Safety Program. The diluted bitumen and conventional crude used for the tests were collected from Alberta pipelines courtesy of the Canadian Association of Petroleum Producers (CAPP).

The analyses of the oil and water samples were carried out at CanmetENERGY Devon by the Analytical Team (hydrocarbon analyses) and the Environmental Impacts Team (water analyses), with the exception of the surface tension and interfacial tension which were performed by Dr. Aleksey Baldygin, with support from his supervisor Dr. Prashant Waghmare, from the University of Alberta Mechanical Engineering Department. The rotary agitator tests were conducted by myself at CanmetENERGY Devon, Alberta. The energy characterization for the rotary agitator jars was completed by Ramin Memarian and Heather Dettman, "*Energy Scaling for Understanding the Effect of Sand Particles on Aggregate Size of Crude Oils"* (unpublished, Appendix A).

The experimental tests, data collection and analysis, and the writing of this thesis are my original work.

Acknowledgements

I would like to express my deepest appreciation to my thesis supervisors, Dr. Suzanne Kresta from the University of Saskatchewan (former Professor at University of Alberta), and my project supervisor, Dr. Heather Dettman from CanmetENERGY Devon. Their knowledge and enthusiasm provided me with the tools I needed to make this learning process fun and exciting! I will always value their continuous guidance, support and encouragement.

I would like to recognize the efforts of Dr. Aleksey Baldygin and his supervisor Dr. Prashant Waghmare, from the University of Alberta Mechanical Engineering Department, for analyzing the surface tensions and interfacial tensions of the oil and water samples.

A very special acknowledgment goes out to my colleagues at CanmetENERGY-Devon for providing the support I needed while I shared my time between the Devon Research Centre and the University of Alberta. I would like to thank NRCan Program of Energy Research and Development (PERD) and the Interdepartmental Tanker Safety Program for funding this study, and the CanmetENERGY Analytical Team and Environmental Impacts team for the water and hydrocarbon analyses.

Finally, I must express my profound gratitude to my parents for providing me with the foundation, support and encouragement to engage in further studies with fulltime work and a family. And to my siblings who have taught me that the challenges we face in life are only meant to make us stronger. I am grateful to be blessed with three bright, compassionate and resilient daughters who seamlessly adapted to a new routine for all the evenings and weekends I had dedicated to completing assignments or writing. Most of all, I am thankful for the unconditional support and patience from my husband who kept me motivated and focussed throughout this journey.

Table of Contents

List of Tables

List of Figures

List of Symbols

A	sediment (input variable)
B	mixing speed (input variable)
b.p.	boiling point
C	temperature (input variable)
CC	conventional crude
D	oil (input variable)
$D_{J,i}$	inside diameter of jar
$D_{J,o}$	outside diameter of jar
D_m	diameter of jar mounting space
D_S	distance between mounting space
DB1	diluted bitumen
E	water (input variable)
FTIR	Fourier transform infrared
FW	fresh water
H_J	height of jar
H_L	height of liquid
H_R	rotation height
N	radius of rotation
NMR	nuclear magnetic resonance
OMA	oil mineral aggregates
OSA	oil solid aggregates
SW	salt water

Equations:

A	represents first main effect, A
C	contrast coefficient
f_i	cumulative frequency at position i of the data value in the ordered list
k	number of variables
n	number of runs or responses
y	output result

Executive Summary

There is much discussion on the transport of diluted bitumen products by pipleline to Canada's Western coastal ports (Government of Canada. (2013a), Government of Canada. (2013b)) where the oil could then be transported via marine tanker or vessel to international markets. This increased volume of marine tankers poses a high risk for accidental oil spills. Therefore, there is a need to advance science and broaden our knowledge on the fate and behaviour of diluted bitumen in water environments. The findings from this study would provide preliminary information to support science regarding oil spill behaviour information that could be used to build oil spills models in different mixing conditions for more effective oil spill response options and strategies.

There were two objectives in this study; the first was to identify key interactions between oil, water and sediment after an oil spill using a 2^k factorial design of experiment, and the second objective was to carry out a detailed hydrocarbon analyses, including elemental (carbon, hydrogen, sulfur, nitrogen and oxygen content) and high temperature simulated distillation data.

The five variables that were selected to study their effect on oil, water, sediment mixing; sediment, mixing speed, mixing temperature, oil type and water type. Each variable was tested at two levels. The two types of sediments used in the tests were diatomaceous earth and sand to observe the effect of sediment particle size on the oil distribution. The mixing speeds were selected to simulate breaking and non-breaking waves while the mixing temperatures were ambient temperature and 30^{o}C. The higher temperature was chosen to simulate warm water oil spills. The two oil types used in the mixing tests were a diluted bitumen and conventional crude for their differences in physical and chemical properties. The diluted bitumen represents the largest volume of diluted bitumen products transported in pipelines in Canada, and the conventional crude oil is the conventionally produced light sweet crude for Western Canada. The water types were fresh water (Devon, AB tap water), and salt water (3.3 wt% NaCl solution in Devon, AB tap water).

Chapter 1 of the thesis addresses the first objective of this study which was to determine the key interactions in oil, water and sediment mixing using a 2^k factorial design of experiment. The mixing of oil, water and sediment was carried out using an end-over-end rotary agitator. The speeds selected to simulate breaking and non-breaking waves were based on an unpublished paper by Memarian and Dettman (unpublished) found in Appendix A ("Energy Scaling for Understanding the Effect of Sand Particles on Aggregate Size of Crude Oils"). Three experimental campaigns were carried out; Campaign 1 identified the overall interactions between oil, water and sediment using a 2^5 design of experiment, Campaign 2 was a 2^4 design to study the effect of mixing in breaking and non-breaking waves and, Campaign 3 was a 2^3 design to study the effect of oil and water mixing in the absence of sediment. The mixing tests were carried out using an-end-over end rotary agitator. Four replicate jars with 1:20 ratio of oil to water and 2000 ppm sediment were prepared and mixed for 12 hours. After the mixing, the floating oil as monitored for emulsion thickness over a period of seven days and the oil, water and sediment were isolated separately. There were five output variables from each mixing test; floating oil recovery, amount of oil dispersed in the water, amount of oil in sediment, water recovery and emulsion thickness. The data from the mixing tests were then analyzed using a 2^k design of experiment where normal probability plots are used to identify significant effects. Parity plots were also constructed to illustrate the oil distribution. From the Campaign 1 it was found that the floating oil recovery is higher in salt water than fresh water, at the highest mixing speed diluted bitumen disperses more in fresh water than conventional crude, conventional crude oil interacts most with sediment compared to diluted bitumen and thicker emulsions were formed when mixing with diluted bitumen. When studying the effect of breaking and non-breaking waves in Campaign 2, the key findings were that at the highest mixing speed diluted bitumen interacts most with sand in the water column, while at the lower mixing speed diluted bitumen interacts most with diatomaceous earth in the water column and settles to the bottom of the mixing jars with sand. From Campaign 3 it was found that in the absence of sediment, conventional crude disperses more in fresh water than diluted bitumen.

Chapter 2 discusses the second objective of the thesis which includes the analytical results (elemental and high temperature simulated distillation) of the oil after mixing from Campaign 1. This information was used to determine the possible causes for the key interactions identified in Chapter 1. The bulk oil properties provided the necessary information to explain the key

interactions during mixing, and analyses of the sub-fractions of the oils identified the significance of polarity of the oils during mixing. A possible cause for a higher oil recovery in salt water could be due to the ionic effects in salt water along with the oils exhibiting a higher interfacial tension in salt water, both allowing for greater oil-water separation. Viscosity and oil composition are important factors that influenced the interaction of oil with water and sediment. According to Stoffyn-Egli & Lee (2002), oil-mineral-aggregates (OMAs) formation is inversely proportional to the oil viscosity. Interfacial tension also contributes to the oil-water mixing (Butt et al., 2006; Israelachvili, 2011). The conventional crude oil used in this study had a lower viscosity and interfacial tension compared to the diluted bitumen allowing for greater mixing with the water and sediment. This phenomenon was also observed during the mixing tests with conventional crude oil. From the elemental results, there was little change in the carbon, hydrogen, nitrogen and sulfur contents after mixing, however, most change was observed in the oxygen content after mixing with conventional crude oil. From the mixing tests, it was observed that the oil type had the greatest impact on the change in oxygen content in the maltenes and asphaltenes fractions. The greatest increase in oxygen content was observed in the asphaltenes fraction of the conventional crude, along with the greatest decrease in oxygen content in the maltenes fraction. There was very little change in the oxygen content for the diluted bitumen tests after mixing. The increase in oxygen content in the conventional crude fractions suggests interaction with sediment along with the presence of bioactivity. The most change in the high temperature simulated distillation data was observed with the conventional crude tests. The increase in material boiling greater than 750^{o}C in the boiling point distrubution curves, could be due to the observed increase in oxygen since oxygenated compounds cause a increase in the heavier boiling fraction.

Chapter 3 proposes future work from this research. Conducting similar mixing tests at cooler temperatures would provide information related to oil spills in icy waters since the melting sea ice makes the Arctic routes more accessible. While a major oil spill has yet to occur in the Arctic, the lack of near by ports and cold weather conditions would make response the more difficult. Obtaining more information on the fate and behaviour of oil when spilled in icy waters would provide valuable information to formulate an appropriate response plan in the event of an oil spill. The diluted bitumen and conventional crude oil used in the mixing tests were fresh oils. Carrying out mixing tests with weathered oils would provide information on the effect of natural

weathering processes (evaporation, photo-oxidation) on the mixing behaviour, since weathering changes the physical and chemical properties of the oil. Studying the effect of water pH on oil-water-sediment interaction would provide useful information on the changes in the oil distribution with changes in pH, and the resulting impact on fish and other underwater organisms in marine and fresh waters.

The findings from this study have shown the effect of salt water and sediment as significant factors affecting the oil distribution after mixing. Characterization of the changes in the physical and chemical composition of the oil that occur after oil is spilled on water is beneficial for building oil spill models for response and remediation. The subsequent impact of an oil spill on water varies greatly depending on the unique chemical composition of the oil, and the dynamic water and environment conditions.

Chapter 1: Identification of the Significant Variables for Conventional Crude and Diluted Bitumen Mixing in Fresh and Salt Water using a Factorial Design of Experiment

1.1 Abstract

With public concern over potential impacts to water environments that could result from a spill of diluted bitumen during transportation, a study is being conducted to determine the mixing characteristics of diluted bitumen and conventional crude in fresh and salt water. The mixing behaviour between water and oil depends on the environment, oil composition and types of water and sediment. To study the relative effects of the different variables, mixing tests in a rotary agitator were conducted varying the oil (fresh conventional crude versus fresh diluted bitumen), water (salt versus fresh), temperature (ambient versus 30^{o}C), sediment (sand versus diatomaceous earth), and mixing speed (38.7 versus 55.4 RPM, where both speeds were turbulent mixing regime).

To sequentially examine the effects of all of variables, a total of 288 runs would be needed. However, a factorial experimental design with five variables (oil, water, sediment, temperature and mixing speed) with two levels reduced the number of tests from 288 to 32, the minimum needed to obtain key information about the effects of all variables (i.e. 5 factors at 2 levels each). This design allowed the study of 5 main effects, 10 two-factor interactions, 10 three-factor interactions, 5 four-factor interactions and 1 six-factor interaction. The data collected for the tests included emulsion formation, and water and oil mass balances.

The objective of this study is to identify the key interactions that occur between oil, water and sediment after an oil spill in a marine or fresh water environment. The mixing tests were conducted using an end-over-end rotary agitator. Three experimental campaigns were carried

out. In the first campaign, all variables were tested at two levels as an initial screening test (2^5 design). The second campaign tested the effect of ionic strength and mixing at lower speeds (2^4 design). The third campaign tested the effect of mixing in the absence of sediment (2^3 design).

The results showed that mixing behaviours in salt and fresh water are different, resulting in interesting patterns for oil loss and sediment interactions for both conventional crude and diluted bitumen. From this study it was found that there is greater oil dispersion in fresh water, conventional crude oil interacts more with sediment, floating oil recovery is greater in salt water compared to fresh water, and in the absence of sediment conventional crude disperses more in fresh water.

1.2 Introduction

The potential increased volume of diluted bitumen product from oil sands being shipped through sensitive marine environments is a concern to environmental groups and to the general public. While the chemical composition and physical properties of conventional and non-conventional petroleum products are available, the behaviour of these oils in a marine environment is not well understood. Currently when an oil spill occurs, response and clean-up do not occur until days after the spill due to a lack of understanding of the mixing behaviour between oil, water and sediment (Gros et al., 2014). Responders to the scene of an oil spill must have a good understanding of the chemical and physical properties of the oil along with the water conditions (temperature, mixing intensity, salinity and sediment composition), and how all of these variables interact, for an effective clean-up response plan. Understanding the risk, fate and behaviour of Canada's diluted bitumen when spilled in marine environments is needed to maintain value of the oil sands and expand to new markets. This study will focus on the behaviour of conventional crude and diluted bitumen when mixed in fresh and marine environments.

When oil and water come into contact, several physical processes occur as shown in Figure 1-1. Oil that is exposed to water will initially float on the water (density of Cold Lake diluted bitumen blend is 0.93 g/ml) (Crude Quality Inc., 2017); however, shortly after the spill the oil undergoes evaporation, photo-oxidation, spreading, and emulsification as a result of the ambient conditions which begin to alter the starting oil properties (Kingston, 2002). The lighter molecular weight compounds present in the oil evaporate which, in turn, increases the density and viscosity of the original floating oil. Teal (1992) carried out controlled lab studies monitoring the oil sedimentation process and found that lighter hydrocarbons (benzene through phenanthrene) underwent evaporation or degradation, while heavier molecules reached the bottom of the water through sedimentation and photo oxidation (Teal et al., 1992). Spreading reduces the thickness of the oil slick. The oil-water interfacial tension influences the extent of spreading and mixing of the oil with water. The lower the interfacial tension between water (salt water or fresh water) and oil the more mixing can be expected. There must be sufficient mixing for emulsification to occur (Jenkins et al., 1991). The stability of emulsions can be categorized as unstable, mesostable, or stable and entrained water is indicative of the oil and water properties

(M. Fingas & Fieldhouse, 2003). In an unstable emulsion (containing less than 10% water), the mixture will separate within a few hours (M. Fingas & Fieldhouse, 2005). The density of a stable water-in-oil emulsion can increase up to 30% over the density of the starting oil and the viscosity can increase by a factor of 1000 (Fingas, M., & Fieldhouse, B. (2004), Fingas, M., & Fieldhouse, B. (2003)). The water content in stable emulsions can be between 60-80% water, thus increasing the volume from two to five times its original volume (M. Fingas & Fieldhouse, 2005). It has been observed that for conventional crude oil spills, emulsions may contain 20-80% water with oil droplets of size 0.1mm or less (Kingston, 2002). Beneath the surface, oil droplets disperse and dissolve in the water as a result of wave action. Sedimentation can occur when the natural sediment present in the water interacts with the dispersed oil droplets (Khelifa et al., 2002; Khelifa et al., 2005; Le Floch et al., 2002; Stoffyn-Egli & Lee, 2002). Approximately 1% of the lower molecular weight compounds in the spilled oil dissolve into the water column, while other fractions of the oil are broken into small droplets of size 0.01-1mm in diameter as a result of wave action (Kingston, 2002). The higher molecular weight compounds detach from the oil and submerge into the water (International Maritime Organization, 2005; International Towing Tank Conference, 2011). Sinking of the oil occurs when the oil mineral aggregate (OMA) density increases such that it can no longer stay suspended in the water column. Biodegradation also takes place at the oil-water interface when the size and molecular weight of the oil droplets are small enough for the bacteria to degrade the hydrocarbons, aiding in remediation.

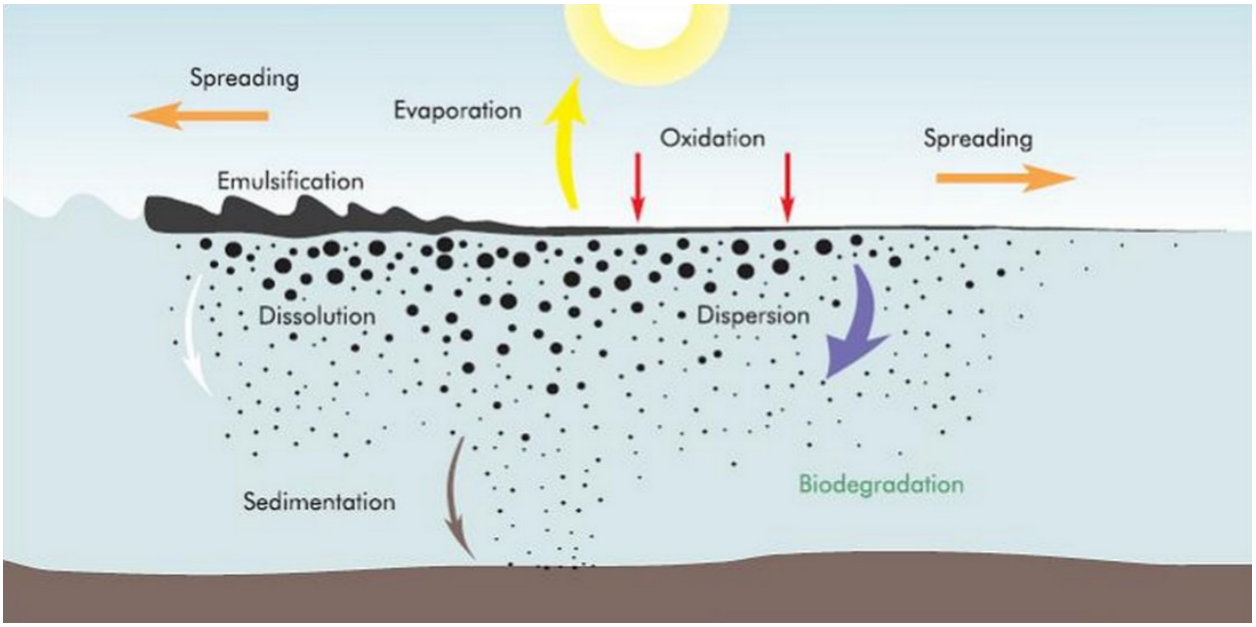

Figure 1-1: Physical processes that occur after an oil spill **(Source: Global Marine Oil Pollution Information Gateway, 'What Happens to Oil in the water' 2014**)

The impact of water salinity is important when predicting behaviour of spills in fresh versus marine waters. The salinity in freshwaters (ponds, lakes, rivers) is approximately 0-0.5 ppt (parts per thousand), in brackish waters (estuaries, brackish seas and lakes) it varies between 0.5-30 ppt., while in sea waters it ranges from 30-50 ppt (National Oceanic and Atmospheric Administration, 2015). The salinity of the water influences oil-water and sediment interaction. According to studies on the interaction of crude oil (density ranging between 0.85 – 0.99 kg/L) with mineral solids in fresh and simulated sea water, the interfacial tension of the crude oils in sea water is less than that in fresh water (Omotoso et al., 2002). With a lower interfacial tension, the spreading coefficient of the oil would be greater in sea water (King et al., 2014). This indicates oil spills in sea water spread to a thinner layer than in fresh water. However, according to Hollebone (2014), the interfacial tension of oils in salt water is greater than the interfacial tension of oils in fresh water. Laboratory studies suggest OMAs (oil-mineral aggregates) readily form in salt water compared to fresh water; however, limited data is available to predict the degree of mineral aggregate formation with varying water salinity levels (Le Floch et al., 2002). As long as the salinity of the water is greater than 2 ppt, oil spill remediation may be accelerated by OMA aggregate formation (Le Floch et al., 2002). King, Robinson, Boufadel & Lee (2014) conducted wave tank studies with sea water from the Bedford Basin (King et al., 2014). They

tested the effect of water salinity on the behaviour of oil and found that oil with higher density had a greater propensity to produce submerged oil-balls that sink with increasing salinity of the water.

Several oil-water mixing studies have been conducted using swirling (Kaku et al., 2006) and baffled flasks (Kaku et al., 2006; Venosa & Holder, 2011), and jars in a rotary agitator (M. Fingas & Fieldhouse, 2003; M. Fingas & Fieldhouse, 2012; M. F. Fingas et al., 2005; Memarian & Dettman,). Kaku et al. (2006) studied the effectiveness of dispersants in oil-water mixtures using swirling and baffled flasks. Mixtures of oil, seawater and dispersant were added to the swirling flasks and then mixed using an orbital shaker. The experimental setup involved using 150 ml swirling flasks and 200 ml baffled flasks with 120 ml of sample in each flask. After the mixing and settling periods were completed, water samples were collected to measure the concentration of oil dispersed in the water. Mixing tests were first carried out in the swirling flasks (only circular motion), and then again using baffled flasks. The four baffles allowed for 3-dimensional mixing to increase dispersant effectiveness. Mixing was carried out at five rotational speeds; 50, 100, 150 175 and 200 RPM, with an orbital diameter of 1.9cm. Venosa (2011) studied the dispersion of oil in water using 150 ml baffled flasks at speeds of 200 RPM. The flasks were modified to include a glass stopcock near the bottom of the flask for water sampling purposes. After mixing and settling times were completed, samples of water were collected and the dispersed oil was extracted using dichloromethane. Oil-water mixing tests have also been carried out in cylindrical jars using a rotary agitator. Fingas & Fieldhouse (2003, 2005, 2012) conducted experiments testing the formation of water-in-oil emulsions using a rotary agitator. The cylindrical jars were 20cm in height and the radius of rotation was about 10cm. Each vessel was filled approximately one quarter full with oil and water (water to oil ratio, w/o=20). Studies performed by the Government of Canada (2013) to assess oil-sediment interaction used 2.2 L wide-mouth HDPE bottles and an end-over-end rotary agitator. This study used 600 ml of water and 30 ml of oil, mixed for 12 hours at 15ºC and 55 RPM. A 33 wt% sodium chloride solution was used to simulate sea water, while reverse osmosis water was used for fresh water runs. After mixing, the contents of the jars were poured into 1 L graduated cylinders for observations. A similar study by Memarian and Dettman (internal report), examined the mixing energy in jars using a rotary agitator and its effect on oil-sediment interaction. The results from Memarian and Dettman tests were used to generate a model and

characterize the mixing flow regimes using the rotary agitator. To derive the model for the water amplitudes in the jars, tests were initially performed with water. This model was defined by a sigmoidal curve with a modelling efficiency (EF) of 0.99, as shown in Figure 1-2. The amplitude at the maximum mixing speed was calculated as the headspace available in the jar when the water height was 8.5cm (height of liquid). Two additional amplitudes were visually observed and measured at lower mixing speeds. These five data points are shown in Figure 1-2, and the amplitudes between these points are defined by the amplitude model data as shown in Table 1-1. For this study, the mixing speeds were selected within the range of the experimentally derived data points to ensure mixing was in a well-defined regime. Two mixing speeds were selected within the non-breaking wave regime and two mixing speeds within the breaking wave flow regime.

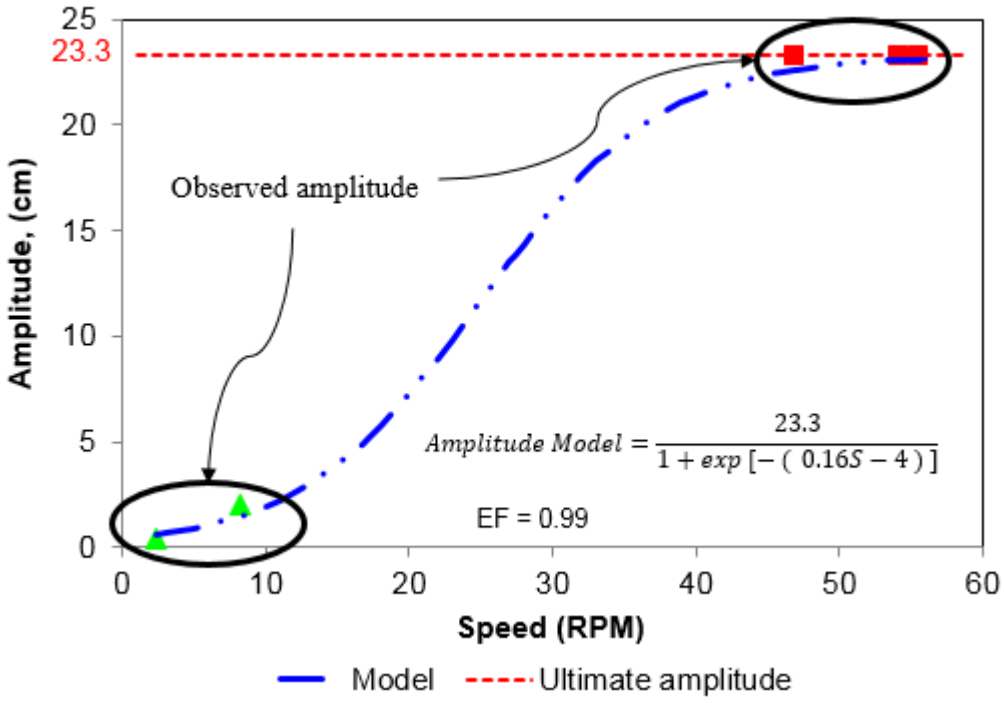

Figure 1-2: Experimental model for determining mixing speeds (**Source: Energy Scaling for Understanding the Effect of Sand Particles on Aggregate Size of Crude Oils; Memarian, R., Dettman, H.D., internal report**)

Table 1-1: Mixing speeds and flow regime

Speed of agitation		Observed Amplitude (cm)	Modelled Amplitude (cm)	Oscillatory Reynolds number	Observed flow regimes	Kinetic energy (J)	Energy Dissipation (m^2/s^3)
rpm	1/s*						
2.3	0.04	0.4**	0.6	96.29	Non-	0.0002	n/a
8.2	0.14	2**	1.48	1,716	breaking waves	0.004	n/a
16.4	0.27	-	4.7	19,568	Breaking	0.018	1.1×10^{-2}
21.4	0.36	-	8.38	31,806	waves	0.036	7.8×10^{-2}
27.3	0.46	-	13.77	47,719		0.064	4.4×10^{-1}
33.1	0.55	-	18.30	64,093		0.1	1.4
39	0.65	-	21.06	80,415		0.14	3
46.9	0.78	23.3	22.62	104,068		0.24	6.1
54.1	0.9	23.3	23.08	122, 309		0.277	9.7
55.6	0.93	23.3	23.14	125, 700		0.281	10.6

* angular frequency
** measured frequency

Source: Energy Scaling for Understanding the Effect of Sand Particles on Aggregate Size of Crude Oils; Memarian, R; Dettman, H.D. (internal report)

This purpose of this work is to identify the key interactions that occur between oil and water after an oil spill using a 2^k factorial design of experiment. The mixing tests were conducted using an end-over-end rotary agitator. Three experimental campaigns were carried out. In the first campaign, all variables were tested at two levels as an initial screening test (2^5 design). The second campaign tested the effect of ionic strength and mixing at lower speeds (2^4 design). The third campaign tested the effect of mixing in the absence of sediment (2^3 design).

1.3 Experimental

The objective of this work is to determine the key interactions between oil and water after an oil spill using a factorial design of experiment. The type of oil, water salinity, sediment type, mixing speed and mixing temperature were selected as the variables for this study, since the physical changes that occur after an oil spill are influenced by these factors (Gong et al., 2014; Government of Canada, 2013b; C. P. Huang & Elliott, 1977; Le Floch et al., 2002; R. F. Lee & Page, 1997; Nordvik et al., 1996; Wei et al., 2003).

The experimental set up includes an end-over-end rotary agitator and four 2.8 L borosilicate jars. A schematic of a jar and top view of the rotary agitator is shown in Figure 1-3. Each jar contained 600.0 ±0.20 ml of water, 30.0 ±0.50 ml of oil and 1.20 ±0.03 g of sediment, giving a total height of 8.5 ±0.20 cm of water-oil-sediment mixture, and 23.5 cm of headspace. Thirty millilitres of oil was added to obtain a 5 mm layer of oil on the surface of the water. An image of the jars mounted on the rotary agitator is shown in Figure 1-4.

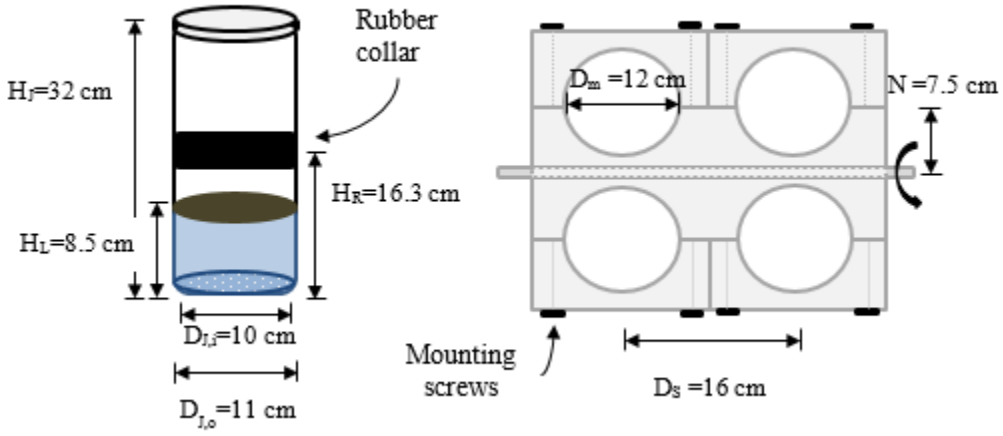

Figure 1-3: Schematic of jar with height of jar (H_J), height of liquid (H_L), inside diameter of jar ($D_{J,i}$), outside diameter of jar ($D_{J,o}$) and rotation height (H_R); top view of rotary agitator with diameter of jar mounting space (D_m), radius of rotation (N), and distance between mounting space (D_S)

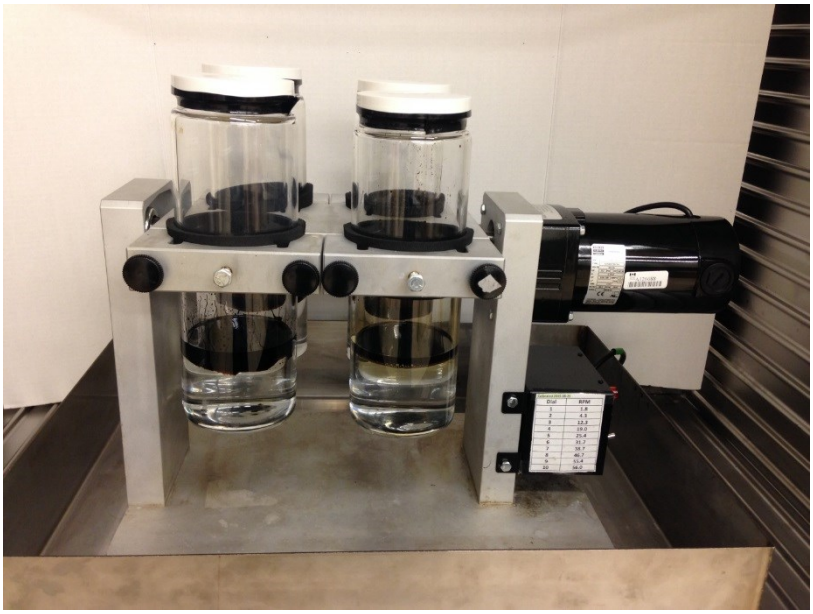

Figure 1-4: Image of the mixing jars mounted on the rotary agitator

An environmental chamber was used to manually control mixing temperatures, as shown in Figure 1-5. The rotary agitator was placed in the chamber to control the mixing temperature at 30ºC. The chamber working temperature ranges from 0ºC – 70ºC, with a temperature setting control accuracy of ±0.1ºC.

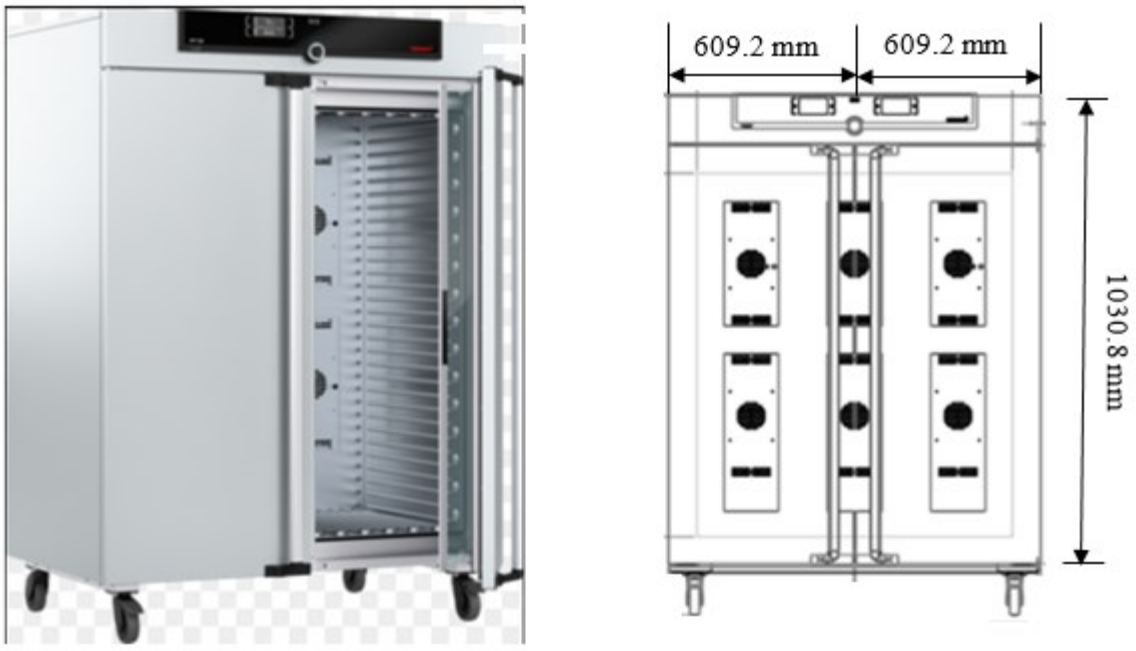

Figure 1-5: Environmental Chamber (dimensions in millimeters)
(www.memmert.com/products/incubators/peltier-cooled-incubator/IPP750/)

1.3.1 Selection of oils

Two types of oils were selected for the mixing tests; a fresh conventional crude (CC) and a fresh diluted bitumen (DB1) derived from the Athabascan Oil Sands. These oils were collected from Alberta pipelines courtesy of the Canadian Association of Petroleum Producers (CAPP). Conventional crude and diluted bitumen were chosen as the two oils for the tests due to their differences in chemical and physical properties listed in Table 1-2. The density was measured using a Mettler Toledo Densitometer (ASTM 4052). The kinematic viscosity was measured according to ASTM D445-01 method. Surface tension was measured using K100 Tensiometer (KRUSS Scientific Instruments Inc.), while the interfacial tension was measured using a Spinning Drop Tensiometer (KRUSS Scientific Instruments Inc.) having a capillary inner diameter of 3.25 mm. For characterization of the fresh oils, each oil was distilled to produce ±204^{o}C boiling point fractions using the ASTM D1160 method. These fractions were generated to study the effect of the heavier fraction in the oil-water-sediment mixing, as the lighter fraction containing the volatile components has the potential to evaporate in actual oil spill conditions.

This is also a standard boiling range cut point for analytical tests when studying class fractions of oil (PIONA ASTM D6839 and SARA ASTMD 2770). The maltenes and asphaltene fractions were separated on the boiling point (b.p.)>204^{o}C fraction by adding pentane as a solvent. The fraction that was insoluble in pentane was separated as the asphaltene fraction, and the remainder of the sample was the maltenes fraction. The elemental carbon, hydrogen and nitrogen were analyzed according to ASTM D5291 and sulfur was determined using ASTM D1552, while the oxygen content is determined by pyrolysis as suggested by the manufacturer of the Elementar instrument.

Table 1-2: Properties of Conventional Crude (CC) and Diluted Bitumen1 (DB1)

Crude Oil		CC	DB1
Density (g/ml)			
	20°C	0.8201	0.9237
	25°C	0.8168	0.9203
	30°C	0.8130	0.9166
Viscosity (cSt)			
	20°C	5.1	218.1
	25°C	4.2	161.5
	30°C	3.7	124.1
Surface tension (mN/m)			
	20°C	25.5	28.9
Interfacial tension (mN/m)			
Fresh water (Devon, AB tap water)			
	20°C	12.24±0.43	16.58±0.12
	30°C	14.16±0.26	16.00±0.09
Salt water (3.3 wt.% NaCl solution)			
	20°C	7.36±0.08	11.74±0.06
	30°C	12.33±0.02	13.94±0.02
+204°C fraction			
Maltenes content (%)		98.48	81.86
	Carbon (%)	85.89	84.12
	Hydrogen (%)	13.05	11.14
	Nitrogen (%)	0.08	0.28
	Sulfur (%)	0.41	3.98
	Oxygen (%)	0.59	0.48
Asphaltenes content (%)		1.52	18.13
	Carbon (%)	84.88	81.50
	Hydrogen (%)	8.09	7.46
	Nitrogen (%)	1.08	1.12
	Sulfur (%)	4.21	8.68
	Oxygen (%)	1.74	1.23

1.3.2 Water type

Fresh water (FW) and salt water (SW) were used for the mixing tests to determine the effect of ionic strength on the electrostatic double layer between the negatively charged oil and sediment particles in water (L. Huang et al., 2012; Le Floch et al., 2002). The fresh water tests were conducted using Devon, Alberta tap water while a solution of 33 ppt (3.3wt%) sodium

chloride (NaCl) solution (Government of Canada, 2013a; Kester & Pytkowicx, 1967; Venosa & Holder, 2011) was prepared for the salt water tests using the same tap water. The NaCl used for the tests was obtained from Fisher Scientific with a purity of ≥99.0%.

1.3.3 Sediment type

Two types of sediment were used for the mixing tests; sand and diatomaceous earth. Sand is mostly silica (90-100%, SIGMA Aldrich MSDS) and is used for many industrial processes, such as manufacturing of glass and bricks, additive to paints to produce textured surfaces, and for concrete production. Sand is also used in the oil spill industry to submerge oil spilled on water as part of the clean-up measures (Boglaienko & Tansel, 2015; Boglaienko & Tansel, 2016; Boglaienko & Tansel, 2017; Muschenheim & Lee, 2002). Sand particles have a complex morphology (non-spherical) and, although there are regions of positive and negative charges, it has an overall negative charge (L. Huang et al., 2012). Diatomaceous earth is the fossilized remains of microscopic diatoms originating from unicellular algae (Calvert, 1930; Özen et al., 2015; Tsai et al., 2006). It is found on the bottoms of oceans and lakes and is mined for many industrial applications (adsorbent, filter and drying agent) due to its high porosity and low density (Özen et al., 2015). It mainly consists of 85% silica along with alumina (Al_2O_3) and iron (Fe_2O_3), and its size can range from 3 micrometers to 1 millimeter (Calvert, 1930). Diatomaceous earth has also been proposed for use in marine oil spill clean-up due to its hydrophilic and oleophilic properties, i.e. it is wet by both water and oil (Özen et al., 2015). The sand and diatomaceous earth were purchased from Sigma-Aldrich for the tests and were not surface treated.

The sediment concentration used in the mixing tests was 2000 ppm to simulate extreme weather conditions with maximum sediment interaction (i.e. storm conditions or in an estuary). As a reference for fresh and salt water body sediment concentrations, the total suspended solids (TSS) in the Bay of Fundy is around 9 ppm (Stewart, 2010), the Gulf of Mexico has been reported to have a sediment concentration ranging between 0.3-1.8 ppm (as cited by Gong et al. 2014), particulate concentration in most oceans is 2 ppm (as cited by Lee and Page 1997), and at the Devon, Alberta monitoring site for the North Saskatchewan River (NSR) sediment loads

average around 100 ppm (Hutchinson Environmental Sciences Ltd., 2014). The suspended sediment concentration in the Fraser River ranges between 30-440 ppm depending on the position of the tidal cycle (Bradley et al., 2013). Tests performed by Environment Canada (2013a) to determine the fate of oil in water used a 10 000 ppm sediment load to simulate coastal river flows.

The median grain size in the Fraser River Estuary ranges from 250 – 320 µm with little seasonal variation (Bradley et al., 2013). The particle size distribution of the sand, diatomaceous earth and a sample of the North Saskatchewan River (NSR) sediment (taken in February 2017 as a reference for natural sediment size) is presented in Table 1-3, showing that most of the sediment particles fall in the range of 45-75 microns, while 33% of the mass of diatomaceous earth is smaller than 45 microns. The sample of the NSR sediment was free from distinctly larger sediment particles. The particle size distributions for sand, diatomaceous earth and NSR sediment were determined by sieving the sediment samples through mesh sizes of 250 µm, 150 µm, 106 µm, 75 µm and 45 µm. The percent of sample passing through each sieve was calculated by subtracting the fraction of sample remaining on each sieve from the initial mass of the sample.

Table 1-3: Particle Size Distribution for Sediment

	Sand	Diatomaceous earth	North Saskatchewan River sediment
Mesh Size (µm)	Percent Passing (%)		
250	27.2	99.9	100.0
150	4.2	99.3	100.0
106	3.7	99.9	99.9
75	3.7	89.6	98.9
45	3.6	67.3	84.5

1.3.4 Mixing speed

The rotary mixer speeds were selected based on studies by Memarian and Dettman (unpublished). This study modelled the energy of mixing in the rotary agitator jars, as shown in Figure 1-2, to characterize the formation of oil-mineral aggregates for CC and DB1. Based on the data collected by Memarian and Dettman (unpublished), mixing speeds for this work were selected in the breaking (38.7 RPM and 55.4 RPM) and non-breaking (2.3 and 8.2 RPM) flow regime. The speeds chosen were within the upper limit of the breaking wave regime and lower limit of the non-breaking flow regime to avoid mixing in a region of transitional flow. These flow regimes were selected to simulate high energy wave conditions and calm wave conditions that occur in natural bodies of water.

1.3.5 Mixing temperature

Two mixing temperatures were selected for the tests; ambient temperature (average 20.3^{o}C±2^{o}C) and 30^{o}C±0.1^{o}C. Ambient temperature was selected so mixing tests could be carried out within the laboratory and the 30^{o}C was selected to simulate oil spills in warm environments. The environmental chamber was used to control only the warmer mixing tests.

1.3.6 Factorial design of experiment

Five main variables were identified in this study: oil, water and sediment types, temperature and mixing speed. A factorial design of experiments approach is necessary when dealing with several factors. This approach allows for the fewest number of experiments while identifying possible variable interactions by allowing all factors to vary in a well ordered way. An initial 2^{k} unreplicated full factorial design was chosen with all five variables at two levels each, to yield a minimal number of experiments for maximum information and screen the variables. Montgomery (2013) suggests selecting extreme values for the high (+) and low (-) levels to avoid misleading conclusions from experiments with only one set of tests. Hence, the levels for each variable were chosen at the maximum range. Each variable was represented by a letter: A

(sediment), B (mixing speed), C (temperature), D (oil), and E (water), and each variable had two levels.

With an unreplicated 2^k design of experiment, the hypothesis is made that data from the experiments will follow a normal distribution (Montgomery, 2013). This means the effects that are negligible will be normally distributed, the significant effects will have non-zero means and will deviate from the normal distribution, and higher order (multivariable) interactions will almost certainly be negligible. Therefore, two factor interactions were discarded after constructing normal probability plots. Factorial designs are used to check for interacting terms and the likelihood of a three factor interaction is small, unless two of the factors are confounded. Normal probability plots of the effects for each campaign were constructed to test the hypothesis, and to identify the significant effects.

The first experimental campaign was carried out to screen the variables with the greatest impact on mixing, followed by two more campaigns which studied the effect of salt water at a range of mixing speeds, and the effect of sediment.

1.3.7 Experimental method

The method for jar preparation and rotary agitator mixing was adapted from the Environment Canada (2013) study where similar mixing tests were performed. Four replicate 2.8 L clear glass jars (Jar I, II, III, IV) with 1:20 (v/v) ratio of oil to water with 2000 ppm sediment were prepared for each test. For salt water runs, 33 g/L of NaCl crystals were added to the jars before addition of oil or sediment and shaken vigorously to dissolve the NaCl. The jars were mounted on the rotary agitator and set to thermally equilibrate for 4 hours. For runs at 30^{o}C, the rotary agitator was placed in the environmental chamber to control the temperature. After the thermal equilibrium period, the jars were agitated for a total of 12 hours, then removed and allowed to settle for one hour. After the settling period, one jar (Jar IV) was set aside to monitor the emulsion thickness and observe changes to the jar contents over a period of seven days. The oil, water and sediment in the remaining three jars (Jars I, II, III) were isolated separately using a separatory funnel. The water and sediment samples were analyzed to determine the oil content in both phases.

The floating oil from Jars I, II, and III was combined then analyzed for high temperature simulated distillation analysis shortly after mixing to determine the boiling point distribution of the oil. After the seven day emulsion test was completed, the oil from Jar IV was added to the floating oil collected from the respective Jars I, II, III for each test. The total floating oil underwent distillation to determine water content, and produce two boiling point fractions, ±204ºC. The water content provided information on the amount of water trapped in the floating oil after each mixing condition. The fraction boiling >204ºC was further separated into the maltenes and asphaltenes fraction via the addition of pentane to the oil sample. The amount of oil in the water phase and on the sediment was determined by carbon disulfide and dichloromethane extraction.

The output variables for this study were floating oil recovery, oil extracted from water, oil extracted from sediment, emulsion thickness and water recovery.

1.4 Overview

According to Montgomery (2013), two important components to any experimental problem are the design of the experiment and the statistical analysis of the data. Analysis of the data from the experimental campaigns will provide valuable information to determine the fate of oil and water after an oil spill.

After each set of tests, the single variable effects (main effects) were calculated for each response variable (output variables) from the experiment. The hypothesis of normality is verified by normal probability plots. Many statistic software packages are available to generate normal probability plots, however, in this study the plots were constructed in excel. In order to construct normal probability plots, the contrast and the effect of each of the main effects and their interactions must be determined.

The contrast of each main effect and the interactions is determined for each output result using equation 1 (Montgomery & Runger, 2010).

$$\boldsymbol{Constrast_A = \sum_{i=1}^{n} (C)_{A_i} y_i} \quad (1)$$

where A is the first main effect, n is the number of runs, C is the contrast coefficient (either +1 or -1) and y is the output variable. The effect of each main effect and the interactions is calculated using equation 2 (Montgomery & Runger, 2010).

$$\boldsymbol{Effect_A} = \frac{\sum_{i=1}^{n}(C)_{A_i} y_i}{2^{k-1}} \tag{2}$$

where k is the number of variables. The magnitude and sign of the effect is an indication of its significance on the output, and in which direction the variable should be adjusted to improve the output. Once the contrast and effect of each main effect and the interactions are determined, the effects are sorted from smallest to largest. The ordered cumulative frequency is then calculated for each effect from equation 3 (Andale Publishing, 2013).

$$\boldsymbol{f_i} = \frac{(i-0.375)}{(n+0.25)} \tag{3}$$

where i is the position of the data value in the ordered list and n is the total number of output responses. From the cumulative frequency ($\boldsymbol{f_i}$), the z-score is obtained using z-score tables.

To identify significant effects of the variables, normal probability plots are used. To construct a normal probability plot, the effect is plotted against the z-score. If the hypothesis of a normally distributed data set is accurate, then the data will fall along a straight line. To confirm the validity of the normal probability distribution hypothesis for a subset of the data, normal probability plots of the maltenes and asphaltenes content in the b.p. >204ºC fraction from the floating oil (Campaign 1) were constructed. Since high-order interactions occur in an unreplicated set of tests, it is expected the effects that are negligible will fit along a straight line with mean zero. The significant effects will deviate from the straight line. In this study, since the variables are both qualitative and quantitative, the presence of a significant variable will be indicated by the letter associated with that variable and then the variable level (refer to Section 1.3.6). From Figure 1-6 we can see the data for the maltenes and asphaltenes fits a straight line with a mean close to zero. The significant effect of D (oil) is clearly an outlier for both the maltenes and asphaltenes. This is an expected result as the content of maltenes and asphaltenes in the starting oil will have the greatest effect on the resulting floating oil, validating the hypothesis. In Figure 1-6a, D has a positive effect (D + level, CC oil) on the maltenes content of the b.p.>204ºC fraction of the floating oil, while in Figure 1-6b D has a negative effect (D –

level, DB1 oil) on the asphaltenes content of the 204ºC fraction. These results are anticipated since CC has greater maltenes content than DB1, and DB1 has greater asphaltenes content than CC (Table 1-2). Based on the clear results shown in Figure 1-6, the use of normal probability plots was accepted for the screening analysis.

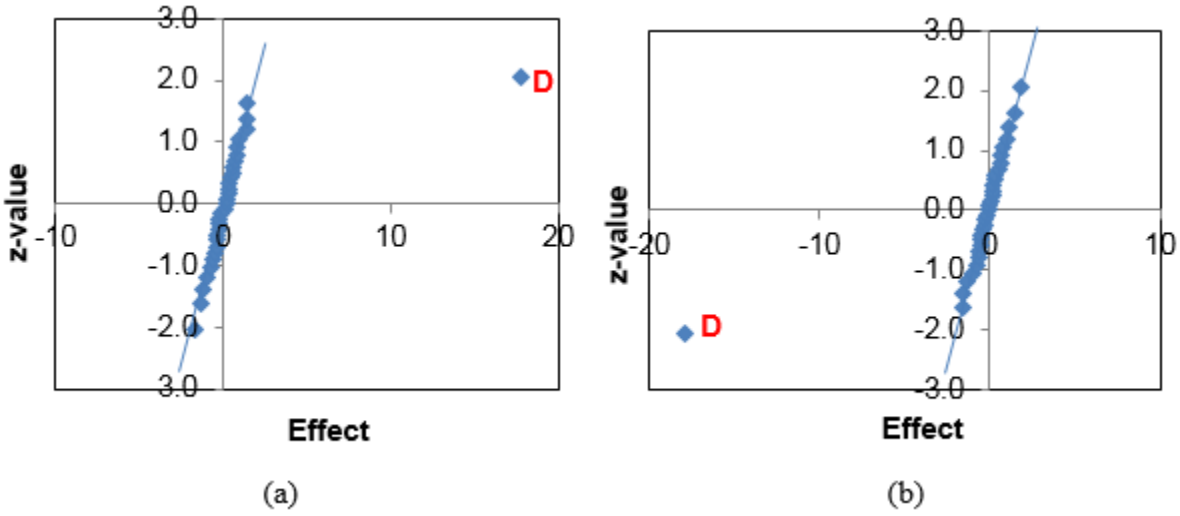

Figure 1-6: Validity of data and hypothesis of normally distributed data. Normal probability plot of effects for >204ºC fraction from Campaign 1 (a) maltenes and (b) asphaltenes content

The first campaign was designed to do an initial screening of the five chosen variables. The results from this campaign would identify which variable(s) play a significant role in oil and water mixing in fresh and marine environments.

1.5 Campaign 1: Variable screening

For Campaign 1, each factor was tested at two levels to give a total of 32 experiments and 31 interactions. The objective of this campaign was to identify the main effects on oil and water

mixing. All five variables were tested at two levels as shown in Table 1-4. Each variable was assigned a letter as an identifier of the effect. Campaign 1 was a 2^5 factorial design focussed on mixing in the breaking waves regime.

Table 1-4: Variable Levels for Campaign 1

Effect	Variable	- level	+ level
A	Sediment	Diatomaceous earth	Sand
B	Mixing Speed	38.7 RPM	55.4 RPM
C	Temperature	Ambient (20.3°C±2°C)	30°C±0.1°C
D	Oil	DB1	CC
E	Water	FW	SW

Table 1-5 shows the matrix of contrast coefficients for Campaign 1 with the columns highlighted in red defining the experimental conditions for each test. It includes all combinations of each variable and their interactions with each other, where '1' and '-1' (contrast coefficients) represent the high and low factor levels of each variable (Montgomery, 2013). This matrix was used to determine the effect of the variables and their interactions on the test outcomes. An experimental design matrix was then constructed to determine the run sequence (and run labeling) for each set of runs. The order of the runs was randomized (Table 1-6). In each run label, the run condition is identified with lower case letters for the input variables (compared to capital letters for input variable IDs). The presence of a letter indicates that the variable was tested at the high level (+). The absence of a letter in a run label indicates that the variable was tested at the lower level (-). The letter 'L' indicates that all variables are tested at the lower level.

Table 1-5: Contrast Coefficients for Campaign 1

A	B	AB	C	AC	BC	ABC	D	AD	BD	ABD	CD	ACD	BCD	ABCD	E	AE	BE	ABE	CE	ACE	BCE	ABCE	DCE	DE	ADE	BDE	ABDE	ABCDE
-1	-1	1	-1	1	1	-1	-1	1	1	-1	1	-1	-1	1	-1	1	1	-1	1	-1	-1	1	-1	1	-1	-1	1	-1
1	-1	-1	-1	-1	1	1	-1	-1	1	1	1	1	-1	-1	-1	-1	1	1	1	1	-1	-1	-1	1	1	-1	-1	1
-1	1	-1	-1	1	-1	1	-1	1	-1	1	1	-1	1	-1	-1	1	-1	1	1	-1	1	-1	-1	1	-1	1	-1	1
1	1	1	-1	-1	-1	-1	-1	-1	-1	-1	1	1	1	1	-1	-1	-1	-1	1	1	1	1	-1	1	1	1	1	-1
-1	-1	1	1	-1	-1	1	-1	1	1	-1	-1	1	1	-1	-1	1	1	-1	-1	1	1	-1	1	1	-1	-1	1	1
1	-1	-1	1	1	-1	-1	-1	-1	1	1	-1	-1	1	1	-1	-1	1	1	-1	-1	1	1	1	1	1	-1	-1	-1
-1	1	-1	1	-1	1	-1	-1	1	-1	1	-1	1	-1	1	-1	1	-1	1	-1	1	-1	1	1	1	-1	1	-1	-1
1	1	1	1	1	1	1	-1	-1	-1	-1	-1	-1	-1	-1	-1	-1	-1	-1	-1	-1	-1	-1	1	1	1	1	1	1
-1	-1	1	-1	1	1	-1	1	-1	-1	1	-1	1	1	-1	-1	1	1	-1	1	-1	-1	1	1	-1	1	1	-1	1
1	-1	-1	-1	-1	1	1	1	1	-1	-1	-1	-1	1	1	-1	-1	1	1	1	1	-1	-1	1	-1	-1	1	1	-1
-1	1	-1	-1	1	-1	1	1	-1	1	-1	-1	1	-1	1	-1	1	-1	1	1	-1	1	-1	1	-1	1	-1	1	-1
1	1	1	-1	-1	-1	-1	1	1	1	1	-1	-1	-1	-1	-1	-1	-1	-1	1	1	1	1	1	-1	-1	-1	-1	1
-1	-1	1	1	-1	-1	1	1	-1	-1	1	1	-1	-1	1	-1	1	1	-1	-1	1	1	-1	-1	-1	1	1	-1	-1
1	-1	-1	1	1	-1	-1	1	1	-1	-1	1	1	-1	-1	-1	-1	1	1	-1	-1	1	1	-1	-1	-1	1	1	1
-1	1	-1	1	-1	1	-1	1	-1	1	-1	1	-1	1	-1	-1	1	-1	1	-1	1	-1	1	-1	-1	1	-1	1	1
1	1	1	1	1	1	1	1	1	1	1	1	1	1	1	-1	-1	-1	-1	-1	-1	-1	-1	-1	-1	-1	-1	-1	-1
-1	-1	1	-1	1	1	-1	-1	1	1	-1	1	-1	-1	1	1	-1	-1	1	-1	1	1	-1	1	-1	1	1	-1	1
1	-1	-1	-1	-1	1	1	-1	-1	1	1	1	1	-1	-1	1	1	-1	-1	-1	-1	1	1	1	-1	-1	1	1	-1
-1	1	-1	-1	1	-1	1	-1	1	-1	1	1	-1	1	-1	1	-1	1	-1	-1	1	-1	1	-1	1	-1	1	-1	-1
1	1	1	-1	-1	-1	-1	-1	-1	-1	-1	1	1	1	1	1	1	1	1	-1	-1	-1	-1	1	-1	-1	-1	-1	1
-1	-1	1	1	-1	-1	1	-1	1	1	-1	-1	1	1	-1	1	-1	-1	1	-1	1	1	-1	-1	1	-1	-1	1	-1
1	-1	-1	-1	-1	1	1	1	1	-1	-1	-1	-1	1	1	1	1	-1	-1	1	1	-1	-1	-1	-1	1	1	-1	1
-1	1	-1	-1	1	-1	1	1	-1	1	-1	-1	1	-1	1	1	-1	1	-1	-1	1	-1	1	-1	1	-1	1	-1	1
1	1	1	-1	-1	-1	-1	1	1	1	1	-1	-1	-1	-1	1	1	1	1	-1	-1	-1	-1	1	1	1	1	1	-1
-1	-1	1	1	-1	-1	1	1	-1	-1	1	1	-1	-1	1	1	-1	-1	1	1	-1	-1	1	1	1	-1	-1	1	1
1	-1	-1	1	1	-1	-1	1	1	-1	-1	1	1	-1	-1	1	1	-1	-1	1	1	-1	-1	1	1	1	-1	-1	-1
-1	1	-1	1	-1	1	-1	1	-1	1	-1	1	-1	1	-1	1	-1	1	-1	1	-1	1	-1	1	1	-1	1	-1	-1
1	1	1	1	1	1	1	1	1	1	1	1	1	1	1	1	1	1	1	1	1	1	1	1	1	1	1	1	1

Table 1-6: Design Matrix for Campaign 1

Campaign 1	Factor						
	A	B	C	D	E	ABCDE	
Run Number	Sediment	Speed	Temperature	Oil	Water		Run label
1	-	-	-	-	-	-	L
2	+	-	-	-	-	+	a
3	-	+	-	-	-	+	b
4	+	+	-	-	-	-	ab
5	-	-	+	-	-	+	c
6	+	-	+	-	-	-	ac
7	-	+	+	-	-	-	bc
8	+	+	+	-	-	+	abc
9	-	-	-	+	-	+	d
10	+	-	-	+	-	-	ad
11	-	+	-	+	-	-	bd
12	+	+	-	+	-	+	abd
13	-	-	+	+	-	-	cd
14	+	-	+	+	-	+	acd
15	-	+	+	+	-	+	bcd
16	+	+	+	+	-	-	abcd
17	-	-	-	-	+	+	e
18	+	-	-	-	+	-	ae
19	-	+	-	-	+	-	be
20	+	+	-	-	+	+	abe
21	-	-	+	-	+	-	ce
22	+	-	+	-	+	+	ace
23	-	+	+	-	+	+	bce
24	+	+	+	-	+	-	abce
25	-	-	-	+	+	-	de
26	+	-	-	+	+	+	ade
27	-	+	-	+	+	+	bde
28	+	+	-	+	+	-	abde
29	-	-	+	+	+	+	cde
30	+	-	+	+	+	-	acde
31	-	+	+	+	+	-	bcde
32	+	+	+	+	+	+	abcde

After completion of Campaign 1, normal probability plots of the effects were constructed as part of the initial screening of the significant effects on each of the output variables.

1.5.1 Normal probability plots for Campaign 1

The results for Campaign 1 are presented in several parts, progressing through the variables which were measured. The first group is the distribution of the oil after mixing: floating oil, oil in water, and oil on sediment based on a material balance. The second group reflects the emulsion formation: the emulsion thickness and the water recovery. After presentation of all 5 sets of normal probability plots, the data is replotted as parity plots, comparing the behavior of diluted bitumen (DB1) to conventional crude (CC). This provides another perspective on the interaction effects and the dominant effects. Finally, the main effects are reviewed and main conclusions for campaign 1 are summarized. The reader (you) may find it helpful to use the three summary figures at the end of this section as they (you) read through the various stages of analysis.

Floating Oil Recovery. The normal probability plot for the recovery of floating oil from Campaign 1 is shown in Figure 1-7a. Many complex physical interactions occur during the mixing of oil, water and sediment. The single variable effects which may be significant in increasing oil recovery are E at the positive level (salt water) and C at the negative level (ambient temperture). Complex interactions between B, C, D, and E also seem to occur but this level of complexity is highly unlikely. To reduce the variable interactions and further study the effect of water type on the recovery of floating oil, the data was separated into two halves and the analysis repeated as if two separate studies were done: one in fresh water and one in salt water. Additional normal probability plots were then constructed. Figure 1-7b and Figure 1-7c show the remaining variable effects (A, B, C and D) on the recovery of the floating oil in salt and fresh water, respectively. The effect of C (30^{o}C) reduces oil recovery when mixing in salt water, but not in fresh water. In the fresh water, the interaction between mixing speed (B) and temperature (C) appears as negative. A second separation of the data was done for C (temperature) to explore these observations further. The effects of the remaining variables (A, B, D, and E) on recovery of floating oil are shown in Figure 1-7d and e for 30^{o}C and ambient

conditions, respectively. The effect of E (salt water) will increase oil recovery when mixing at both temperatures, but is more prominent at ambient mixing. Taking all of the data together and reviewing the effects and interactions, a number of 4-factor and 3-factor interactions appear in the plots. Some of these persist, even in smaller data sets, reflecting substantial complexity in the data. The dominant variables are the type of water (E) and the temperature (C) with mixing speed (B) appearing only in triple interaction effects.

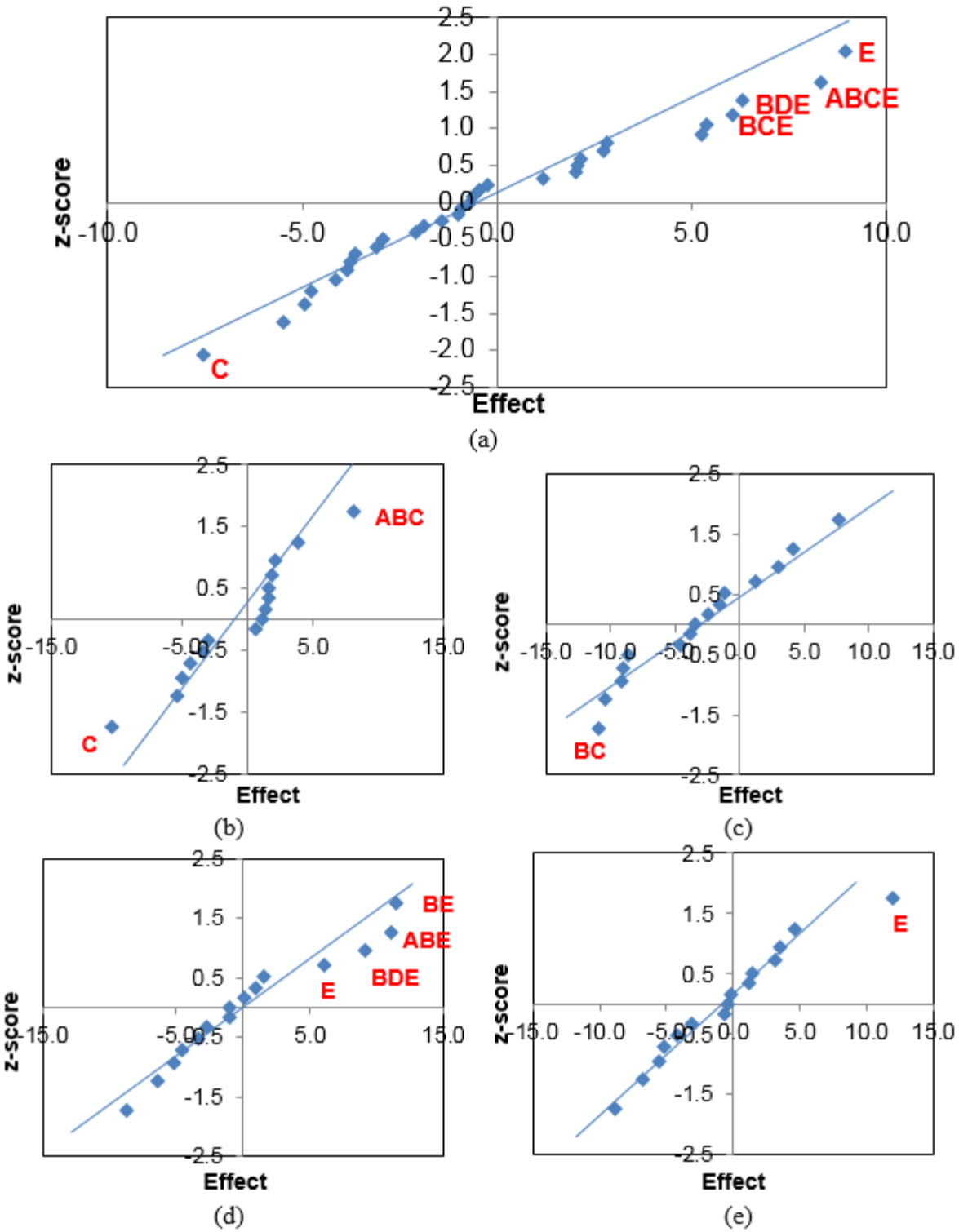

Figure 1-7: Normal probability plot of effect for (a) recovery of floating oil, and the effect of water type (b) SW, (c) FW, and mixing temperature of (d) 30°C and (e) ambient for Campaign 1

Oil in Water. The significant variables that cause an increase in the amount of oil dispersed in the water phase are D (DB1 oil) and E (fresh water), as shown in Figure 1-8.

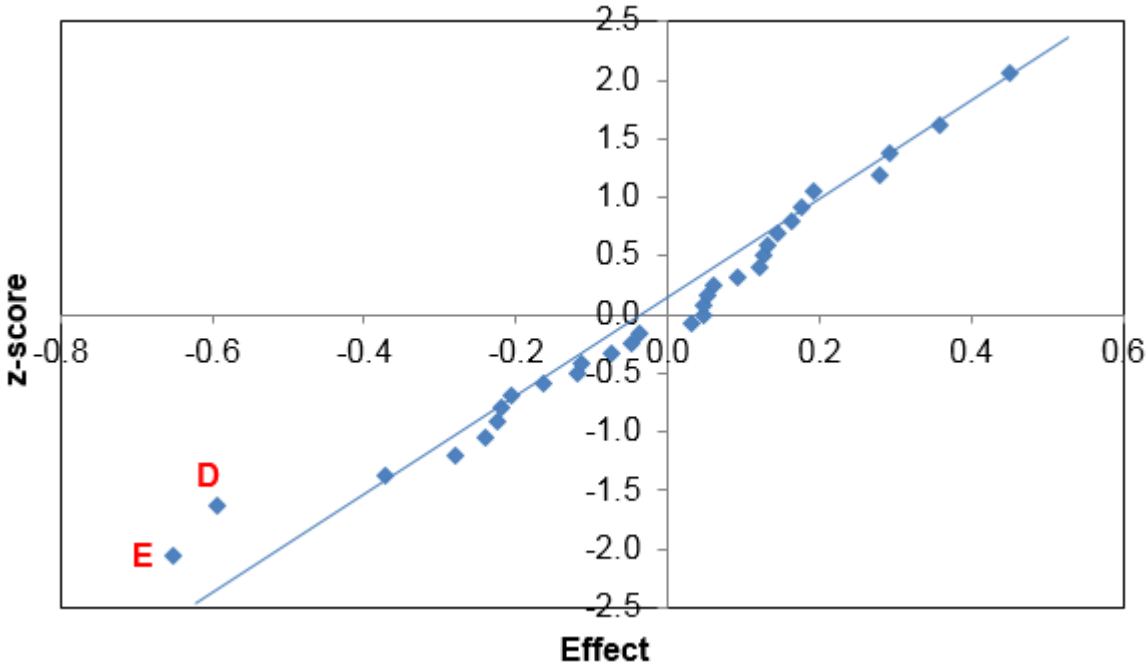

Figure 1-8: Normal probability plot of effects for oil in water (g oil/kg water) for Campaign 1

Oil on Sediment. The factors affecting the amount of oil recovered from sediment are shown Figure 1-9. The amount of oil recovered from sediment increases with D (CC oil)) along with a complex interaction between ABC. Water type E (salt water) causes a decrease in oil on sediment. This point is highlighted in Figure 1-9a since water type has shown to have an effect on mixing with sediment (multivariable interactions in Figure 1-7a). The effect of oil type and water type on the oil recovered from sediment for Campaign 1 is shown in Figure 1-9b-e, respectively. The effect of E (salt water) causes a decrease in the oil on the sediment for both oil types (Figure 1-9b and c) and the presence of D (CC oil) and A (diatomaceous earth) show up for both water types (Figure 1-9d and e). However, variable D (CC oil) is not considered significant due to its close proximity to the rest of the data (normally distributed). Variable A (diatomaceous earth) is significant in increasing the amount of oil recovered from sediment in both fresh and salt water.

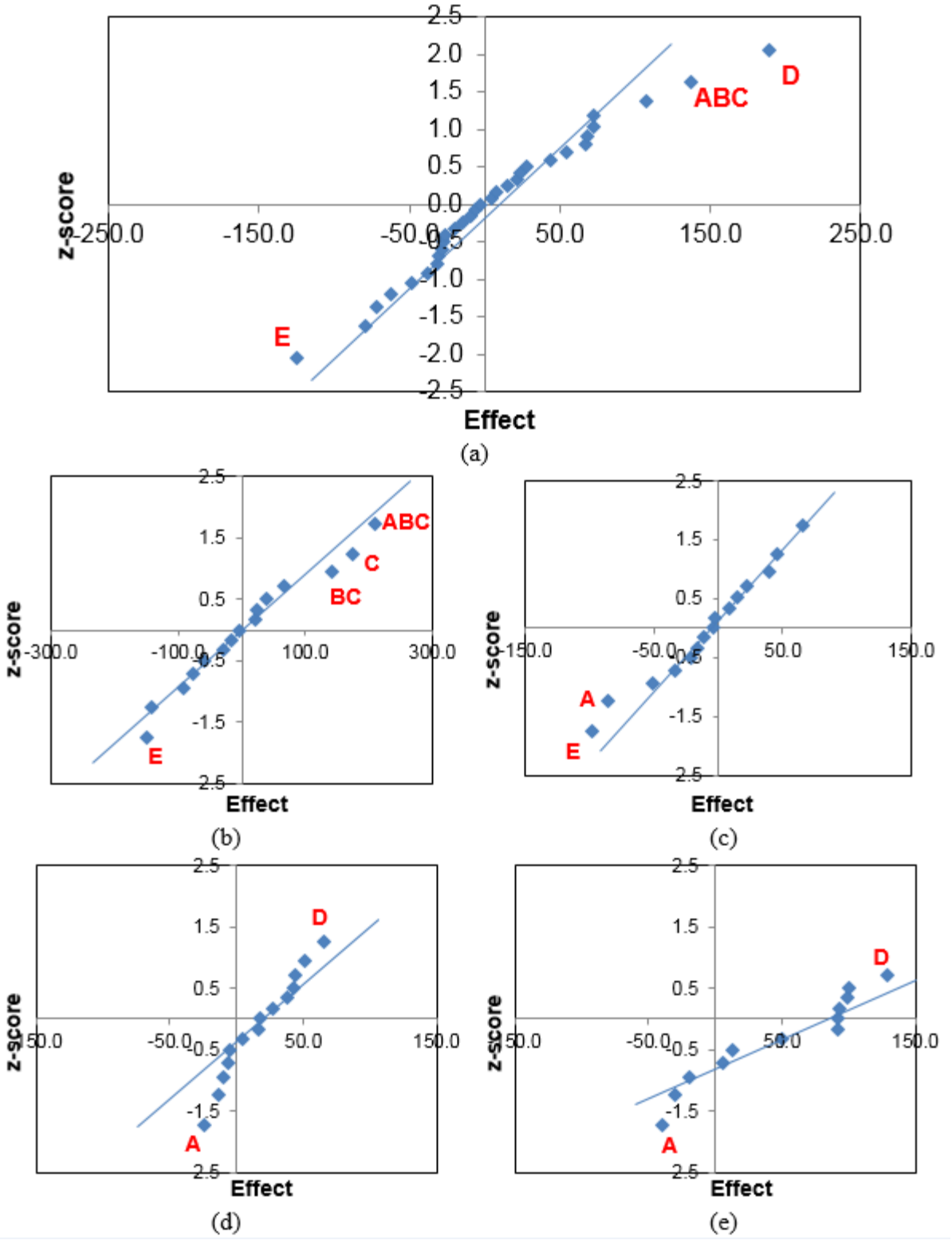

Figure 1-9: Normal probability plot of effects for (a) recovery of oil from sediment (g oil/kg sediment) and effect of oil (b) CC, (c) DB1 and water (d) SW and (e) FW for Campaign 1

Emulsion Thickness. The emulsion thickness for each run was monitored over a series of seven days. The significant effects are shown in Figure 1-10. The emulsions thickness is greatest with D (CC oil) with a small effect of E (salt water). The effect of oil type on the emulsion thickness was plotted as shown in Figure 1-10b and c. For CC, the interaction of AE is significant, however, for DB1 variables A (sand) and E (salt water) are single variable effects. In Figure 1-10d the effect of water type shows that D (DB1 oil) and A (sand) will cause an increase in emulsion thickness in salt water. In fresh water, D (DB1 oil) is significant and will increase the emulsion thickness (Figure 1-10e).

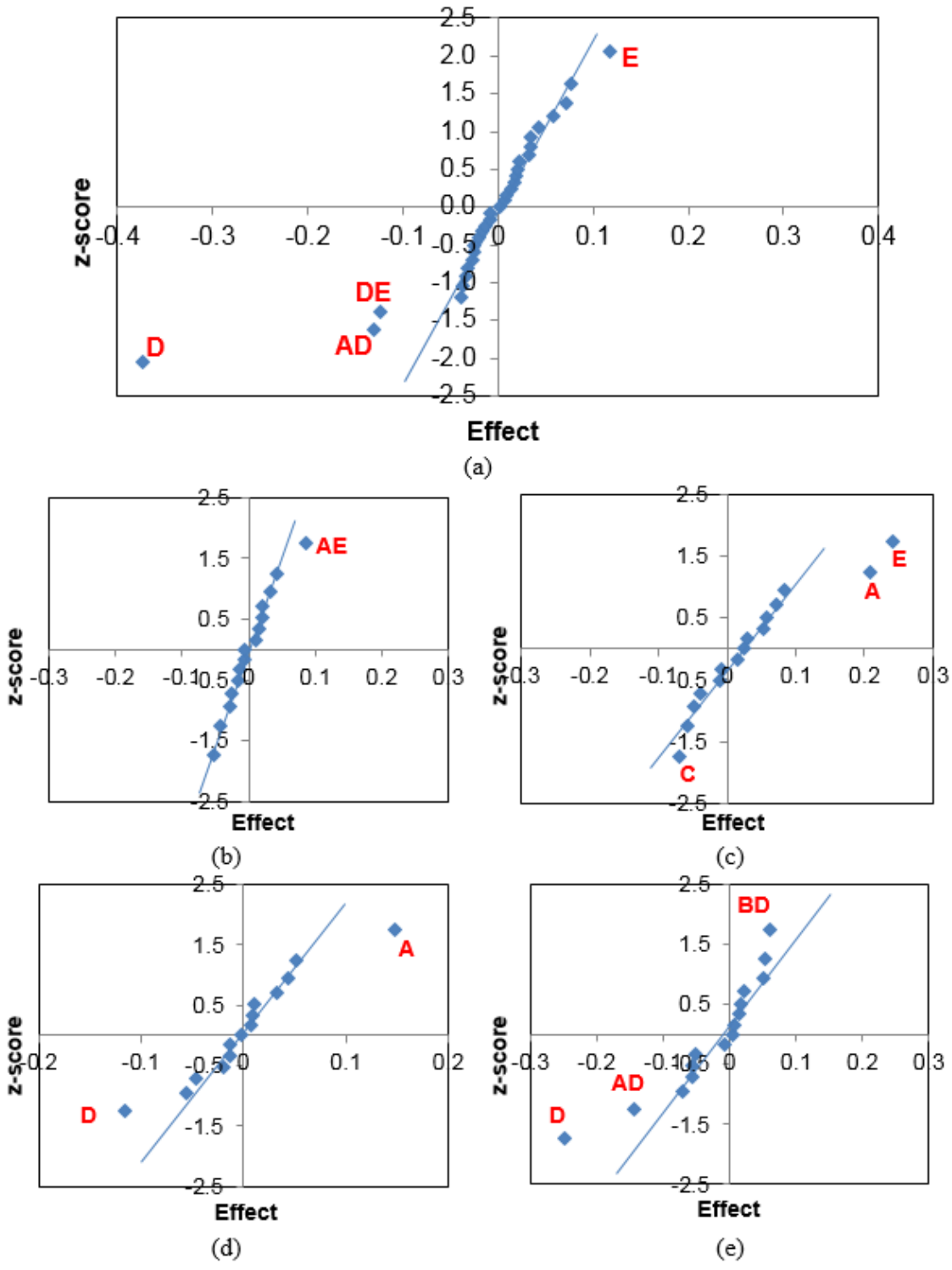

Figure 1-10 Normal probability plot of effects for (a) average emulsion thickness and the effect of oil type (b) CC and (c) DB1 and water type (d) SW and (e) FW for Campaign 1

Water Recovery. The significant effects on water recovery for Campaign 1 are E (salt water) and D (CC oil), as shown in Figure 1-11a. The effect of E and D on water recovery are shown in Figure 1-11b and c, and Figure 1-11d and e, respectively. The effect of D (CC oil) causes an increased in water recovery in salt water with a little effect on fresh water (Figure 1-11b and c). Variable E (salt water) clearly causes an increase in water recovery for both CC and DB1 while A (diatomaceous earth) shows some effect for DB1 (Figure 1-11d and e).

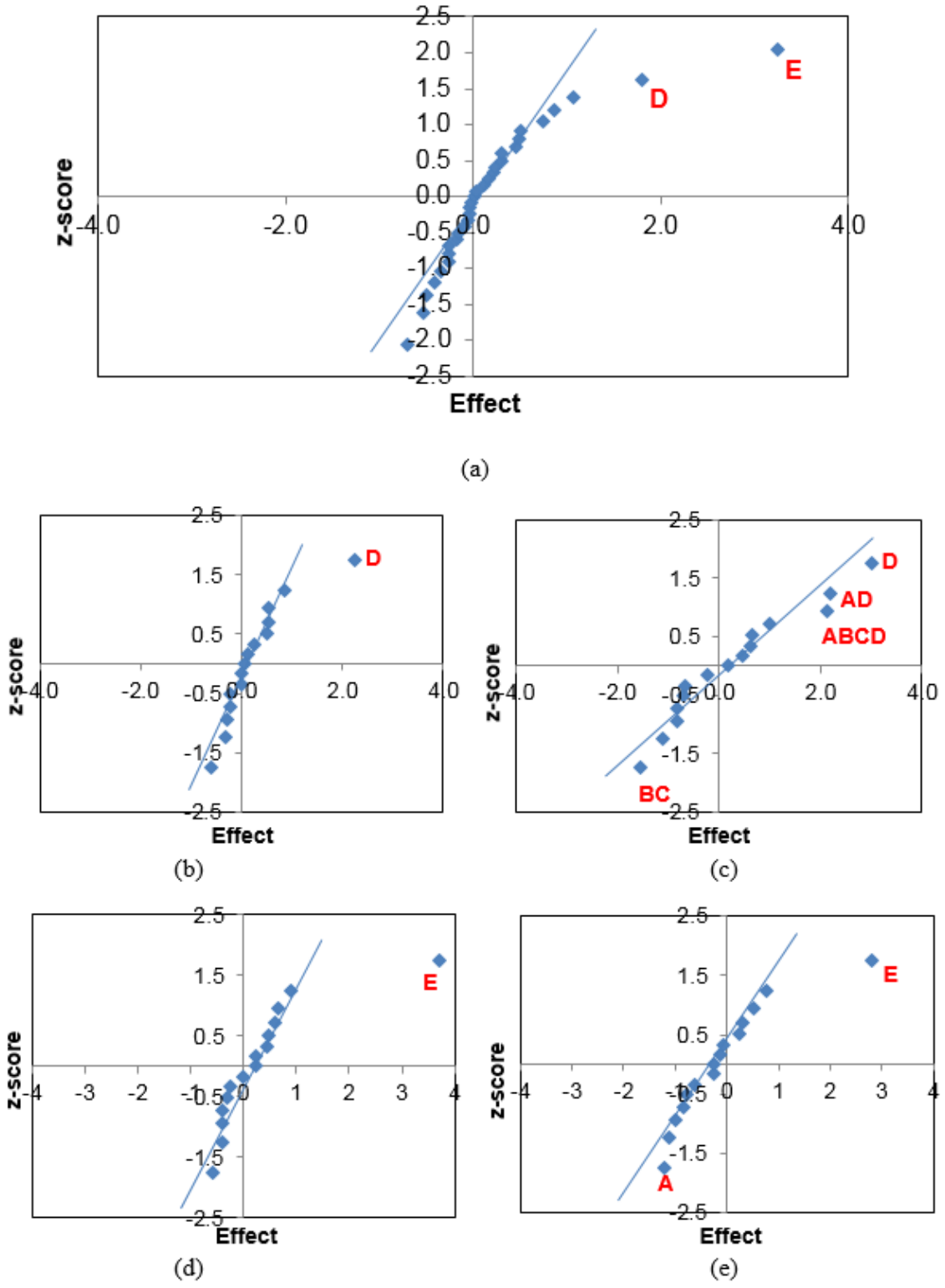

Figure 1-11 Normal probability plot of effects for (a) water recovery and the effect of water type (b) SW and (c) FW and oil type (d) CC and (e) DB1 for Campaign 1

1.5.2 Significant effects on output variables

Floating Oil

As shown in Figure 1-7, the main factors that affect the recovery of the floating oil from the surface of the water are C (ambient temperature) and E (salt water) based on the 32 runs. This indicates that the mixing at ambient temperatures and the presence of salt ions improve the recovery of floating oil. The buoyancy of oil is determined by its density while the rate of spreading and dispersion into the water column is influenced by the viscosity (Government of Canada, 2013b). As shown in Table 1-2, the density and viscosity for the oils decrease with increasing temperature, as expected. Studies conducted by Bridie (1980) show that heavier oils (density around 0.97 g/ml) did not mix as easily in synthetic sea water at 15^{o}C compared to lighter crude oils (densities between 0.83-0.87 g/ml), which supports our findings of improved recovery of DB1 in salt water mixing. The effect of E (salt water) is supported by the fact that water-in-oil emulsion stability decreases with an increase in salt concentration (Butt, Graf, & Kappl, 2006; Israelachvili, 2011). The higher ionic strength reduces the thickness of the electric double layer, causing agglomeration of the oil drops (Butt et al., 2006; Halboose, 2010; Israelachvili, 2011; Trefalt & Borkovec, 2014). From Figure 1-7, the temperature and type of water both affected the floating oil recovery, with salt water increasing recovery. The effect of mixing temperature and water type on recovery of floating oil is further illustrated in Figure 1-12. Recovery of DB1 from the surface of salt water is higher than recovery of CC, with all other mixing conditions constant. In fresh water, the points are distributed around the parity line, meaning that either CC or DB1 may give higher recovery depending on other factors. This nicely illustrates the interaction effects and reinforces the importance of revisiting some of the interactions as potentially significant effects.

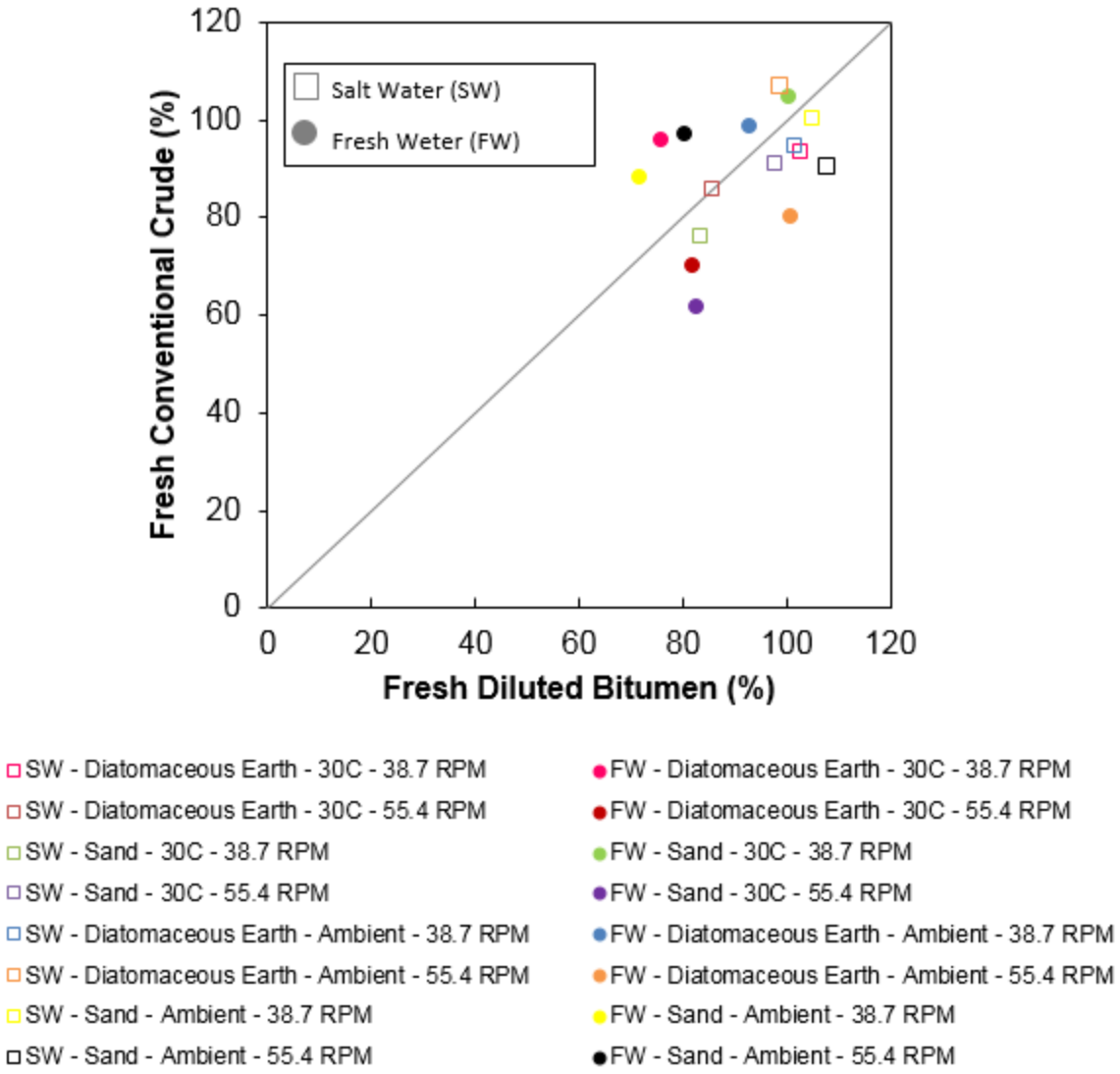

Figure 1-12: Floating oil recovered from salt and fresh water in Campaign 1

Oil recovered from the water phase

It was observed that D (DB1 oil) and E (fresh water) affect the amount of oil that migrates to the water phase (Figure 1-8), indicating that mixing DB1 in fresh water will produce the greatest amount of oil in the water column. This supports the idea that the oil droplets in fresh water have a higher surface charge density allowing the oil particles to disperse easily due to electrostatic repulsion (Butt et al., 2006; Israelachvili, 2011; Trefalt & Borkovec, 2014). From

Figure 1-13, it can be seen that the greatest amount of DB1 is extracted from the fresh water column at the higher mixing speed and temperature, with diatomaceous earth. Similar mixing conditions produce the same result when mixing with CC, but with sand. A study by Lafargue and Barker (1988) was conducted to understand the effect of the water soluble fractions in crude oils for the effectiveness of water washing after an oil spill. They found in the four oils studied, the lighter ends of crude oils were more soluble (saturates and aromatics fractions) (LaFargue & Barker, 1988). The soluble fractions of oil become a risk to aquatic life (M. Fingas, 2015; Gong et al., 2014). Detailed analysis of the water soluble components of the oils would provide a better understanding of the susceptibility of the oil to dispersing/solubilizing in water environments; however this is beyond the scope of this study.

Colloidally dispersed oil particle sizes range between 1nm - 1μm (Butt et al., 2006; Israelachvili, 2011), while larger droplets of oil (>~50μm) will resurface (Fingas, M., 2014). The dispersed oil particle sizes from the mixing tests were not measured, however, similar dispersion behaviour of a high viscosity oil was observed in the tests carried out by Environment Canada (2013a). A high mixing speed is necessary to disperse a high viscosity oil which may then remain dispersed depending on sediment and water salinity conditions (Fingas, M., 2014; Gong et al., 2014). Further study on oil particle sizes and changes in interfacial stability would provide more information on the stability of the oil dispersed in the water column.

Due to the presence of ions in salt water, less oil disperses in salt water compared to fresh water. The influence of the ions causes a decrease in the electric double layer around the particles in the water allowing them to approach each other and interact (Butt et al., 2006; Israelachvili, 2011; Lima, De Melo, Baptista, & Paredes, 2013; Trefalt & Borkovec, 2014). The surface charge density decreases on the negatively charged oil particles which then approach each other as the energy barrier is reduced and the electrostatic repulsion decreases (Trefalt & Borkovec, 2014; Butt et al., 2006; Israelachvili, 2011). The Van der Waals attractive force then becomes the dominating force between the oil particles encouraging separation of the oil from the water phase (Le Floch et al., 2002).

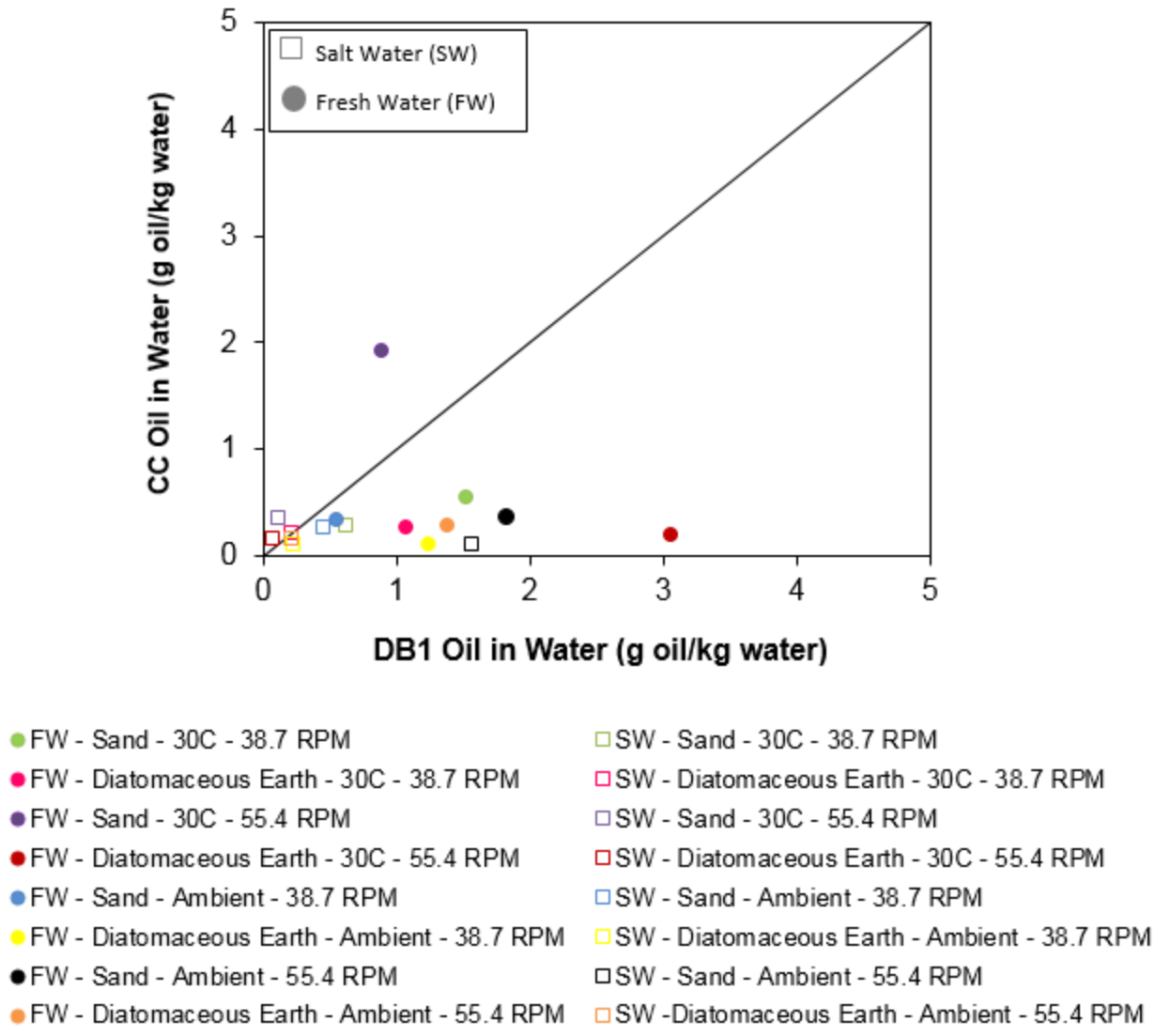

Figure 1-13: Oil in salt and fresh water from Campaign 1

Oil recovered from sediment

Along with oil dispersing into the water column, sediment interaction occurs in the form of OMAs, also referred to as OSAs (Oil Sediment Aggregates), when oil is spilled in fresh and marine waters (Le Floch et al., 2002; Lima et al., 2013; Nordvik et al., 1996). Colloidal forces determine whether particles will attract or repel; van der Waal forces are attractive and almost

always present (promote aggregation), and Double Layer forces are repulsive. Most particles in marine waters have a negative charge including oil particles and silica in sand (C. P. Huang & Elliott, 1977; Kanicky, Lopez-Montilla, Pandey, & Shah, 2001). According to Stoffyn-Egli & Lee (2002), the formation of OMAs is dependent on the viscosity of the oil (inversely proportional to viscosity). Based on the inverse relationship between OMA formation and viscosity of the oil, it is expected the CC would interact more with sediment, compared to DB1, since CC has a lower viscosity than DB1 oil. From Figure 1-9, it was found that the effect of D (CC oil) is the most significant causing an increase of oil on sediment in fresh water. As shown in Figure 1-14, lab tests revealed that CC becomes trapped within the sediment in fresh water. However, the OMAs formed are not stable and break upon agitation or sample handling, the same phenomena experienced during tests performed by Stoffyn-Egli and Lee (2002). Low viscosity oils used in other studies produced negatively buoyant OMAs causing them to sink (Gong et al., 2014; Khelifa et al., 2002; R. F. Lee & Page, 1997). To form OMAs, sufficient polar fractions are needed as this component of the oil increases the adhesion of the oil onto the sediment (as cited in Gong et al, 2014). The oil composition of CC has a greater maltenes fraction compared to DB1 and thus interacts more with the sediment.

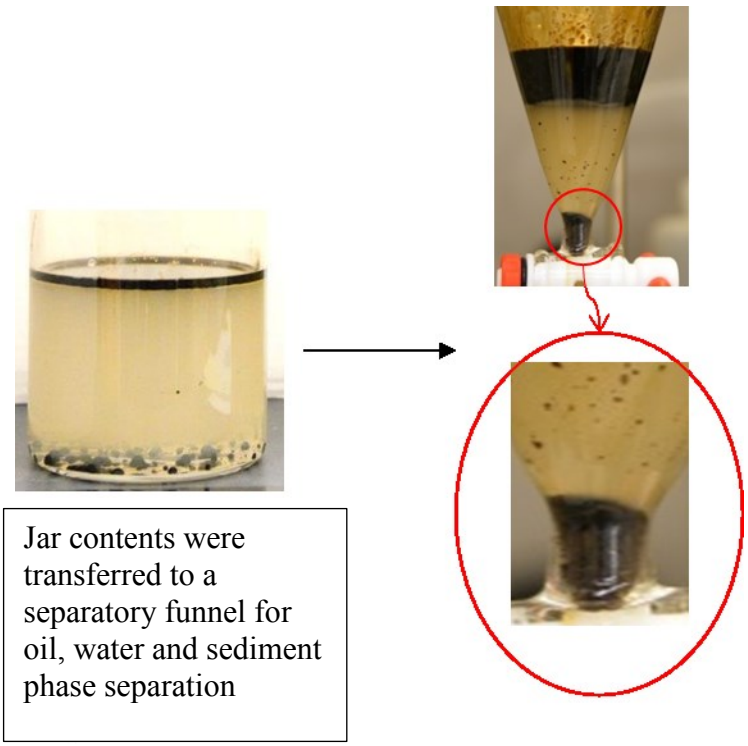

Figure 1-14: Mixing tests with CC, sand and fresh water at ambient conditions (20.3°C±2°C) showing oil trapped in the sediment

Earlier results suggest a relationship between CC and diatomaceous earth in sedimentation for both fresh and salt water (Figure 1-9). A parity plot of the results for oil extracted from sediment data is shown in Figure 1-15. It is evident that CC interacted more with both sediments than DB1 as all of the data falls above the parity line.

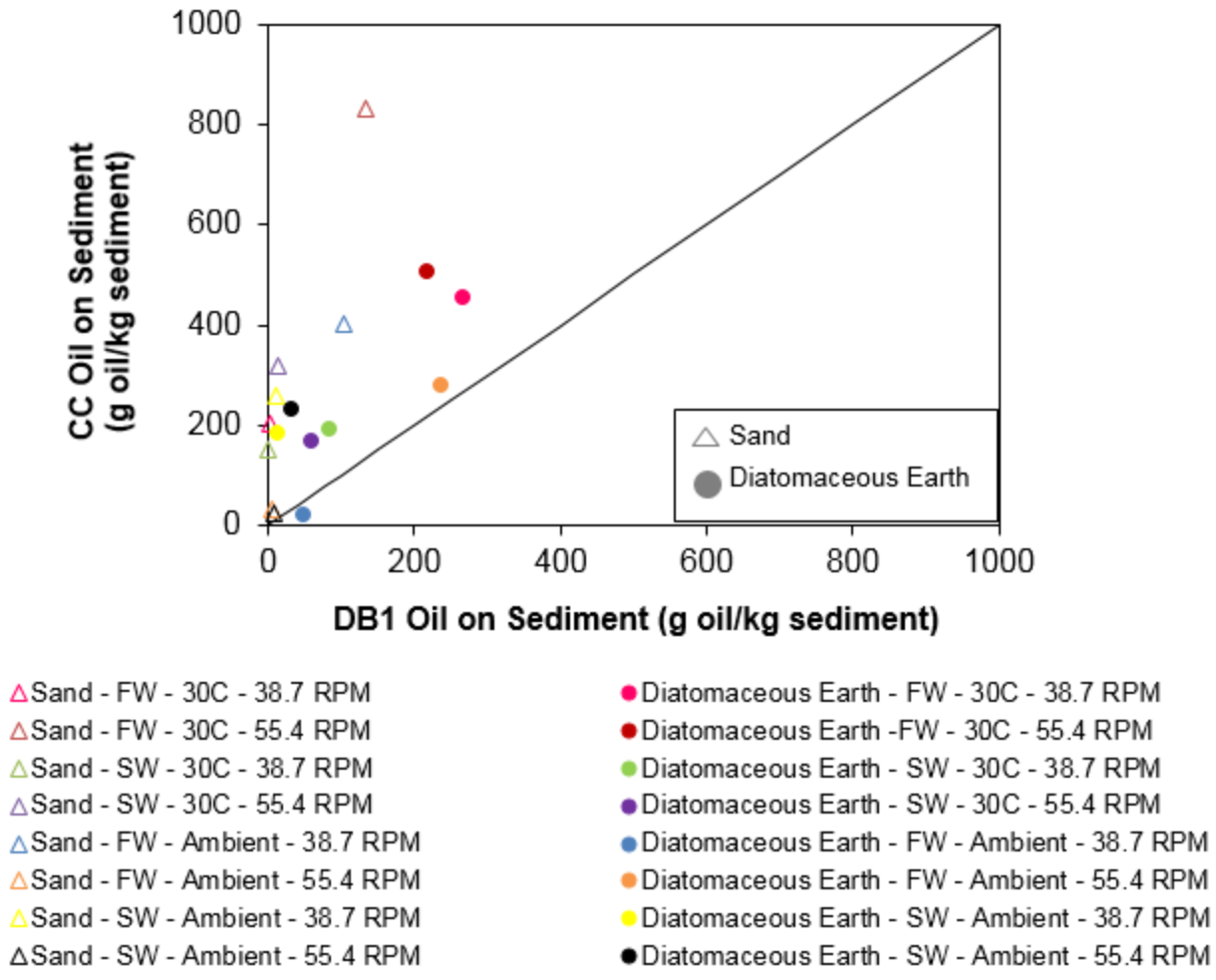

Figure 1-15: Oil recovered from sediment for CC and DB1 from Campaign 1

Emulsion thickness

Several studies have shown that water-in-oil emulsions are stabilized by the viscous and elastic forces resulting from the presence of resins and asphaltenes at the interface (Abdel-Rauf, 2012; M. Fingas & Fieldhouse, 2003; M. Fingas, Fieldhouse, & Mullin, 2005; M. Fingas, 2015; National Research Council, 2003). The floating oil phase was monitored for emulsion thickness after each mixing test. The jars were maintained at ambient lab conditions over a period of 7 days. It was noted that most of the change in emulsion thickness occurred within the first 24-36 hours after mixing. According to Fingas and Fieldhouse (2005), emulsions are considered stable

if there is no change in 5 days at 15^{o}C. The formation of an emulsion can cause volume swell making oil spill clean-up a difficult task. The most significant effect on emulsion thickness is the type of oil (DB1 oil), as shown in Figure 1-10a. This emphasizes the importance of oil properties on the formation of water-in-oil emulsions (Gong et al., 2014; King et al., 2014; Stoffyn-Egli & Lee, 2002). Oils with higher asphaltene and resin content will produce more stable water-in-oil emulsions (M. F. Fingas et al., 2005; Nordvik et al., 1996; Poindexter, Chuai, Marble, & Marsh, 2005; Sjoblom et al., 2003; Wei et al., 2003). When oil is mixed with salt water, the asphaltenes in the oil form micelles and are adsorbed by electrostatic attraction in the salt water preventing water particles from coalescing, promoting emulsion formation. The effect of E, water type, (although not as significant as D, type of oil) is also highlighted as a single variable effect in Figure 1-10a. The presence of E (salt water) supports the findings that salt water has an impact on the recovery of the floating oil. The effect of oil type was further studied. As show in Figure 1-10b, a complex interaction between A and E occurs with CC, while A (sand) and E (salt water) are significant with DB1. This indicates emulsion formation with DB1 is most significant in salt water with sand (Figure 1-10c).

Water recovery

The effect of mixing on the water column was also studied in the form of water recovery post mixing. Water recovery is reduced when water is lost to the formation of water-in-oil emulsions. Studies have shown that 60-85% of water is lost to form stable emulsions, also referred to as mousse (M. FINGAS, 1995; M. Fingas & Fieldhouse, 2003; M. Fingas & Fieldhouse, 2008; M. F. Fingas et al., 2005). From Figure 1-11a, the greatest impact on water recovery for Campaign 1 are variables D (CC oil) and E (salt water). The effect of D (CC oil) is significant in both salt water and fresh water (Figure 1-11b and c, respectively), while the effect of E (salt water) is significant for both CC and DB1 (Figure 1-11d and e, respectively). These results are in agreement with the water salinity effect improving water recovery by destabilizing emulsion formation (C. P. Huang & Elliott, 1977; Khelifa et al., 2005; Lima et al., 2013). In Figure 1-11e, the effect of A (diatomaceous earth) also proves important for DB1 runs.

A parity plot for water recovery is shown in Figure 1-16, where the water recovery is greater in salt water for all runs. The variable E (salt water) causes an increase in emulsion thickness and water recovery (Figure 1-10a and Figure 1-11a, respectively), while D (CC oil) causes an increase in water recovery and a decrease in emulsion thickness. This implies that DB1 will produce a thicker emulsion while CC will allow for greater water recovery. Another similarity is the presence of variable A and E when mixing with DB1. Variable E (salt water) is significant at the positive level for emulsion thickness (Figure 1-10c) and water recovery (Figure 1-11e), while A is significance at the positive level (sand) for emulsion thickness (Figure 1-10c) and less significant at the negative level (diatomaceous earth) for water recovery (Figure 1-11e).

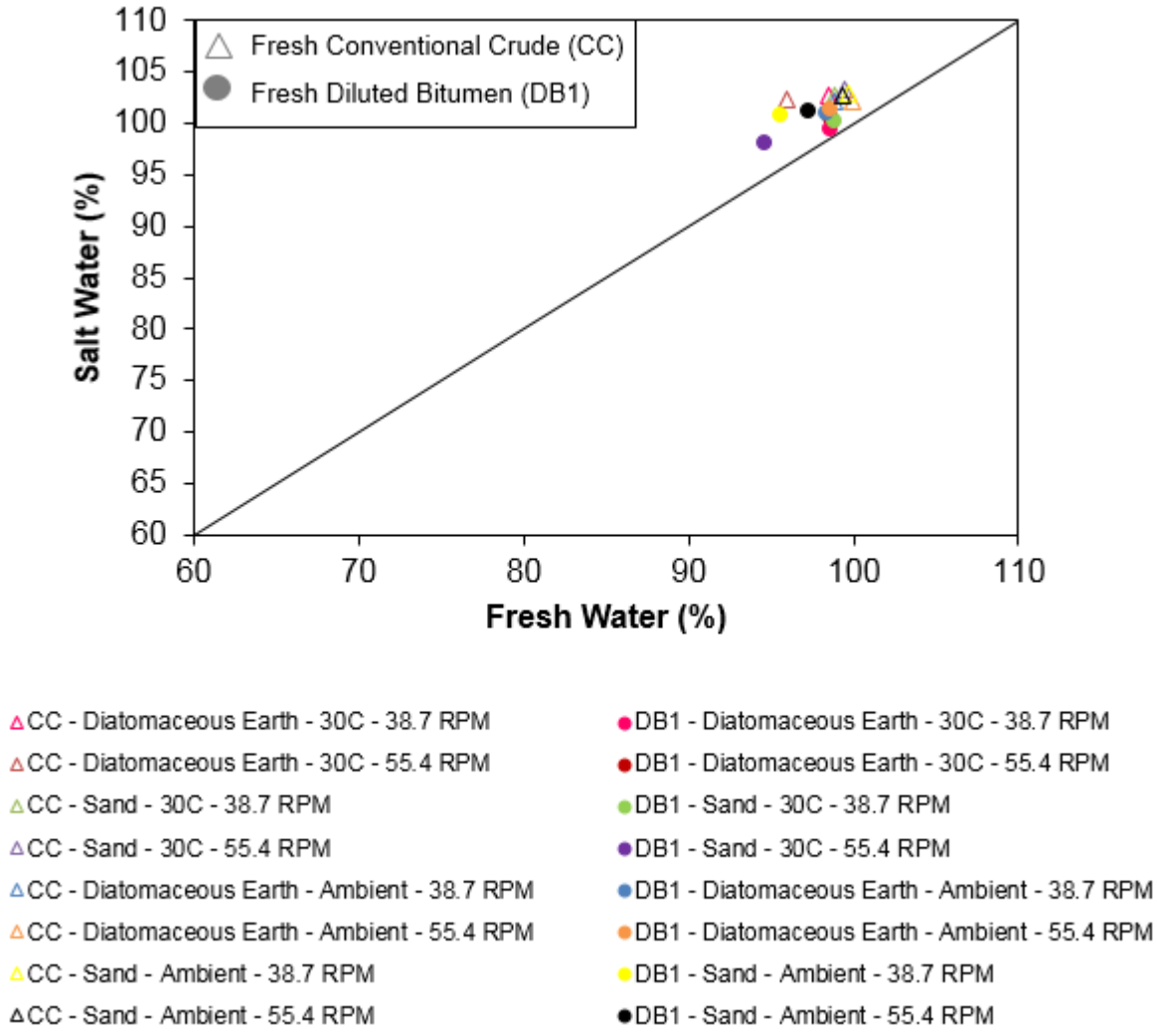

Figure 1-16: Water recovery in fresh and salt water in Campaign 1

A summary of the significant effects for the oil distribution, emulsion thickness, and water recovery from Campaign 1 is shown in Figure 1-17a, b, and c, respectively. The significant effects identified with a triangular shape are the results from the first level of the normal probability plots and the circular shapes represent the second level of the normal probability plots. The input variables are color coded as follows: brown is for type of sediment, green is for mixing speed, yellow is for temperature, grey is for type of oil and blue is type of water. The size of each shape represents the magnitude of the effect relative to other effects. The sign below each shape is an indication if the variable is present at the positive or negative level.

Since the type of water showed the most consistently important effects in Campaign 1, the salt water data was expanded in a second campaign.

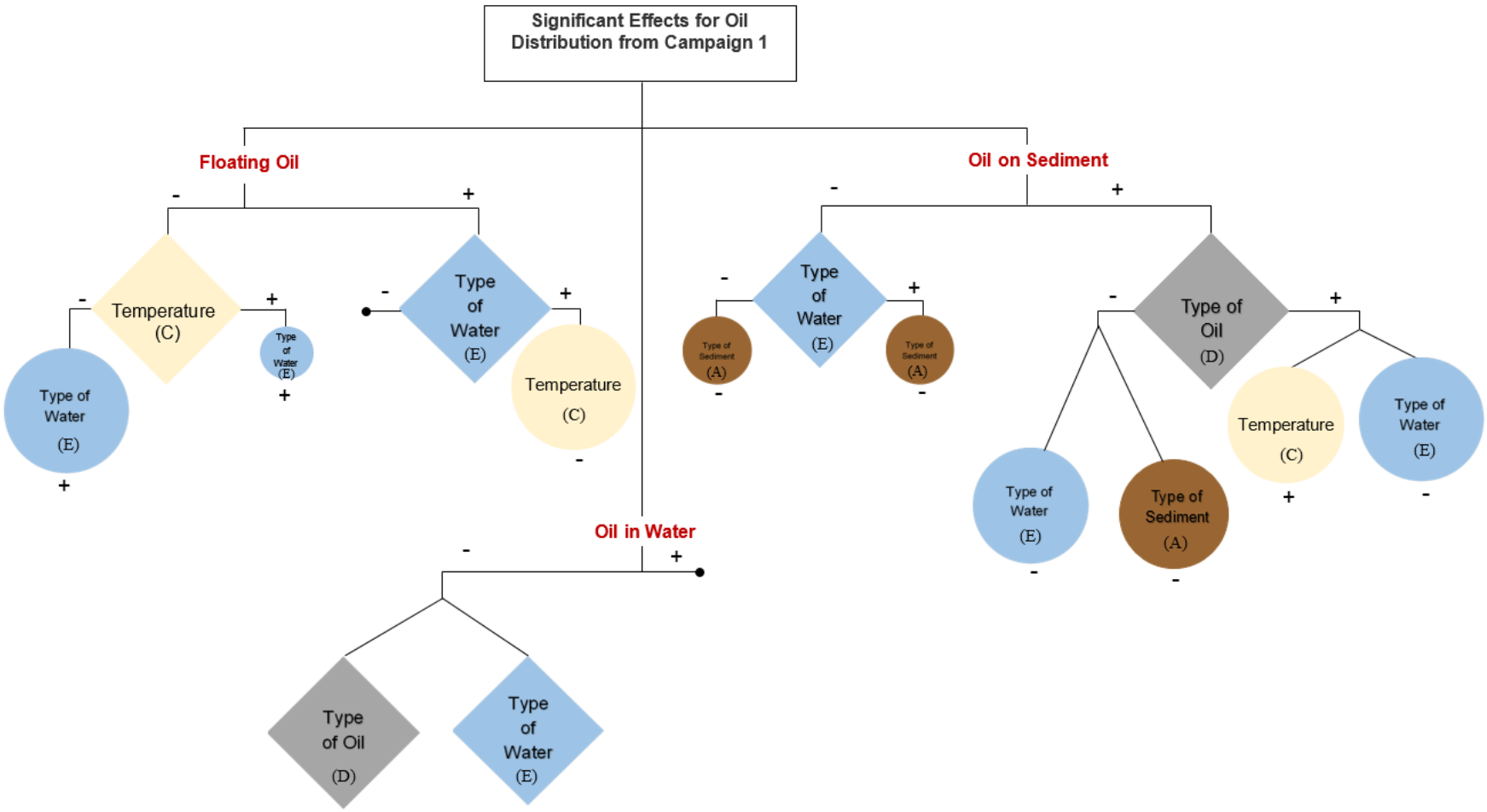

(a) Oil Distribution

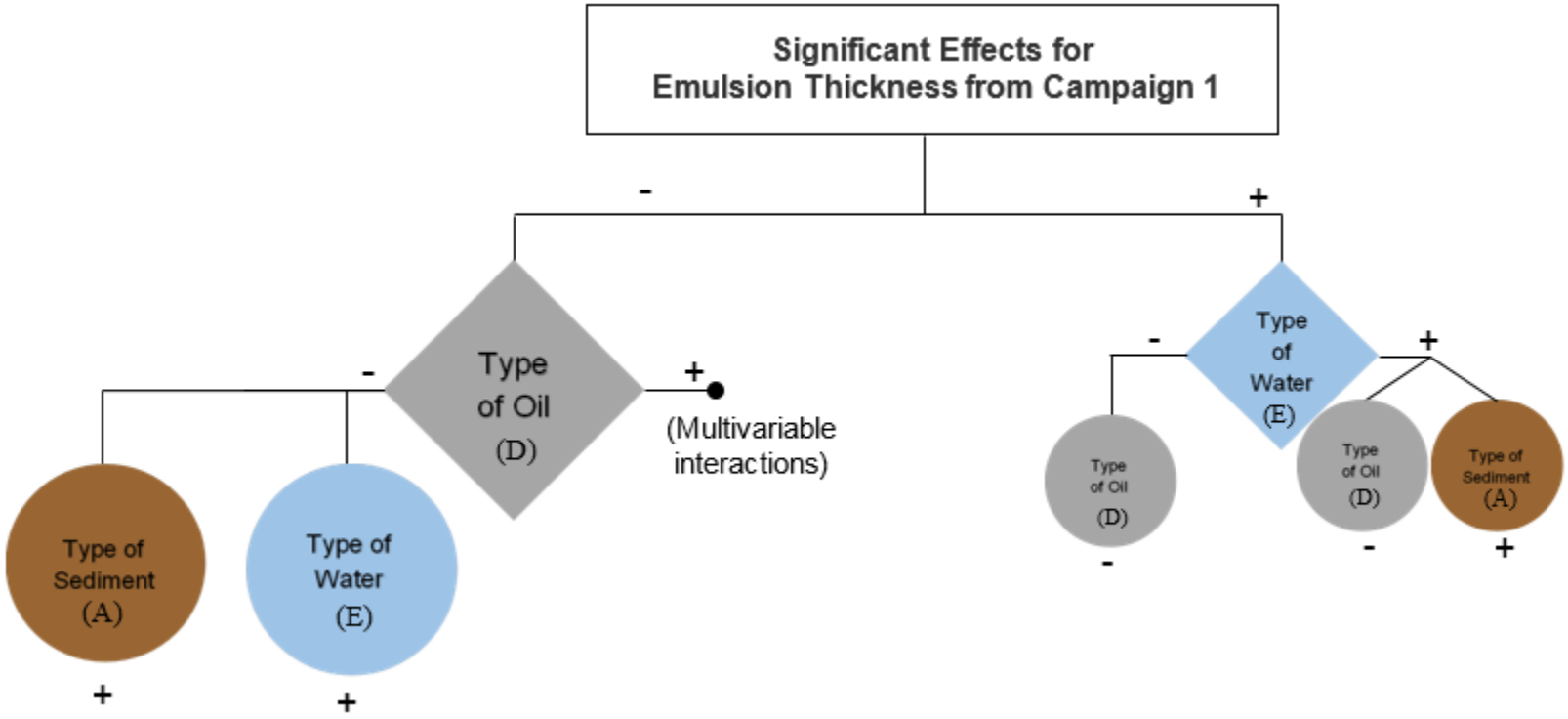

(b) Emulsion Thickness

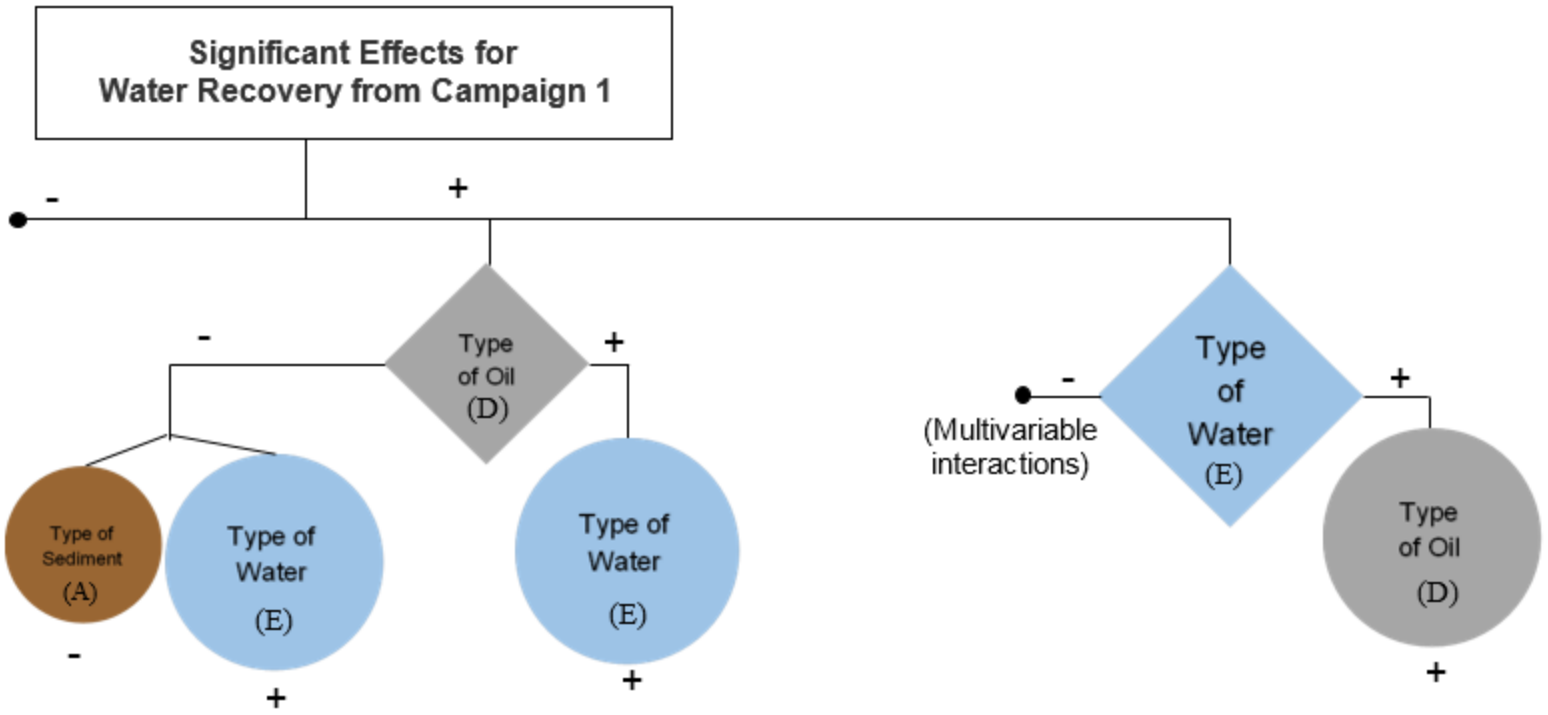

(c) Water Recovery

Figure 1-17: Summary of significant effects from Campaign 1 (a) Oil distribution, (b) Emulsion thickness and (c) Water recovery

1.6 Campaign 2: Effect of salt water

After completion of Campaign 1, an additional eight runs were carried out to obtain more information on the effect of mixing speed and ionic strength. The variable levels for Campaign 2 are shown in Table 1-7. The tests were carried out using diluted bitumen (DB1) in salt water only, while varying sediment and temperature at two-levels. The new mixing speeds for Campaign 2 were shifted to the non-breaking wave flow regime. The higher mixing speed data (breaking waves) from Campaign 1 was combined with Campaign 2 to assess the effect of the two different flow regimes in order to confirm whether mixing intensity has a significant effect when dramatically different conditions are present.

Campaign 2 completes a mixed level 2^4 factorial design with eleven interactions; two variables were tested at two levels (A, sediment, and C, temperature), and one variable at four levels (B, mixing speed) while the oil data used on DB1 and water data used only the salt water runs. Using the method of replacement, the four levels of B were replaced by two 2-level factors (B_1 and B_2) (Montgomery, 2013). Any interactions containing both B_1 and B_2 are ignored since there is no interaction between the speeds simultaneously. The contrast coefficients and design matrix are shown in Table 1-8 and Table 1-9, respectively.

Table 1-7: Variable Levels for Campaign 2

Effect	Variable	- level	+ level
A	Sediment	Diatomaceous earth	Sand
B	Mixing Speed	2.3 RPM	8.2 RPM
C	Temperature	Ambient (20.3°C±2°C)	30°C±0.1°C
D	Oil	DB1	*
E	Water	*	SW

*: not tested at that level

Table 1-8: Contrast Coefficients for Campaign 2

B_1	B_2	X=speed @ 4-levels	C	A	CA	B_1C	B_1A	B_2C	B_2A	B_1CA	B_2CA
-1	1	x_4	-1	-1	1	1	1	-1	-1	-1	1
-1	1	x_4	-1	1	-1	1	-1	-1	1	1	-1
1	1	x_3	-1	-1	1	-1	-1	-1	-1	1	1
1	1	x_3	-1	1	-1	-1	1	-1	1	-1	-1
-1	1	x_4	1	-1	-1	-1	1	1	-1	1	-1
-1	1	x_4	1	1	1	-1	-1	1	1	-1	1
1	1	x_3	1	-1	-1	1	-1	1	-1	-1	-1
1	1	x_3	1	1	1	1	1	1	1	1	1
-1	-1	x_1	-1	-1	1	1	1	1	1	-1	-1
-1	-1	x_1	-1	1	-1	1	-1	1	-1	1	1
1	-1	x_2	-1	-1	1	-1	-1	1	1	1	-1
1	-1	x_2	-1	1	-1	-1	1	1	-1	-1	1
-1	-1	x_1	1	-1	-1	-1	1	-1	1	1	1
-1	-1	x_1	1	1	1	-1	-1	-1	-1	-1	-1
1	-1	x_2	1	-1	-1	1	-1	-1	1	-1	1
1	-1	x_2	1	1	1	1	1	-1	-1	1	-1

Table 1-9: Design Matrix for Campaign 2

Campaign 2	Factor						
	A	B	C	D	E	ABCDE	
Run Number	Sediment	Speed	Temperature	Oil	Water		Run label
33	-	-	-	-	+	+	e
34	+	-	-	-	+	-	ae
35	-	+	-	-	+	-	be
36	+	+	-	-	+	+	abe
37	-	-	+	-	+	-	ce
38	+	-	+	-	+	+	ace
39	-	+	+	-	+	+	bce
40	+	+	+	-	+	-	abce

1.6.1 Normal probability plots for Campaign 2

Floating Oil Recovery. As shown in Figure 1-18, there is no significant impact of the input variables on the floating oil recovery.

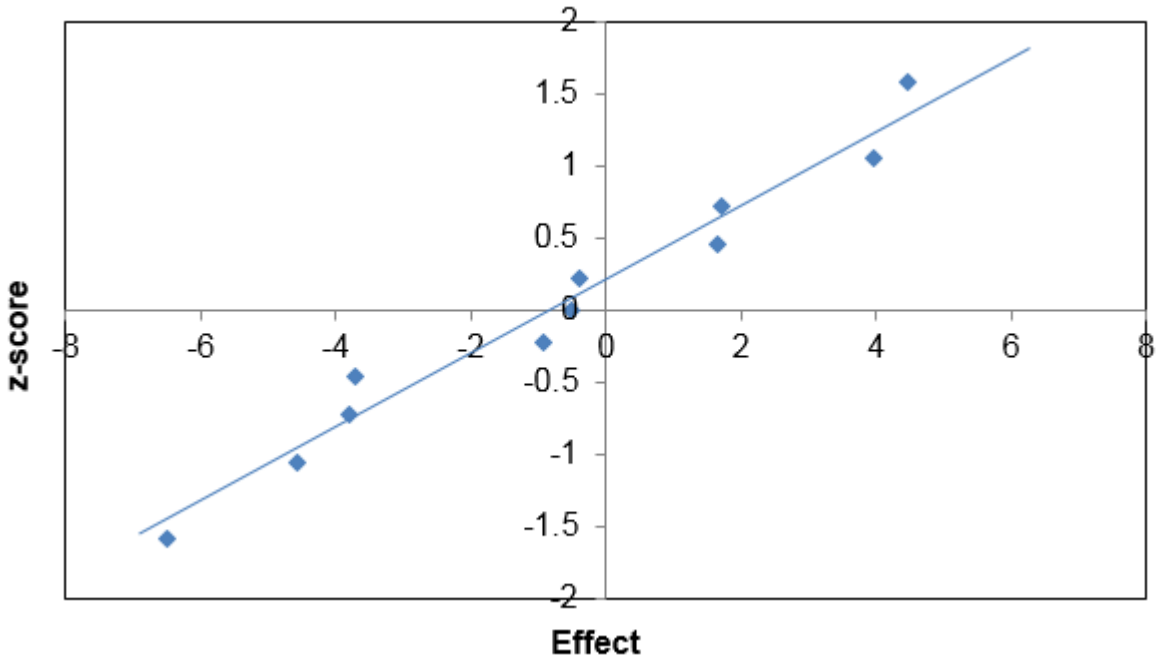

Figure 1-18: Normal probability plot of effects for recovery of floating oil from Campaign 2

Oil in Water. The significant effects on the amount of oil which remains in the water phase for DB1 in salt water (Campaign 2) is shown in Figure 1-19. Variable A (sand) has the greatest effect, along with complex interactions between B, C and A (Figure 1-19a). The results for sand and diatomaceous earth are separated in Figure 1-19b and Figure 1-19c, respectively. For sand, increasing the mixing speed increases the amount of oil in the water, while for diatomaceous earth, the effect is reversed.

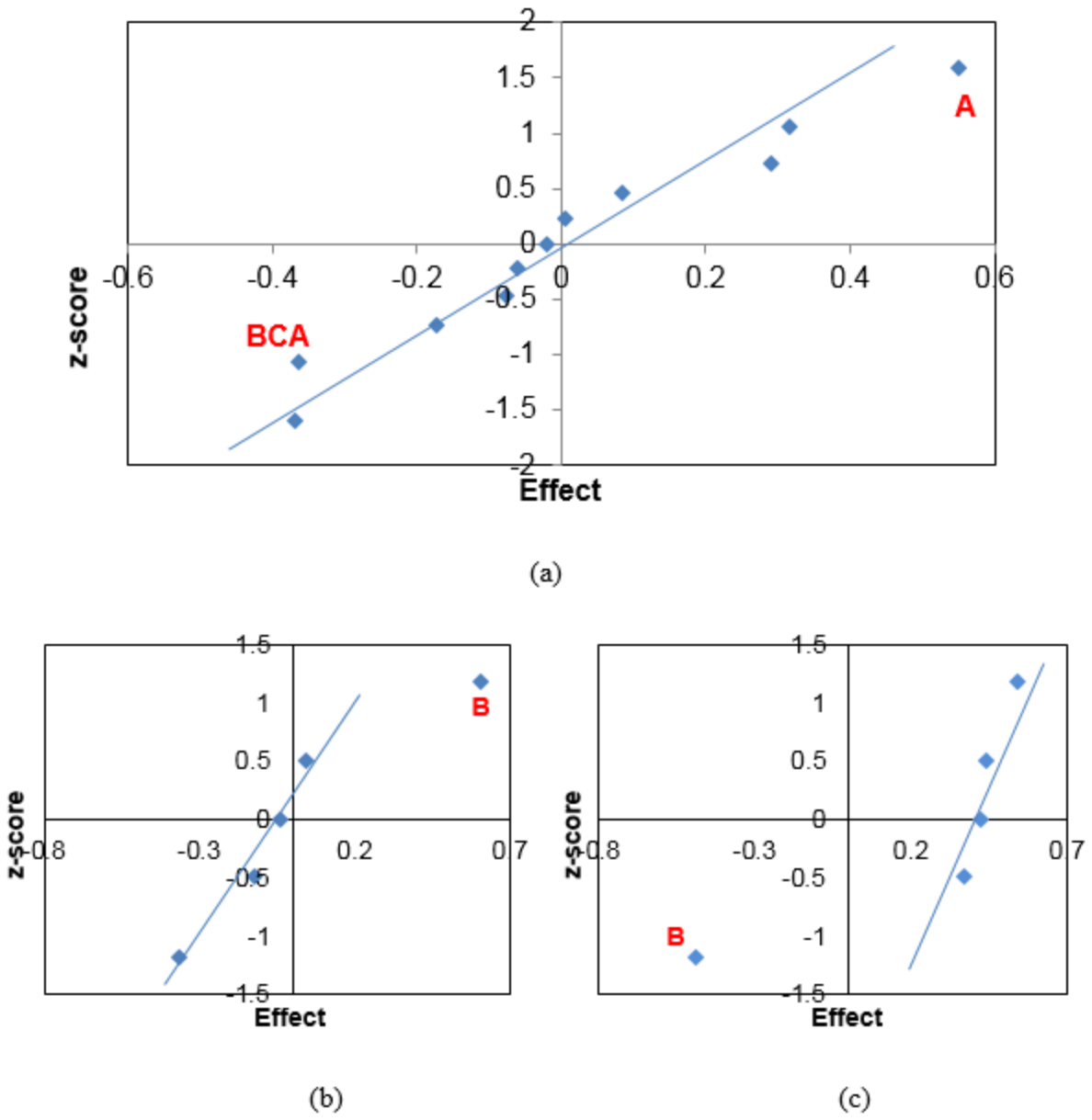

Figure 1-19: Normal probability plot of effects for (a) DB1 oil in salt water (g oil/kg water), and effect of sediment, (b) sand and (c) diatomaceous earth for Campaign 2

Oil on Sediment. The significant effects for oil trapped in sediment for Campaign 2 are shown in Figure 1-20. Sediment type (sand) has the greatest impact on how much DB1 is recovered from the sediment layer. There were no significant effects when mixing with sand

(Figure 1-20b), while C (30°C) is significant when mixing with diatomaceous earth (Figure 1-20c).

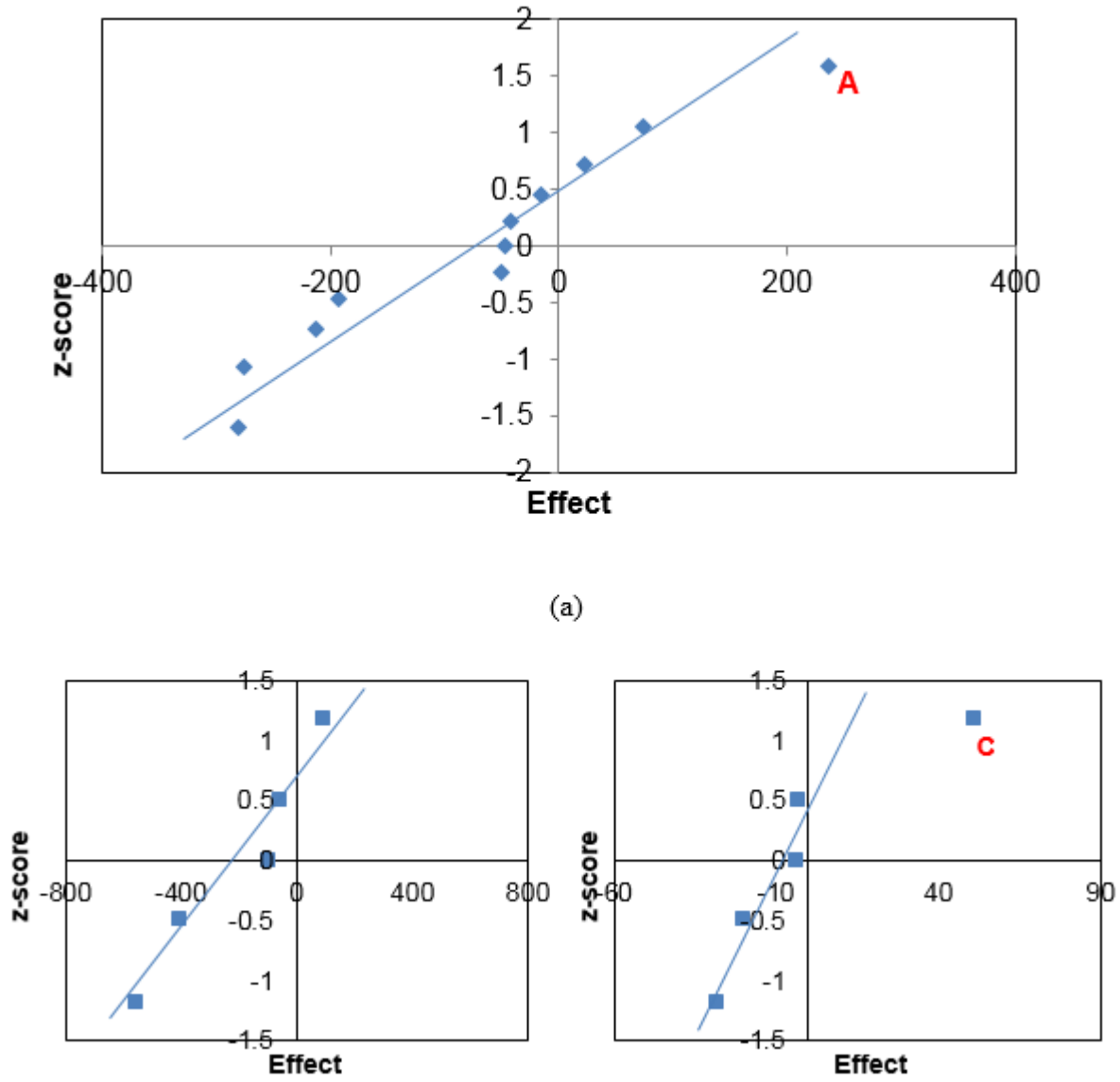

Figure 1-20: Normal probability plot of effects for (a) recovery of oil from sediment (g oil/kg sediment) and the effect of sediment, (b) sand and (c) diatomaceous earth for Campaign 2

Emulsion Thickness. The significant effect on emulsion thickness in Campaign 2 is B (mixing speed) as shown in Figure 1-21. Increasing the mixing speed produces a greater

emulsion thickness, as would be expected. This was not observed in Campaign 1 as the range of mixing speeds was much smaller.

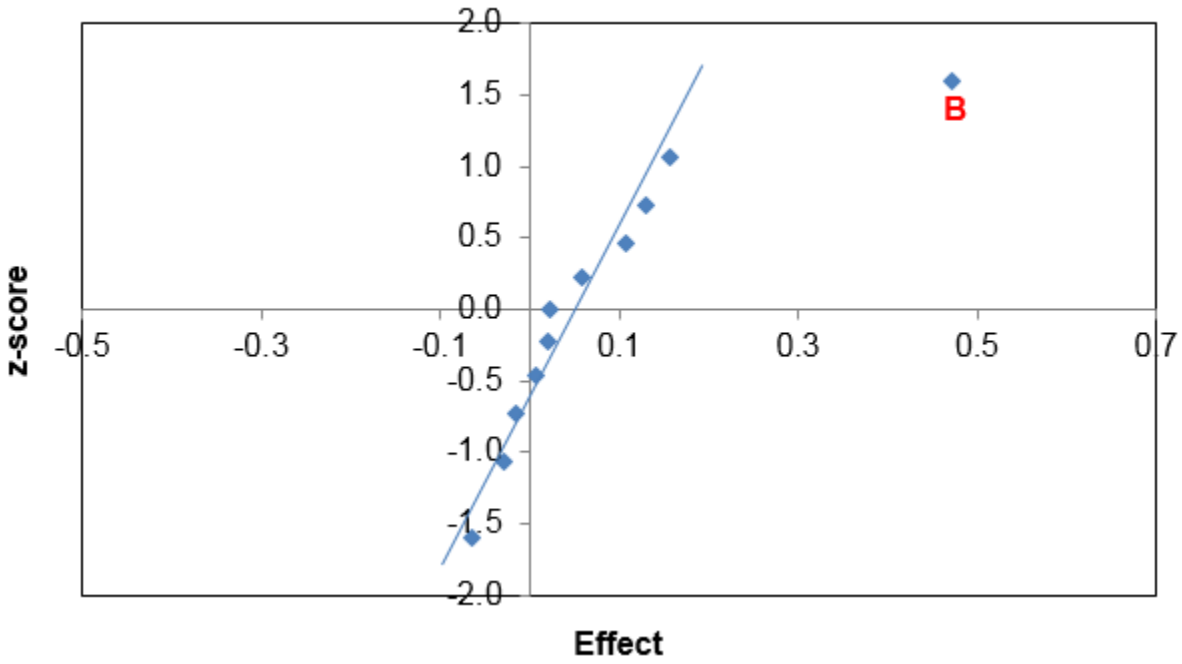

Figure 1-21: Normal probability plot of effects for average emulsion thickness for Campaign 2

Water Recovery. As shown in Figure 1-22, C (temperature) has the greatest impact on water recovery in Campaign 2. As the temperature increases, less of the water is recovered and more is lost to the emulsion layer.

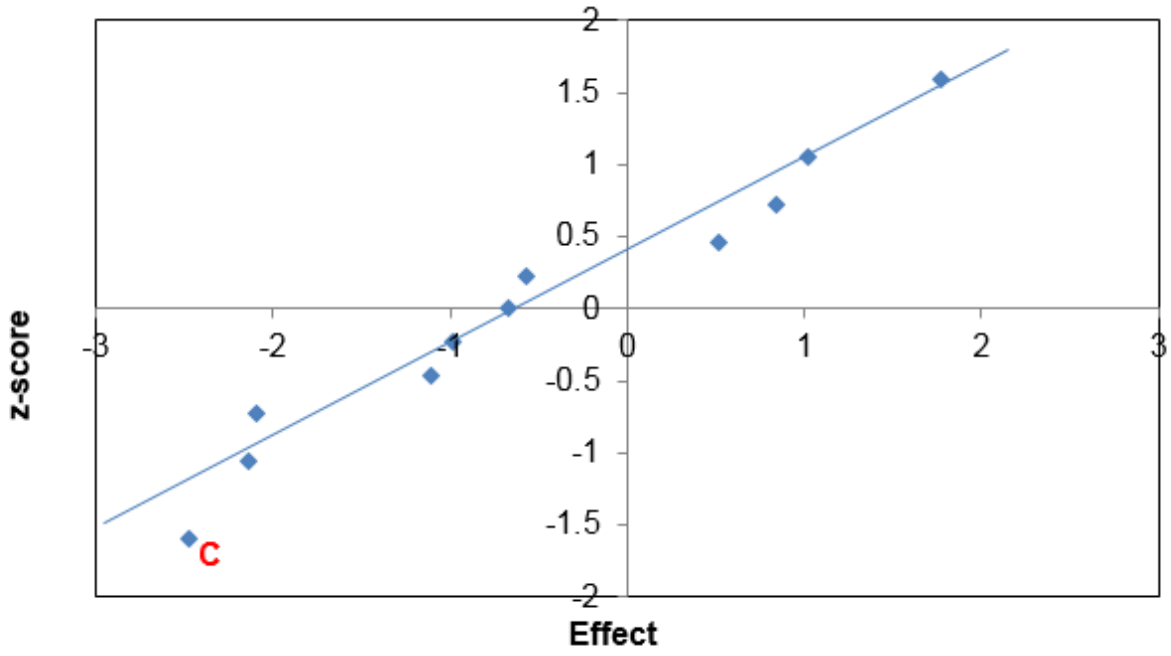

Figure 1-22: Normal probability plot of effects on water recovery for Campaign 2

1.6.2 Parity plots for mixing of diluted bitumen in salt water

Floating oil

From Campaign 2, there was no apparent effect of the input variables (Figure 1-18) which indicates there is no significant impact of different mixing energies on floating oil recovery for DB1 in SW.

Oil in water

The results from Campaign 2 show the effect of sediment (sand) as significant in increasing the amount of DB1 dispersing into the water column (Figure 1-19). This is further illustrated in Figure 1-23 where the greatest amount of oil is recovered from salt water when sand is present in the system, thus, encouraging the interaction between oil and water during mixing. However, it

was noted that the water column almost completely cleared up after the 1-h settling time and oil-sediment particles settled to the bottom of the jar.

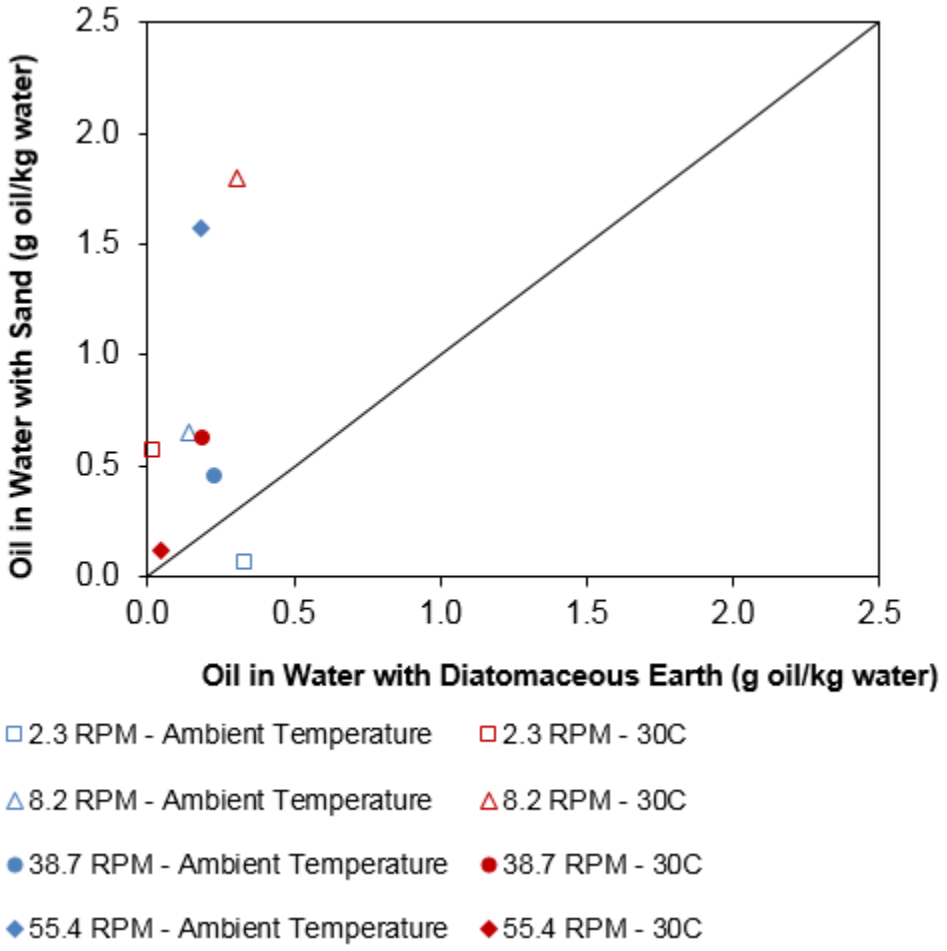

Figure 1-23: Oil in salt water runs from Campaign 2

Lab images taken after mixing DB1 with sand and salt water, at varying mixing speeds and temperatures, are show in Figure 1-23. These images are taken one day after mixing, and obvious interactions occurred between the oil and sand at the bottom of each jar. Oil can be found as dispersed droplets or dissolved oil components interacting with sediment in water environments. Since oil and mineral particles have a negative surface charge in salt water, and the presence of ions in the water thins out the electrostatic double layer repulsion between the oil and mineral particles, the oil then settles at the bottom with the sediment (Gong et al., 2014). The results of the effect of sediment on the dispersion of DB1 into the water column (Figure

1-19b and c) indicate that a high mixing energy is needed for DB1 to adhere to sand while low mixing energy is required when mixing with diatomaceous earth. Mixing temperature does not have an effect since oil-sediment interaction is seen at both mixing temperatures in Figure 1-24. Oil-sediment interaction at the oil-water interface is shown in images Figure 1-24b, c and d. The lighter OSAs rise to the oil-water surface. This interaction is defined as positively buoyant OSAs since the oil-sediment particles rise to the oil-water interphase and remain there (Omotoso et al., 2002).

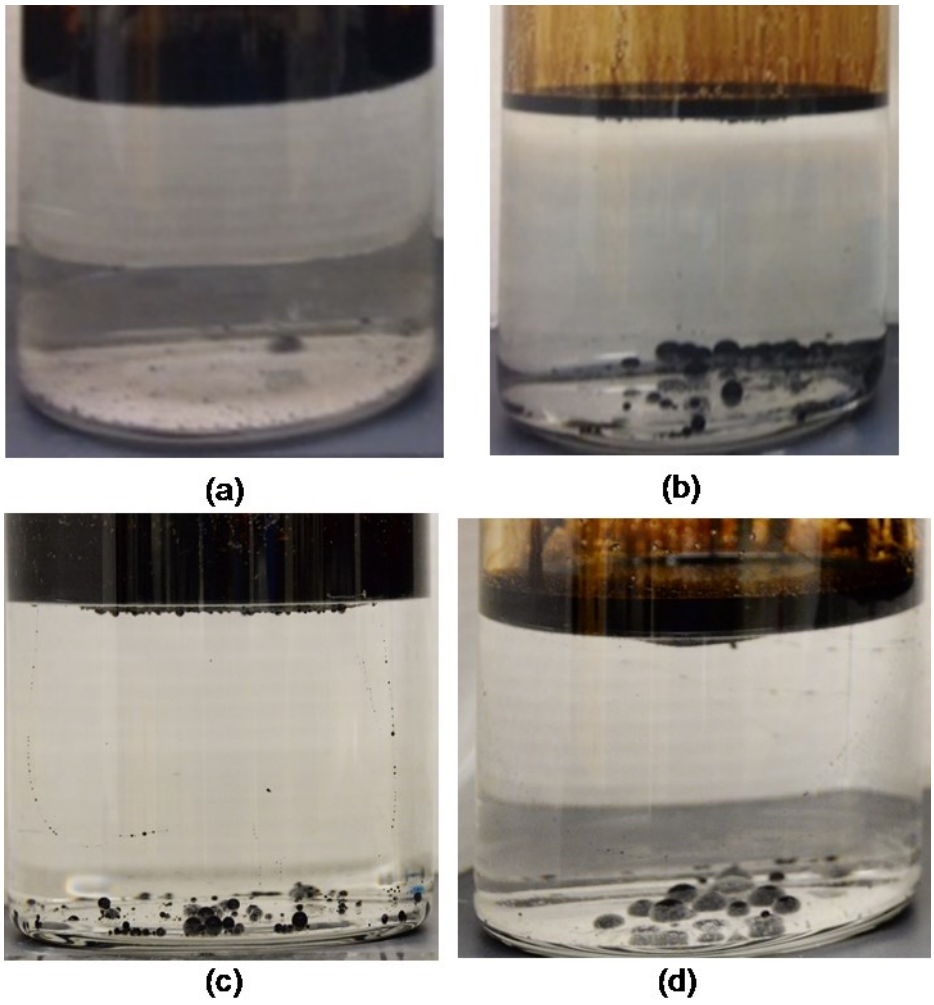

Figure 1-24: DB1 with salt water and Sand (a) 8.2 RPM and 30ºC, (b) 38.7 RPM and 30ºC, (c) 2.3 RPM and ambient temperature, and (d) 8.2 RPM and ambient temperature

Oil on sediment

In Campaign 2, the most significant effect when mixing DB1 in salt water was A (sand) as shown in Figure 1-20a. Images to support DB1 and sand interaction are shown in Figure 1-24; spherical oil drops covered in a layer of sand are settled at the bottom of the jars. The ionic strength effect, as discussed previously, encourages the interaction between the negatively charged oil and sand particles. The effect of sediment type on the oil extracted from sediment phase is shown in Figure 1-20b and c, for sand and diatomaceous earth respectively. No obvious significant effects are shown in Figure 1-20b for sand, however, C (temperature) in Figure 1-20 implies a relation between diatomaceous earth and warmer mixing temperature on the amount of oil extracted from the sediment layer.

Emulsion thickness

The main effect when mixing DB1 in salt water is the mixing speed (B + level, higher mixing speed) as shown in Figure 1-21. Higher mixing energy encourages interaction between the water and oil phases, trapping more water into the floating oil.

Water recovery

It was found from Campaign 2 that mixing DB1 in salt water with sand will produce a thicker emulsion, while mixing DB1 in salt water with diatomaceous earth will improve water recovery. From Figure 1-22, the significant effect on water recovery in Campaign 2 is C (ambient temperature). At ambient temperature, there would be minimal effect on reducing the viscosity of DB1 in salt water, which in turn, would minimize oil-water interaction.

A summary of the significant effects on the oil distribution, emulsions thickness and water recovery is shown in Figure 1-25a, b, and c respectively. Output variables with no main effect are marked with a '•'.

The results from Campaign 1 and 2 both show complex interactions between the oil and sediment. A third campaign was set up with no sediment to isolate some of the other effects.

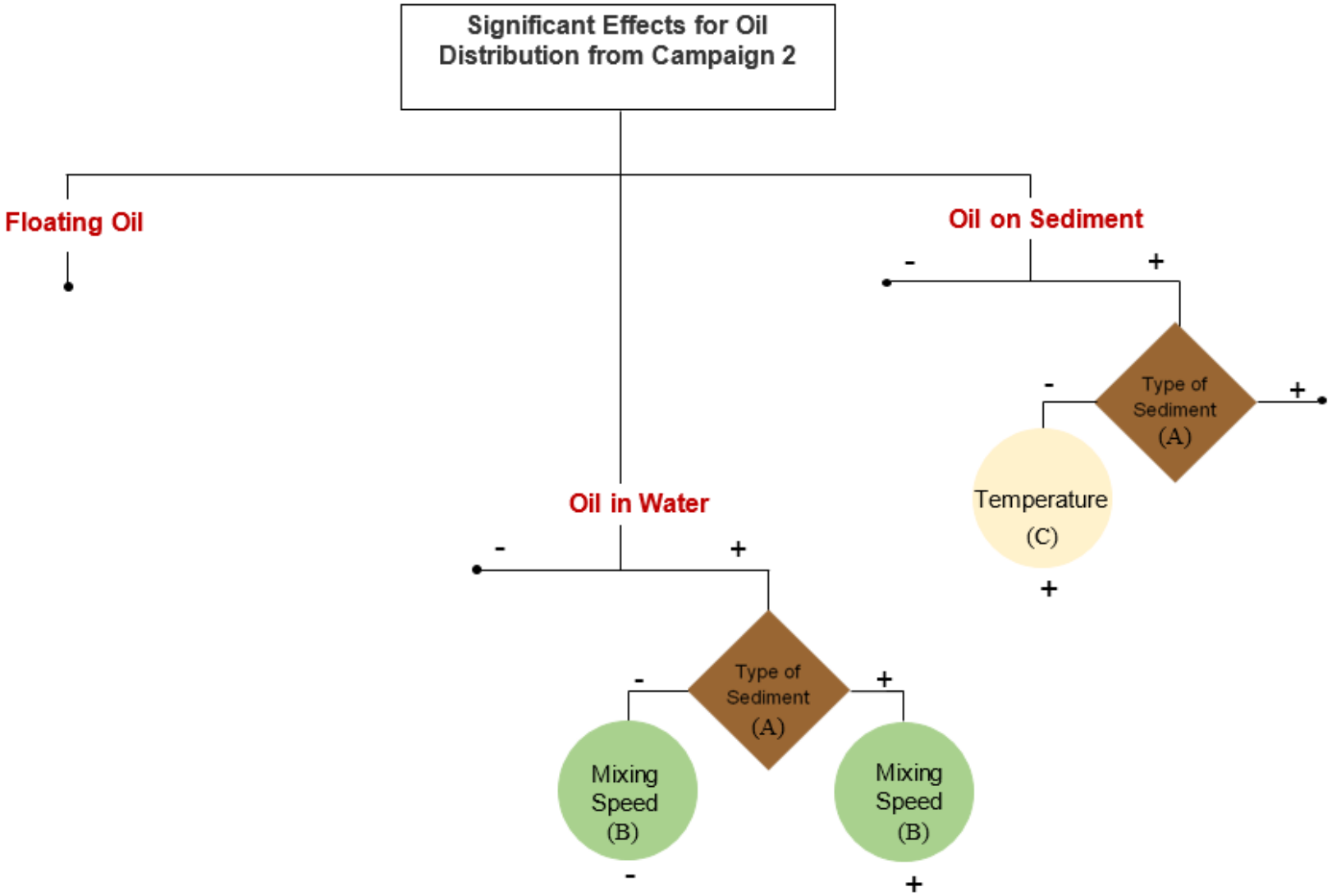

(a) Oil Distribution

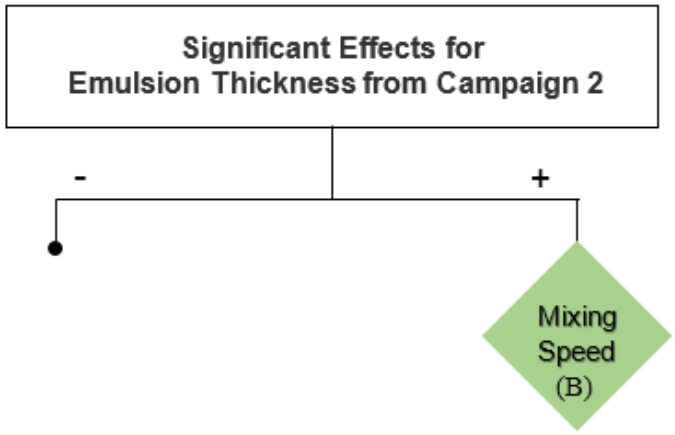

(b) Emulsion Thickness

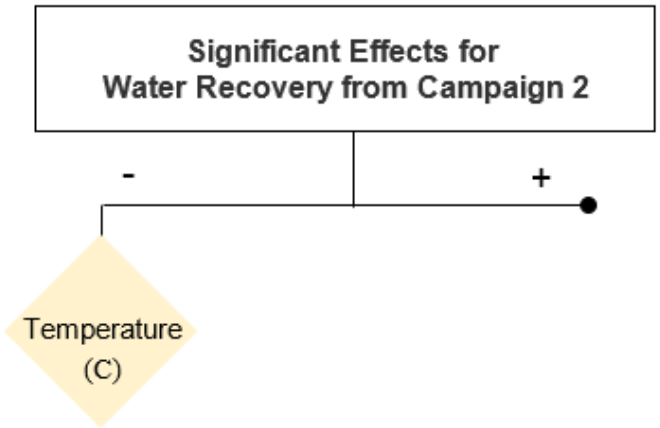

(c) Water Recovery

Figure 1-25: Summary of significant effects from Campaign 2 (a) Oil distribution, (b) Emulsion thickness and (c) Water recovery

1.7 Campaign 3: Mixing in the absence of sediment

A third Campaign was designed with no sediment to isolate its effect on the oil distribution and emulsion formation (eliminating sediment and mixing at the highest speed, Table 1-10). The third Campaign was a 2^3 design, with seven interactions. The temperature (C), oil type (D) and water type (E) were tested at two-levels.

The contrast coefficients and design matrix for Campaign 3 are shown in Table 1-11 and Table 1-12, respectively.

Table 1-10: Variable Levels for Campaign 3

Effect	Variable	- level	+ level
A	Sediment	(No sediment)	
B	Mixing Speed	*	55.4 RPM
C	Temperature	Ambient (20.3°C±2°C)	30°C±0.1°C
D	Oil	DB1	CC
E	Water	FW	SW

*: not tested at the low level

Table 1-11: Contrast Coefficients for Campaign 3

C	D	CD	E	CE	DE	CDE
-1	-1	1	-1	1	1	-1
1	-1	-1	-1	-1	1	1
-1	1	-1	-1	1	-1	1
1	1	1	-1	-1	-1	-1
-1	-1	1	1	-1	-1	1
1	-1	-1	1	1	-1	-1
-1	1	-1	1	-1	1	-1
1	1	1	1	1	1	1

Table 1-12: Design Matrix for Campaign 3

Campaign 3	Factor						
Run Number	A Sediment	B Speed	C Temperature	D Oil	E Water	ABCDE	Run label
41	(no sediment added for these runs)	+	-	-	-	-	b
42		+	+	-	-	+	bce
43		+	-	+	-	+	bd
44		+	+	+	-	-	bcd
45		+	-	-	+	+	be
46		+	+	-	+	-	bce
47		+	-	+	+	-	bde
48		+	+	+	+	+	bcde

1.7.1 Normal probability plots for Campaign 3

Floating Oil Recovery. The normal probability plot for the floating oil show no significant effects as shown in Figure 1-26 since the points are almost equally deviated from the straight line.

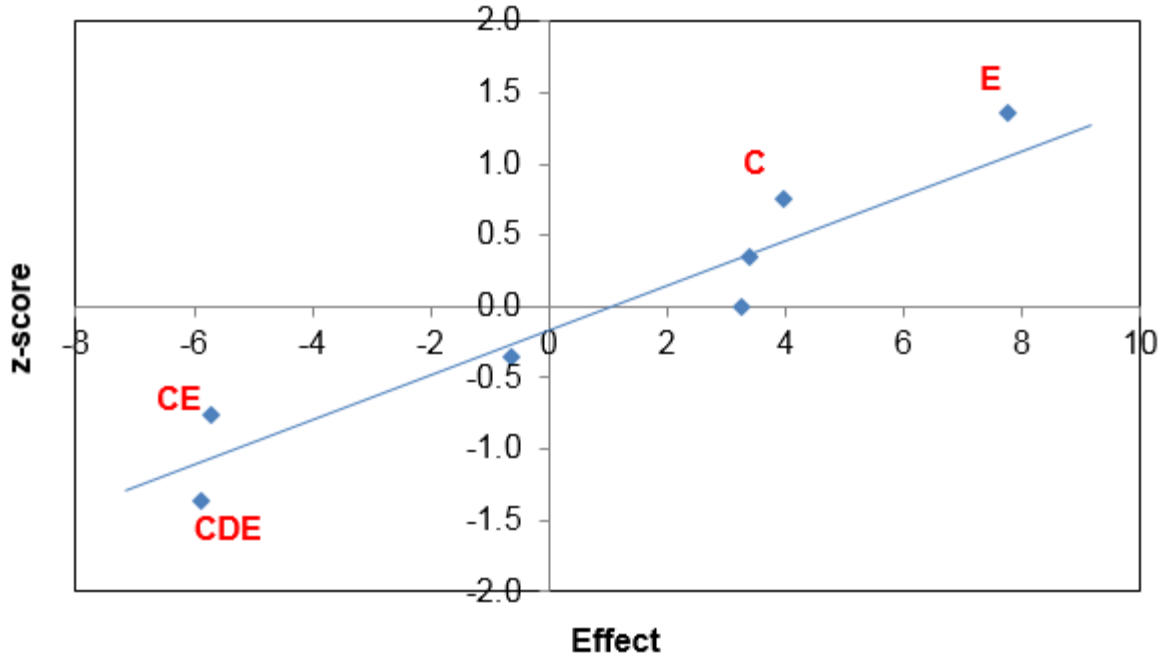

Figure 1-26: Normal probability plot of effects for recovery of floating oil from Campaign 3

Oil in Water. The water type (fresh water) has the greatest impact on increasing the amount of oil extracted from the water phase as shown in Figure 1-27.

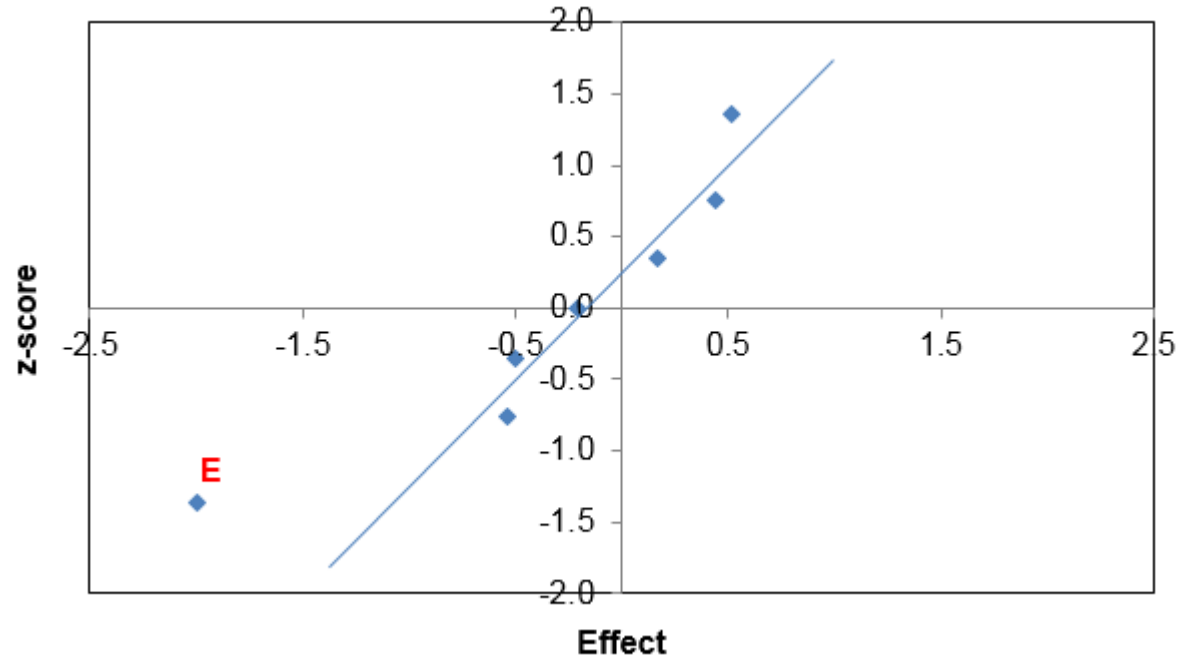

Figure 1-27: Normal probability plot of effects of oil in water (g oil/kg water) for Campaign 3

Emulsion Thickness. No main effects of the variables were identified as significant on the emulsion thickness formed after mixing in Campaign 3 (Figure 1-28).

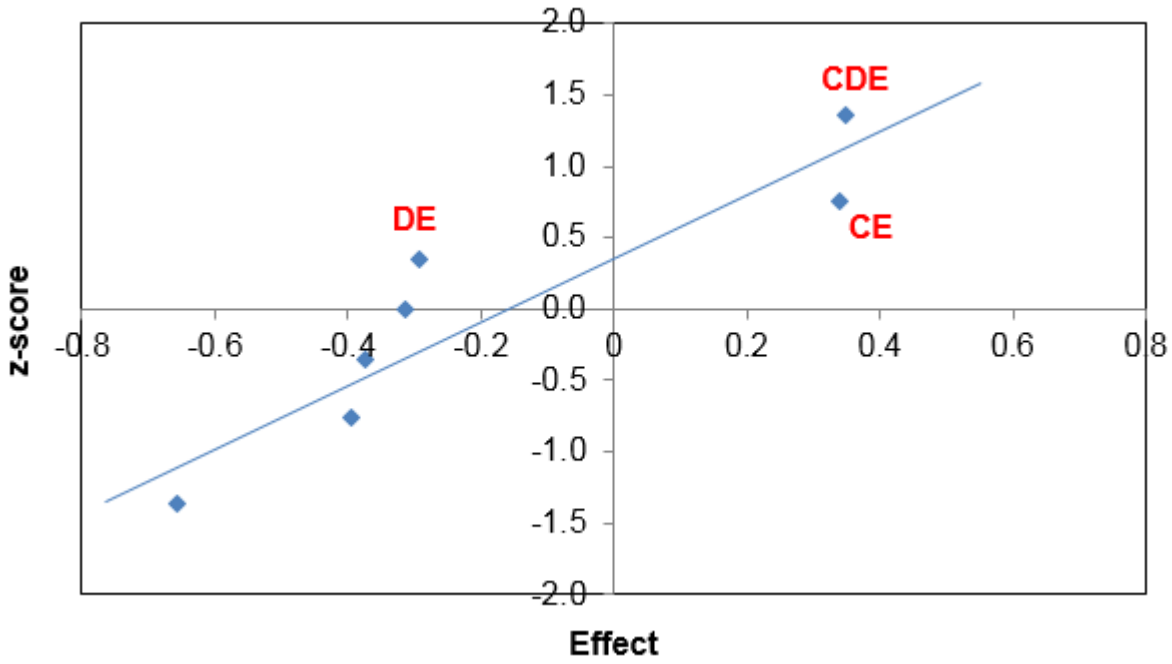

Figure 1-28: Normal probability plot of effects for average emulsion thickness for Campaign 3

Water Recovery. As shown in Figure 1-29, no key effects were identified on the water recovery in the absence of sediment.

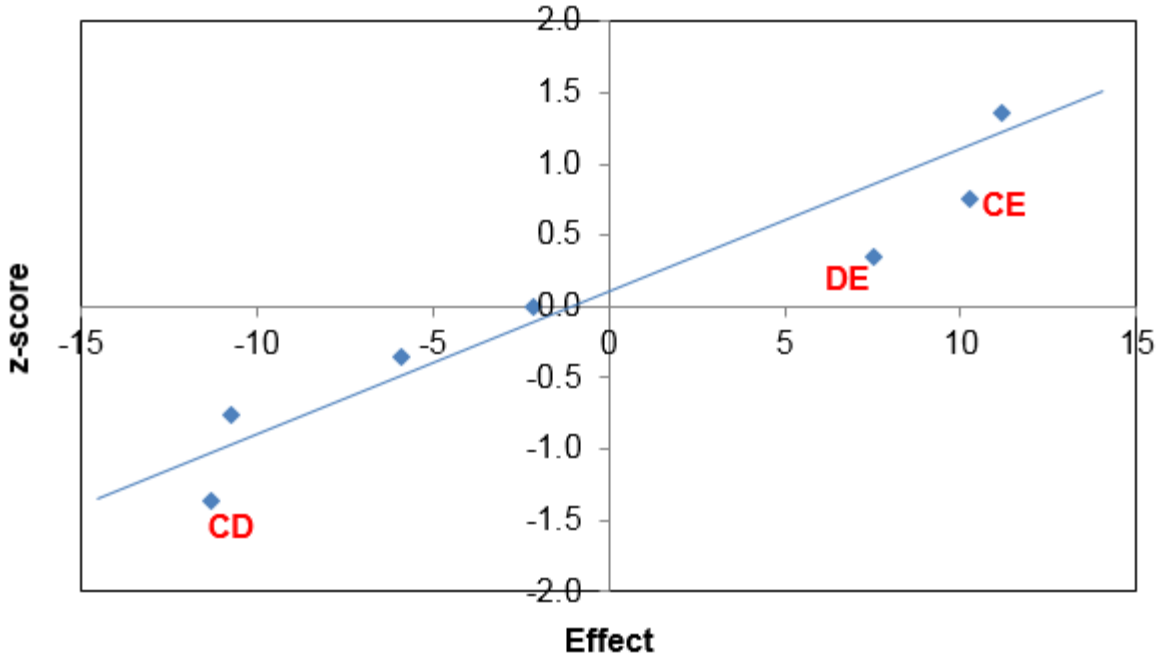

Figure 1-29: Normal probability plot of effects on water recovery for Campaign 3

1.7.2 Significant effects when mixing in the absence of sediment

In the absence of sediment and mixing at the highest speed, the water type (fresh water) was identified as the single significant effect which only impacts the amount of oil dispersed into the water. As expected, oil particles disperse more freely in fresh water than salt water.

A summary of the significant effects for oil distribution, emulsion thickness and water recovery are shown in Figure 1-30a, b and c, respectively.

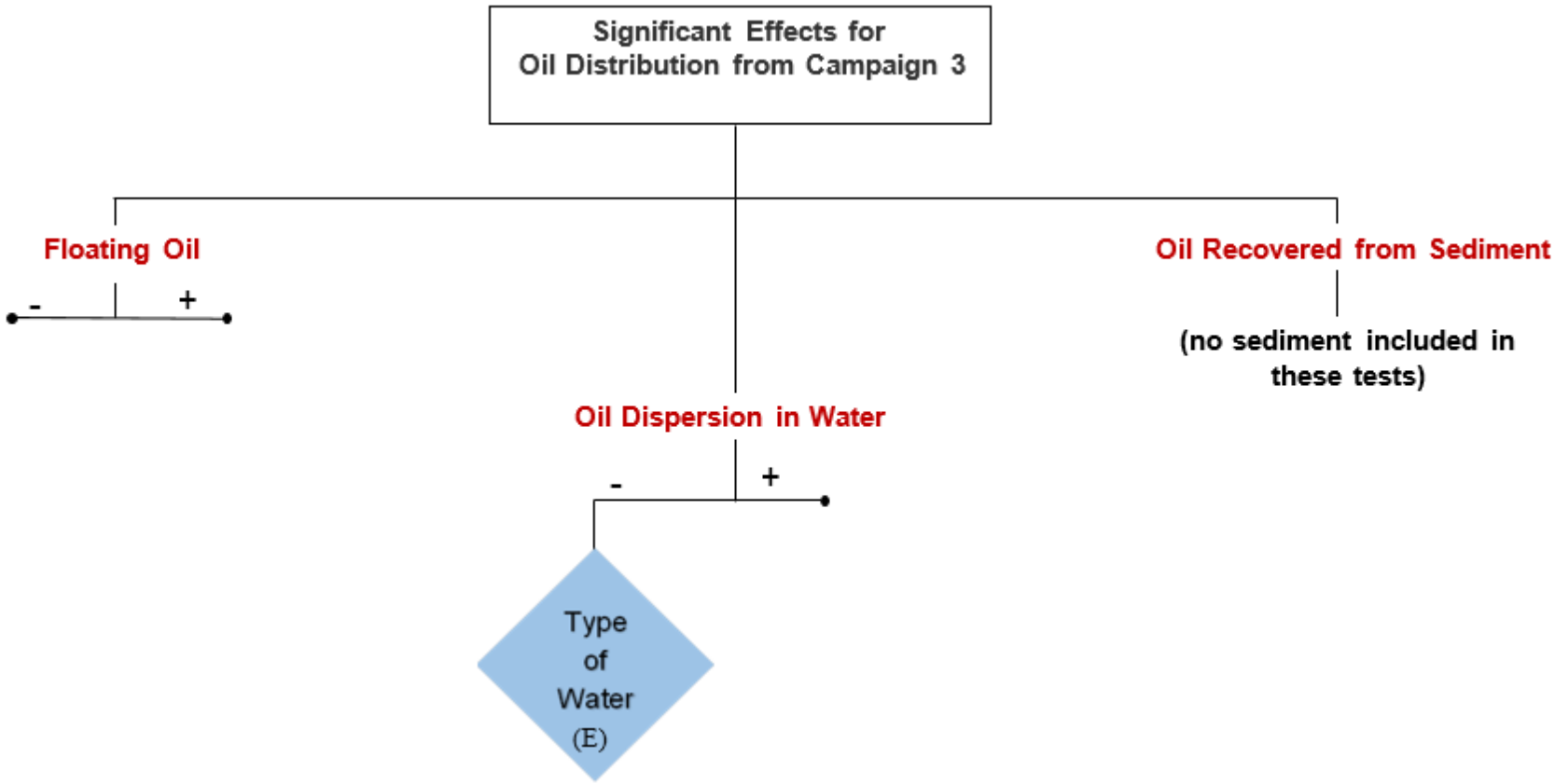

(a) Oil Distribution

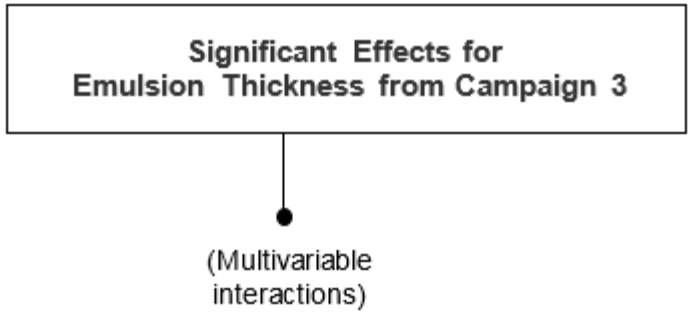

(b) Emulsion Thickness

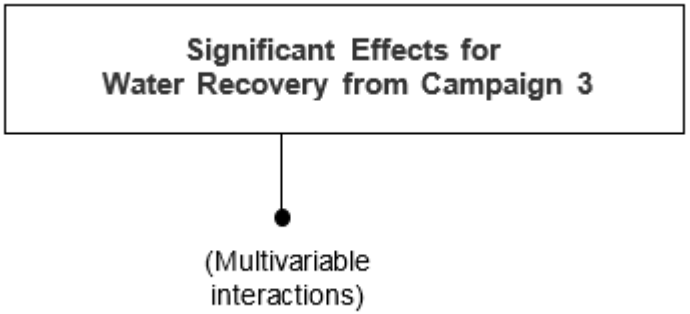

(c) Water Recovery

Figure 1-30: Summary of significant effects from Campaign 3 (a) Oil distribution, (b) Emulsion thickness and (c) Water recovery

1.8 Conclusions

The idea of deepening Canada's ties with growing economies in Asia leads towards the need to better understand the fate and behaviour of oil when spilled in fresh and marine environments. The interactions that occur between oil, water and sediment after an oil spill are complex. There is a strong dependence on the composition of the oil, nature of the sediment particles, ionic strength of the aqueous phase, along with mixing intensity and temperature.

This study was conducted to identify the main significant effects that occur when mixing oil, water and sediment under the chosen mixing conditions. From the initial variable screening tests, it was concluded that the mixing was complex. To simplify the mixing, the effects of the variables were reduced in subsequent campaigns. It was found that in the absence of sediment (Campaign 3), the type of water (fresh water) was the main effect that only impacted the amount of oil dispersed into the water. CC dispersed more in fresh water than DB1. When studying the impact of mixing speed with DB1 in salt water (Campaign 2), the type of sediment (sand) had the greatest effect on the interaction with water and sediment. These two campaigns highlighted the significance of water type and sediment type in mixing. Similar results were also seen in the overall screening of the results (Campaign 1) where salt water proved to have the greatest effect on increasing oil recovery, while in fresh water more DB1 dispersed into the water at the highest mixing speed. Furthermore, thicker emulsion layers formed with DB1 in fresh water with sand. Both types of sediment interacted more with CC.

1.9 Acknowledgments

The authors would like to thank NRCan Program of Energy Research and Development (PERD) and the Interdepartmental Tanker Safety Program for funding this study, and the CanmetENERGY Environmental Impacts Team for the water analyses and the Analytical Team for the hydrocarbon analyses. We would also like to acknowledge the Canadian Association of Petroleum Producers (CAPP) for providing the two oils for this study.

1.10 Nomenclature

A	sediment (input variable)
B	mixing speed (input variable)
b.p.	boiling point
C	temperature (input variable)
CC	conventional crude
D	oil (input variable)
$D_{J,i}$	inside diameter of jar
$D_{J,o}$	outside diameter of jar
D_m	diameter of jar mounting space
D_S	distance between mounting space
DB1	diluted bitumen
E	water (input variable)
FW	fresh water
H_J	height of jar
H_L	height of liquid

H_R	rotation height
N	radius of rotation
OMA	oil mineral aggregates
OSA	oil solid aggregates
SW	salt water

Equations:

A	represents first main effect, A
C	contrast coefficient
f_i	cumulative frequency at position *i* of the data value in the ordered list
k	number of variables
n	number of runs or responses
y	output result

1.11 References

Abdel-Rauf, M. E. (2012). Emulsions- composition stability and characterization Chapter 10. http://www.intechopen.com/books/crude-oil-emulsions-composition-stability-and-characterization/factors-affecting-the-stability-of-crude-oil-emulsions

Andale Publishing. (2013). Normal probability plots.

Boglaienko, D., & Tansel, B. (2015). Instantaneous stabilization of floating oils by surface application of natural granular materials (beach sand and limestone). Marine Pollution Bulletin, 91(1), 107-112.

Boglaienko, D., & Tansel, B. (2016). Partitioning of fresh crude oil between floating, dispersed and sediment phases: Effect of exposure order to dispersant and granular materials. Journal of Environmental Management, 175, 40-45.

Boglaienko, D., & Tansel, B. (2017). Submergence patterns of floating crude oil by granular particles. Chemical Engineering Journal, 314, 548-553.

Bradley, R. W., Venditti, J. G., Kostaschuk, R. A., Church, M., Hendershot, M., & Allison, M. A. (2013). Flow and sediment suspension events over low-angle dunes: Fraser estuary, Canada. Journal of Geophysical Research: Earth Surface, 118(3), 1693-1709.

Bridie, A. L., Wanders, T. H., Zegveld, W., & Van der Heijde, H B. (1980). Formation, prevention and breaking of sea water in crude oil emulsions 'chocolate mousses'. Marine Pollution Bulletin, 11(12), 343-348.

Butt, H., Graf, K., & Kappl, M. (2006). Physics and chemistry of interfaces John Wiley & Sons.

Calvert, R. (1930). Diatomaceous earth. J.Chem.Educ, 7(12), 2829.

Crude Quality Inc. (2017). Crude monitor. http://www.crudemonitor.ca/home.php

Dapkunas, S. J., Jillavenkatesa, A., & Lum, L. H. (2001). Particle size characterization.

Fingas, M. (1995). Water-in-oil emulsion formation - a review of physics and mathematical-modeling. Spill Science & Technology Bulletin, 2(1), 55-59.

Fingas, M. (2015). Diluted bitumen (dilbit): A future high risk spilled material. Proceedings of Interspill. Edmonton, Alberta, Canada. Spill Science, 24

Fingas, M. (2014). Oil physical properties. Handbook of oil spill science and technology (Chapter 20) John Wiley & Sons, Inc.

Fingas, M., & Fieldhouse, B. (2003). Studies of the formation process of water-in-oil emulsions. 47(9-12), 369-396. http://dx.doi.org/10.1016/S0025-326X(03)00212-1

Fingas, M., & Fieldhouse, B. (2005). How to model water-in-oil emulsions. Paper presented at the 2005 International Oil Spill Conference, IOSC 2005, May 15, 2005 - May 19, 11354-11361.

Fingas, M., & Fieldhouse, B. (2008). Water-in-oil emulsions: Studies on water resolution and rheology over time. Paper presented at the 31st AMOP Technical Seminar on Environmental Contamination and Response, June 3, 2008 - June 5, , 1 1-34.

Fingas, M., & Fieldhouse, B. (2012). Studies on water-in-oil products from crude oils and petroleum products. Marine Pollution Bulletin, 64(2), 272-283. http://dx.doi.org/10.1016/j.marpolbul.2011.11.019

Fingas, M., Fieldhouse, B., & Mullin, J. (2005). Water-in-oil emulsions: How they are formed and broken. Paper presented at the 2005 International Oil Spill Conference, IOSC 2005, May 15, 2005 - May 19, 9058-9060.

Fingas, M. F., Fieldhouse, B., Lane, J., & Mullin, J. V. (2005). What causes the formation of water-in-oil emulsions? Paper presented at the 2005 International Oil Spill Conference, IOSC 2005, May 15, 2005 - May 19, 9120-9125.

Gong, Y., Zhao, X., Cai, Z., O'Reilly, S. E., Hao, X., & Zhao, D. (2014). A review of oil, dispersed oil and sediment interactions in the aquatic environment: Influence on the fate, transport and remediation of oil spills. Marine Pollution Bulletin, 79(1-2), 16-33. 10.1016/j.marpolbul.2013.12.024

Government of Canada. (2013a). Federal government technical report: Properties, composition and marine spill behaviour, fate and transport of two diluted bitumen products from the Canadian oil sands. http://www.ec.gc.ca/Publications/default.asp?lang=En&xml=D6AB8B67-73F5-48B6-B3D1-AAE1B06FF9A2

Government of Canada. (2013b). Properties, composition and marine spill behaviour, fate and transport of two diluted bitumen products from the Canadian oil sands. (Canadian Federal Government Technical Report No. Cat. No.: En84-96/2013E-PDF). ISBN 978-1-100-23004-7

Gros, J., Nabi, D., Würz, B., Wick, L. Y., Brussaard, C. P., Huisman, J., Arey, J. S. (2014). First day of an oil spill on the open sea: Early mass transfers of hydrocarbons to air and water. Environmental Science & Technology, 48(16), 9400-9411.

Halboose, A. T. (2010). Effect of pH and salinity on stability of crude oil water emulsions. Misan Journal for Academic Studies, 9(17)

Huang, C. P., & Elliott, H. A. (1977). The stability of emulsified crude oils as affected by suspended particles. Fate and Effects of Petroleum Hydrocarbons in Marine Organisms and Ecosystems. D.A.Wolfe, Ed., Pergammon Press, 413-420.

Huang, L., Fang, H., & Chen, M. (2012). Experiment on surface charge distribution of fine sediment. Science China Technological Sciences, 55(4), 1146-1152.

Hutchinson Environmental Sciences Ltd. (2014). North Saskatchewan River: Water quality and related studies (2007-2012) final report.

International Maritime Organization. (2005). Spills of heavy fuel oils - features and countermeasures. Manual on oil pollution: Combating oil spills (pp. 195). UK: Polestar Wheatons, Exeter.

International Towing Tank Conference. (2011). Fresh water and seawater properties. (No. 7.5-02-01-03).

Israelachvili, J. N. (2011). Intermolecular and surface forces Academic press.

Jenkins, R. H., Grigson, S. J. W., & McDougall, J. (1991). Formation of emulsions at marine oil spills and the implications for response strategies. Paper presented at the Proceedings of the First International Conference on Health, Safety and Environment in Oil and Gas Exploration and Production Part 2 (of 2), November 11, 1991 - November 14, 437-443.

Kaku, V. J., Boufadel, M. C., Venosa, A. D., & Weaver, J. (2006). Flow dynamics in eccentrically rotating flasks used for dispersant effectiveness testing. Environmental Fluid Mechanics, 6(4), 385-406. 10.1007/s10652-006-0003-3

Kanicky, J. R., Lopez-Montilla, J., Pandey, S., & Shah, D. (2001). Surface chemistry in the petroleum industry. Handbook of applied surface and colloid chemistry (pp. 251-267) John Wiley and Sons Ltd New York.

Kester, D. R., & Pytkowicx, R. M. (1967). Determination of the apparent dissociation constants of phosphoric acid in seawater. Limnology and Oceanography, 12(2), 243-252.

Khelifa, A., Stoffyn-Egli, P., Hill, P. S., & Lee, K. (2002). Characteristics of oil droplets stabilized by mineral particles: Effects of oil type and temperature. Spill Science and Technology Bulletin, 8(1), 19-30. http://www.sciencedirect.com/science/article/pii/S1353256102001172

Khelifa, A., Stoffyn-Egli, P., Hill, P. S., & Lee, K. (2005). Effects of salinity and clay type on oil–mineral aggregation. Marine Environmental Research, 59(3), 235-254. http://www.sciencedirect.com/science/article/pii/S0141113604001680

King, T. L., Robinson, B., Boufadel, M., & Lee, K. (2014). Flume tank studies to elucidate the fate and behavior of diluted bitumen spilled at sea. Marine Pollution Bulletin, 83(1), 32-37.

Kingston, P. F. (2002). Long-term environmental impact of oil spills. Spill Science & Technology Bulletin, 7(1-2), 53-61. 10.1016/S1353-2561(02)00051-8

LaFargue, E., & Barker, C. (1988). Effect of water washing on crude oil compositions. AAPG Bulletin, 72(3), 263-276.

Le Floch, S., Guyomarch, J., Merlin, F. X., Stoffyn-Egli, P., Dixon, J., & Lee, K. (2002). The influence of salinity on oil-mineral aggregate formation. Spill Science & Technology Bulletin, 8(1), 65-71. 10.1016/S1353-2561(02)00124-X

Lee, R. F., & Page, D. S. (1997). Petroleum hydrocarbons and their effects in subtidal regions after major oil spills. Marine Pollution Bulletin, 34(11), 928-940. 10.1016/S0025-326X(97)00078-7

Lima, E. R., De Melo, B. M., Baptista, L. T., & Paredes, M. (2013). Specific ion effects on the interfacial tension of water/hydrocarbon systems. Brazilian Journal of Chemical Engineering, 30(1), 55-62.

Memarian, R., & Dettman, H. D. Energy scaling for understanding the effect of sand particles on aggregate size of crude oils (unpublished)

Montgomery, D. C. (2013). Design and analysis of experiments (Eighth ed.). Hoboken, NJ: John Wiley & Sons, Inc. http://catdir.loc.gov/catdir/enhancements/fy1206/2012000877-t.html

Montgomery, D. C., & Runger, G. C. (2010). Applied statistics and probability for engineers John Wiley & Sons.

Muschenheim, D. K., & Lee, K. (2002). Removal of oil from the sea surface through particulate interactions: Review and prospectus. Spill Science & Technology Bulletin, 8(1), 9-18.

National Oceanic and Atmospheric Administration. (2015). Why is the ocean salty? Salinity data. http://oceanservice.noaa.gov/facts/whysalty.html

National Research Council. (2003). Oil in the sea III: Inputs, fates, and effects National Academies Press.

Nordvik, A. B., Simmons, J. L., Bitting, K. R., Lewis, A., & Strm-Kristiansen, T. (1996). Oil and water separation in marine oil spill clean-up operations. Spill Science & Technology Bulletin, 3(3), 107-122.

Omotoso, O. E., Munoz, V. A., & Mikula, R. J. (2002). Mechanisms of crude oil-mineral interactions. Spill Science & Technology Bulletin, 8(1), 45-54. 10.1016/S1353-2561(02)00116-0

Özen, İ, Şimşek, S., & Okyay, G. (2015). Manipulating surface wettability and oil absorbency of diatomite depending on processing and ambient conditions. Applied Surface Science, 332, 22-31.

Poindexter, M. K., Chuai, S., Marble, R. A., & Marsh, S. C. (2005). Solid content dominates emulsion stability predictions. Energy & Fuels, 19(4), 1346-1352.

Sjoblom, J., Aske, N., Auflem, I. H., Brandal, O., Havre, T. E., Sther, O., Kallevik, H. (2003). Our current understanding of water-in-crude oil emulsions. Recent characterization techniques and high pressure performance. Advances in Colloid and Interface Science, 100-102, 399-473. http://dx.doi.org/10.1016/S0001-8686(02)00066-0

Stewart, P. L. (2010). Oceanographic measurements - salinity, temperature, suspended sediment, turbidity, minas passage study Site.

Stoffyn-Egli, P., & Lee, K. (2002). Formation and characterization of oil–mineral aggregates. Spill Science & Technology Bulletin, 8(1), 31-44.

Teal, J. M., Farrington, J. W., Burns, K. A., Stegeman, J. J., Tripp, B. W., Woodin, B., & Phinney, C. (1992). The west Falmouth oil spill after 20 years: Fate of fuel oil compounds and effects on animals. Marine Pollution Bulletin, 24(12), 607-614.

Trefalt, G., & Borkovec, M. (2014). Overview of DLVO theory www.colloid.ch/dlvo

Tsai, W., Lai, C., & Hsien, K. (2006). Characterization and adsorption properties of diatomaceous earth modified by hydrofluoric acid etching. Journal of Colloid and Interface Science, 297(2), 749-754.

Venosa, A. D., & Holder, E. (2011). Laboratory-scale testing of dispersant effectiveness of 20 oils using the baffled flask test. US Environmental Protection Agency, 600-699.

Wei, Q., Mather, R. R., Fotheringham, A. F., & Yang, R. D. (2003). Characterization of water-in-crude oil emulsions in oil spill response. Journal of Environmental Sciences, 15(4), 506-509.

Chapter 2: Chemical Characterization of Oil after Mixing in Fresh and Salt Water

2.1 Abstract

The unique physical and chemical nature of a crude oil directly impacts its fate and behaviour when spilled in fresh and salt water environments. The composition of the oil will determine the extent of mixing, spreading, dispersion and evaporation after an oil spill. An experimental campaign was conducted in an initial study to identify the significant variables in oil and water mixing for diluted bitumen and conventional crude oil (Section 1.5). Mixing behaviours in salt and fresh water were different, resulting in interesting patterns for oil loss and sediment interactions for both oils. From the first study of the two oils, the significant physical effects were that salt water had the greatest impact on floating oil recovery, there is greater oil dispersion in fresh water than salt water, conventional crude oil interacted more with sediment than diluted bitumen, and a thicker emulsion layer was formed when mixing with diluted bitumen (Section 1.5) .

In this study, the chemical characteristics of the oil were determined for each fraction and for different conditions. After each mixing test three fractions were collected; the floating oil, the water fraction and the sediment. The floating oil was distilled to remove water and the boiling point (bp) >204°C fraction was separated into maltenes and asphaltenes fractions. The maltenes and asphaltenes fractions were then analyzed using high temperature simulated distillation (SimDis), and elemental (carbon, hydrogen, nitrogen, sulfur, oxygen) analyses. For the water and sediment phases, oil was isolated first by carbon disulfide, then methylene chloride extraction and analyzed using high temperature simulated distillation.

The purpose of this work was to identify the chemical reasons underlying the significant physical differences in separation of the oil between the floating oil, oil in water and the oil attached to sediment – and the associated emulsion formation - identified in the mixing study.

2.2 Introduction

The demand for oil and its derivatives is only increasing with the increasing global population as a source of energy and as feedstock for the manufacturing of goods. Due to the limited geographic locations of oil sources, it must be transported from the point of extraction for use to other countries. Canada recognizes the benefits and opportunities new markets for oil will bring to the Canadian economy; however, there is much concern over the risk of transporting oil through coastal waters. In recent years, there have been several high-profile oil spills in water environments that have captured public interest (i.e. Gulf of Mexico April 2010, Kalamazoo River July 2010). Oil spills occur as accidental leaks from drilling rigs, pipelines, tankers, and barges (National Research Council, 2003). Release of oil and chemicals into fresh and salt waters leads to environmental and economic damage that can last for decades.

Conventional and non-conventional oil is made up of a wide range of hydrocarbons, from very volatile compounds such as butane and benzene to more complex heavy compounds such as asphaltenes, resins and waxes. The main physical properties that affect the behaviour of oil spilled in fresh or sea water are density and viscosity. The density will determine whether the oil can sink or float, while the viscosity, along with the interfacial tension, influence the oil's resistance to flow or spread over and into the water. More viscous oils will not spread on nor mix into the water and will not penetrate soils rapidly. The chemical characteristics of interest in this work are the relative amounts of volatile components and asphaltenes, both of which influence oil-water mixing. Oils which form stable water-in-oil emulsions will persist on the water surface, while oil-in-water emulsions are found below the surface of the water (Wang et al., 2003). Several studies have been carried out investigating the influence of asphaltenes on the stability of an emulsion (Czarnecki et al., 2012; M. Fingas & Fieldhouse, 2004; M. Fingas & Fieldhouse, 2005; M. Fingas & Fieldhouse, 2009; M. Fingas & Fieldhouse, 2012; McLean & Kilpatrick, 1997; Sjoblom et al., 2003; Tchoukov et al., 2014). The asphaltenes content in diluted bitumen (approximately 13% for Cold Lake Bitumen) is

greater than conventional crude oils (approximately 2% for a Mixed Sweet Conventional Crude) (McLean & Kilpatrick, 1997). Asphaltenes contain compounds that can be found at the oil-water interface and which tend to act as a mechanical barrier. According to McLean and Kilpatrick, if the asphaltenes are molecularly dissolved, they will not contribute to emulsion formation; however, if they are colloidally dispersed they will form a stable emulsion. According to their studies, resins aid in solubilizing the colloidally dispersed asphaltenes to form aggregates. They then adsorb on to the oil-water interface and decrease the interfacial tension (Abdel-Rauf, 2012). Fingas and Fieldhouse (2004, 2005 and 2009) found emulsions formed have viscoelastic behaviour. Studies have shown that water-in-oil emulsions are stabilized when resin content in the oil is slightly greater than the asphaltenes content, however, an excess of resins (asphaltene/resin ratio >0.6) may lead to instability of the emulsion (M. Fingas & Fieldhouse, 2009). A study carried out by Czarnecki et al. (2012) examined the contribution of asphaltenes to emulsion formation by testing properties of a thin oil film separating two water droplets using the microinterferometric thin liquid film technique. It was found that only small amounts of surface active agents are present in the asphaltenes fraction.

When two immiscible liquids are in contact with each other, as in oil and water, an interfacial area is formed. The fate of oil in water depends on the forces acting between the oil and water molecules. The interaction energy between atoms and molecules can be described by the van der Waals attraction forces and electrostatic repulsive forces (Trefalt & Borkovec, 2014). At close distances between emulsion droplets, there is a strong van der Waals attraction which increases with decreasing separation distance (attraction forces varies inversely to separation distance) (Tadros, 2013). Droplets of oil and sediment particles are negatively charged causing electrostatic repulsion between the oil and sediment in fresh water. According to the theory of colloidal stability (DLVO theory), an increase in water salinity reduces the surface charge density of the ions which in turn weakens the electrostatic repulsion and allows the oil and sediment to aggregate (Trefalt & Borkovec, 2014). According to the study by Gundlach and Hayes, sedimented

oil can sink 15-25 cm into steeper, medium to coarse grain sand beaches (0.25-2.0 mm size) under high energy environments such as the Atlantic and Pacific coasts (Gundlach & Hayes, 1978). Studies conducted in the Prudhoe Bay in Alaska found dissolved hydrocarbons adsorbed onto mineral fines sinking to the bottom of the water column, while some oil droplets interacted with the suspended particulates in the water to form stable emulsions (Bragg & Owens, 1994). Sediment particulate concentrations greater than 100 mg/L are required for oil-particulate suspensions to occur (R. F. Lee & Page, 1997). Water energy (in the form of waves or current) aid in increasing oil surface area by breaking oil particulates into micron sized particles. The oil particles disperse easier in the water column allowing solid particulates to adsorb to the surface (K. Lee, 2002; R. F. Lee & Page, 1997). Tests have been conducted to identify the formation of flocs (masses of fine oil-mineral particles) when oil is spilled in water and found mineral particles attach to the oil droplets due to hydrophobic bonding (Omotoso et al., 2002). As long as the size of the OMA (oil-mineral aggregate) exceeds the electrical double-layer surrounding the particle, the particle acts as a surfactant preventing the oil droplets from recoalescing (Stoffyn-Egli & Lee, 2002). The wettability, or contact angle, of a solid particle determines the stability of the emulsion. When the three-phase contact angle is slightly less than 90 degrees it will ensure the solid particles are held at the oil-water interface and stabilize oil-water emulsions (when contact angle is greater than 90 degrees, water-oil emulsions will be stabilized) (Tambe & Sharma, 1994).

Tests were conducted to identify the key interactions when conventional crude (CC) and diluted bitumen (DB1) are mixed with water and sediment (Section 1.5). Mixing tests were carried out in 2.2L borosilicate glass jars using an end-over-end rotary agitator. The oil distribution after mixing from Campaign 1 of the study outlined in Section 1.5 was quantified by isolating the oil, water and sediment fractions and conducting oil mass balances.

From the initial screening of the design factors (Campaign 1, Section 1.5), it was found that salt water had the greatest impact on floating oil recovery. In terms of oil

dispersion into the water column, DB1 dispersed more in fresh water than CC at the highest mixing speed and warmer mixing temperature. It was also found that CC interacted more with sediment than DB1. A thicker emulsion layer was formed when mixing with DB1.

The purpose of this study is to identify mechanisms for the significant effects identified in Campaign 1 (Section 1.5) by conducting detailed hydrocarbon analyses of the floating oil, and the oil samples isolated from the water and sediment.

2.3 Methods

2.3.1 Materials

The diluted bitumen and conventional crude oils chosen for this study were selected because of their extensive transportation via pipelines, railways, and over water and, because of their relative differences in chemical and physical properties (Table 2-3). These oils were collected from Alberta pipelines courtesy of the Canadian Association of Petroleum Producers (CAPP). The sand and diatomaceous earth were purchased from Sigma-Aldrich Canada Co. for the tests and were used as received (more details on sediment properties are available in Section 1.3.3). The solvents, carbon disulfide and methylene chloride, used to extract the oil from the water and sediment were also purchased from Sigma Aldrich Canada Co.

2.3.2 Analytical Methods

Density – ASTM 4052. The density was measured using a Mettler Toledo Digital Densitometer according to the method recommended by the manufacturer.

Kinematic viscosity – ASTM D445-01. The kinematic viscosity was measured using the Stabinger instrument according to ASTM D445-01 method.

High Temperature Simulated Distillation –ASTM D7169: The boiling range distribution determination by distillation was simulated by the use of the Agilent 6890N gas chromatograph and PAC software for processing the data. Boiling points were assigned to the time axis from a calibration curve obtained under the same chromatographic conditions by analyzing a known mixture of hydrocarbons covering the boiling range expected in the sample. From this data, the boiling range distribution up to 750ºC was measured. The data was processed first by fixing the mass and then by fixing the boiling point. The latter method was used to merge the boiling point distribution data obtained when oil was extracted from the water using the two different solvents based on the yields from both extractions.

Distillation – ASTM D1160: To remove the water from the floating oil, and create the ±204ºC fractions, the sample was distilled at reduced pressures. Each fraction was distilled from the sample, collected, then gravimetrically measured and recorded. Distillation yields by mass were calculated from the mass of each fraction relative to the total mass recovery.

Pentane Insolubles (Separation of Asphaltenes & Maltenes fractions) – Modified ASTM D4055: To isolate the maltenes and asphaltenes fractions, the asphaltenes were removed from the +204ºC fraction of the oil by precipitation with pentane. A weighed amount of sample was dissolved in 40 volumes of pentane and sonicated for 60 minutes. The mixture was then filtered through an 8.0 μm nylon filter membrane under vacuum. The filter and insolubles were washed, dried and weighed to calculate the insolubles (asphaltenes). The filtrate was collected and transferred to a rotary evaporator flask and the pentane is removed by rotary evaporation. The oil obtained was the maltenes fraction.

Carbon, Hydrogen, Nitrogen, Sulfur (CHNS) – ASTM D5291 (CHN) and ASTM D1552 (S): The carbon, hydrogen, nitrogen and sulfur contents were measured using an Elementar Variomicrocube Analyzer.

Oxygen (in house): The oxygen contents of the samples were measured by an Elementar Variomicrocube Analyzer according to the method recommended by the manufacturer. The repeatability of measurements for this instrument is estimated to be ± 0.2wt%.

Surface tension and Interfacial tension: The surface tension was measured using K100 Tensiometer (KRUSS Scientific Instruments Inc.) according to the method suggested by the manufacturer. To determine the interfacial tension between the two oils (CC and DB1) and the two types of water (salt and fresh) a spinning drop tensiometer instrument (SDT), manufactured by KRÜSS, was used according to the method recommended by the manufacturer.

Dean Stark (CanmetENERGY Devon): Another method used to quantitatively determine the water content of an emulsion, was by Dean Stark extraction at CanmetENERGY Devon. The solvent used for extraction was toluene. The oil was extracted from the sample using the modified Soxhlet extractor apparatus by means of heating toluene so that its vapors washed over the sample, separating the oil from the water. The water was collected in the water trap, and the oil was collected in the boiling flask, together with the toluene. The extraction was complete when there was a clear colorless drip of toluene from the bottom of the thimble, and when the glassware was dry, indicating that all of the water from the sample has been collected in the water trap.

Solvent extraction of oil in water (CanmetENERGY Devon): To determine the mass of oil dispersed and dissolved in the water phase after mixing, the oil in the water sample was first extracted using carbon disulfide followed by extraction with dichloromethane. The two solvents were used because of their different solubility in oil. Solvent was added to the separatory funnel containing the oil and water. The solvent-oil layer was separated

from the bulk water layer. The vial containing the solvent, oil and any water that may have been collected during separation was placed in a dry-ice bath to freeze the water. The solvent-oil layer was transferred to a vial using a syringe and then filtered through a 0.45 μm filter to remove any suspended particulates, then collected for analysis. To determine the yield of the oil from the carbon disulfide extraction, a drop of the oil and carbon disulfide was placed on a pre-weighed Whatman glass microfiber filter paper (1.5 μm pore size). The solvent was allowed evaporate and the weight of oil was obtained. Any remaining oil in the bulk water sample was then extracted using dichloromethane. The procedure for dichloromethane extraction was the same as carbon disulfide extraction, except the dichloromethane was evaporated using nitrogen in an evaporation chamber (TurboVap^{R} LV) to isolate the oil sample. The yield of the oil collected in water was calculated as g oil/kg water.

Solvent extraction of oil on sediment (CanmetENERGY Devon): To determine the mass of oil on the sediment, the oil on sediment was extracted with dichloromethane. Dichloromethane was added to the sediment sample vial (which also contained trace water). The solvent-oil layer was transferred to a new vial using a syringe, and then placed in a dry-ice bath to freeze any water that may have entered the syringe. The solvent-oil layer was then filtered through a 0.45 μm filter to remove any suspended particulates. The dichloromethane was evaporated using nitrogen in an evaporation chamber (TurboVap^{R} LV) to isolate the oil sample. The yield of the oil collected from the sediment was calculated as g oil/g sediment.

2.3.3 Experimental design

The objective of this study was to characterize the floating oil, oil in water and oil on sediment fractions after the mixing tests performed in Campaign 1 (Section 1.5). All five variables (sediment, mixing speed, temperature, oil and water) were tested at two levels as shown in Table 2-1. For each run label, the run condition is identified with lower case

letters for the input variables (compared to capital letters for input variable IDs). The presence of a letter indicates that the variable was tested at the high level (+). The absence of a letter in a run label indicates that the variable was tested at the low level (-). The letter 'L' indicates that all variables are resent at the lower level (Table 2-2).

Table 2-1: Variable Levels for Campaign 1

Effect	Variable	- level	+ level
A	Sediment	Diatomaceous earth	Sand
B	Mixing Speed	38.7 RPM	55.4 RPM
C	Temperature	Ambient (20.3°C±2°C)	30°C±0.1°C
D	Oil	DB1	CC
E	Water	Fresh	Salt

Table 2-2: Design Matrix for Campaign 1

Campaign 1	Factor						
	A	B	C	D	E	ABCDE	
Run Number	Sediment	Speed	Temperature	Oil	Water		Run label
1	-	-	-	-	-	-	L
2	+	-	-	-	-	+	a
3	-	+	-	-	-	+	b
4	+	+	-	-	-	-	ab
5	-	-	+	-	-	+	c
6	+	-	+	-	-	-	ac
7	-	+	+	-	-	-	bc
8	+	+	+	-	-	+	abc
9	-	-	-	+	-	+	d
10	+	-	-	+	-	-	ad
11	-	+	-	+	-	-	bd
12	+	+	-	+	-	+	abd
13	-	-	+	+	-	-	cd
14	+	-	+	+	-	+	acd
15	-	+	+	+	-	+	bcd
16	+	+	+	+	-	-	abcd
17	-	-	-	-	+	+	e
18	+	-	-	-	+	-	ae
19	-	+	-	-	+	-	be
20	+	+	-	-	+	+	abe
21	-	-	+	-	+	-	ce
22	+	-	+	-	+	+	ace
23	-	+	+	-	+	+	bce
24	+	+	+	-	+	-	abce
25	-	-	-	+	+	-	de
26	+	-	-	+	+	+	ade
27	-	+	-	+	+	+	bde
28	+	+	-	+	+	-	abde
29	-	-	+	+	+	+	cde
30	+	-	+	+	+	-	acde
31	-	+	+	+	+	-	bcde
32	+	+	+	+	+	+	abcde

A detailed experimental method for the mixing tests is given in Section 1.3.7 and is summarized here. Four replicate 2.8 L clear glass rotary agitator jars (Jar I, II, III, and IV) with 1:20 (v/v) ratio of oil to water with 2000 ppm sediment were prepared for each test. For salt water tests, 33 g/L of sodium chloride (NaCl) crystals were added to the jars before addition of oil or sediment and shaken vigorously to dissolve the NaCl. The jars were agitated for a total of 12 hours, then allowed to settle for one hour. After the settling period, one jar (Jar IV) was set aside to monitor the emulsion thickness and observe changes to the jar contents over a period of seven days. The oil, water and sediment in the remaining three jars (Jars I, II, III) were isolated separately using a separatory funnel. The water and sediment samples were analyzed to determine the oil content in both phases. Shortly after mixing, the floating oil from Jars I, II, III was analyzed using high temperature simulated distillation to determine the boiling point distribution of the oil. After the seven day emulsion test was completed for each test, the oil from Jar IV was added to the floating oil collected from Jars I, II, and III for each test. The total floating oil underwent distillation to determine water content, and produce two boiling point fractions, ±204ºC. The water content provided information on the amount of water trapped in the floating oil after each mixing condition. The fraction boiling >204ºC was further separated into the maltenes and asphaltenes fraction via the addition of pentane to the oil sample. Elemental (carbon, hydrogen, sulfur, nitrogen and oxygen content) and high temperature simulated distillation analysis were obtained for the maltenes and asphaltenes fraction. The oil in the water and sediment was extracted using carbon disulfide and dichloromethane. These oil samples were analyzed by high temperature simulated distillation.

2.4 Results

To identify the chemical reasons for the key physical interactions as identified in Section 1.5, the original oils, conventional crude (CC) and diluted bitumen (DB1), were analyzed. The densities, viscosities, surface tension and interfacial surface tension results

are shown in Table 2-3. The original oils and floating oils were also analyzed by high temperature simulated distillation for their boiling point distributions as shown in Figure 2-1. During an oil spill the light ends with boiling point less than 204ºC (boiling point, b.p.<204ºC) would be lost due to evaporation (Zhou, Dettman, & Bundred, 2015). Consequently, the fraction of oil boiling greater than 204ºC (b.p.>204ºC) was prepared by distillation for the original and floating oils. To determine whether interactions with water and sediment would cause changes to the hydrocarbons in the oils, the original oils and floating oils were separated into two fractions based on polarity; maltenes (pentane soluble) and asphaltenes (pentane insoluble). Their compositions by elemental analysis are given in Table 2-3.

For the figures that follow, the naming convention for each of the data points (runs) include the number sixteen (16) which is used to represent the batch number, followed by the variable letter(s) (a, b, c, d, e) representing the run condition. As explained in Section 1.5, the presence of a letter indicates that the variable was tested at the high level (+). The absence of a letter in a run label indicates that the variable was tested at the low level (-).

Table 2-3: Properties of Conventional Crude (CC) and Diluted Bitumen (DB1)

Crude Oil	CC	DB1
Density (g/ml)		
20ºC	0.8201	0.9237
25ºC	0.8168	0.9203
30ºC	0.8130	0.9166
Viscosity (cSt)		
20ºC	5.1	218.1
25ºC	4.2	161.5
30ºC	3.7	124.1
Surface tension (mN/m)		
20ºC	25.5	28.9
Interfacial tension (mN/m)		
Fresh water (Devon, AB tap water)		
20ºC	12.24	16.58
30ºC	14.16	16.00
Salt water (3.3 wt.% NaCl solution)		
20ºC	7.36	11.74
30ºC	12.33	13.94
+204ºC fraction		
Carbon (wt.%)	86.65	84.26
Hydrogen (wt.%)	13.04	10.24
Nitrogen (wt.%)	0.03	0.46
Sulfur (wt.%)	0.66	4.33
Oxygen (wt.%)	<0.1	0.81
H/C ratio	0.15	0.12
Maltenes content (wt.%)	98.48	81.86
Carbon (wt.%)	85.89	84.12
Hydrogen (wt.%)	13.05	11.14
Nitrogen (wt.%)	0.08	0.28
Sulfur (wt.%)	0.41	3.98
Oxygen (wt.%)	0.59	0.48
H/C ratio	0.15	0.13
Asphaltenes content (wt.%)	1.52	18.13
Carbon (wt.%)	84.88	81.50
Hydrogen (wt.%)	8.09	7.46
Nitrogen (wt.%)	1.08	1.12
Sulfur (wt.%)	4.21	8.68
Oxygen (wt.%)	1.74	1.23
H/C ratio	0.10	0.09

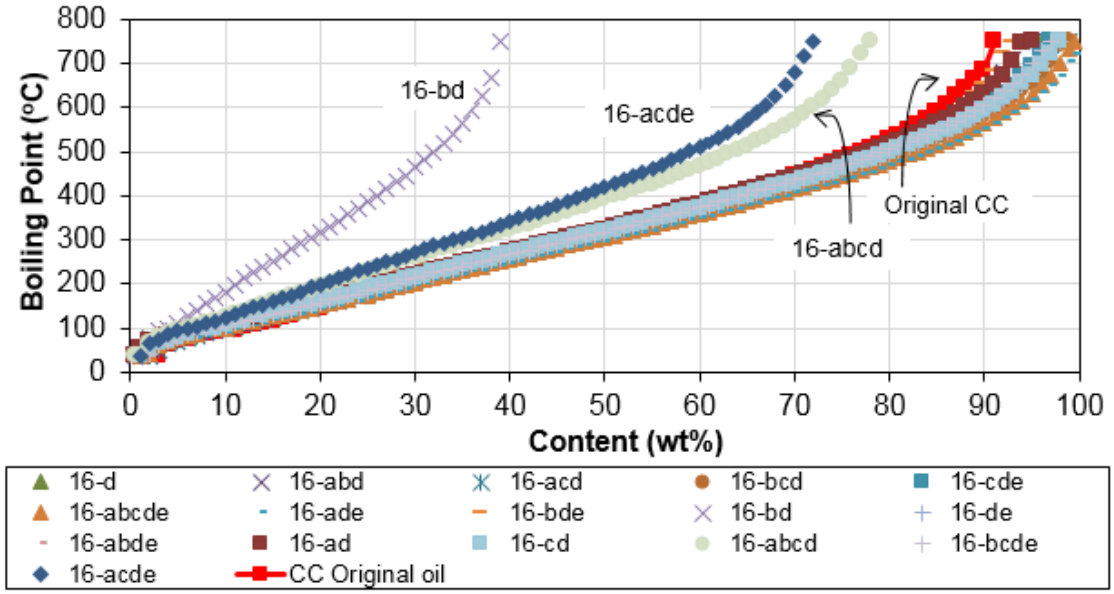

(a)

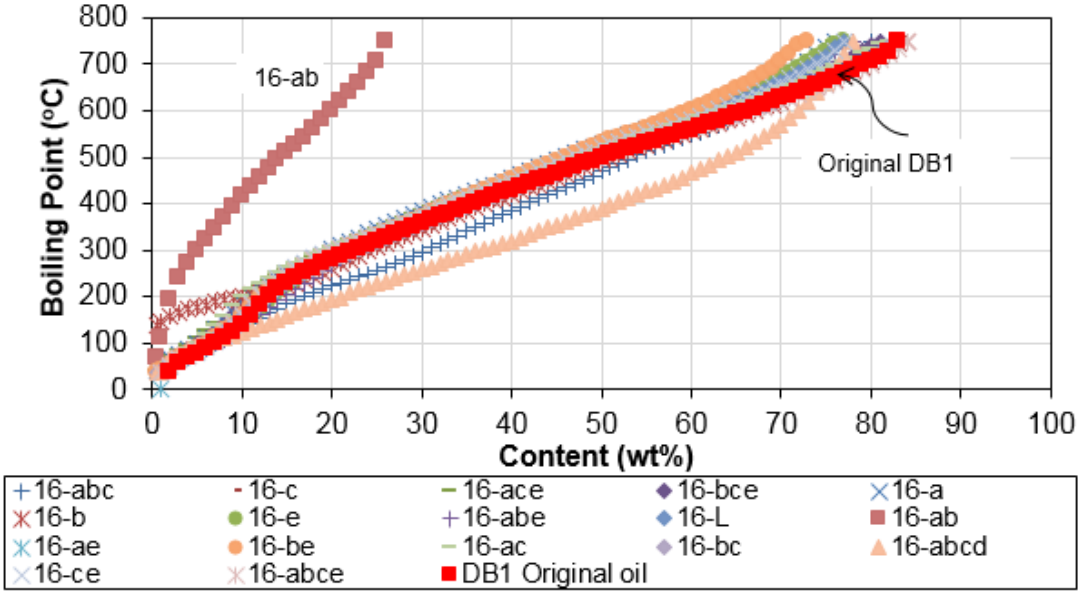

(b)

Figure 2-1: Floating oil boiling point distributions for (a) CC and (b) DB1 tests

After the mixing tests, the maltenes and asphaltenes fractions were also obtained for the >204ºC fraction of the floating oils. The changes in the maltenes and asphaltenes content from the original oil are shown in Figure 2-2. The percent change of maltenes and asphaltenes contents from the original oil is calculated based on the absolute mass of the maltenes and asphaltenes fractions in the floating oil relative to the mass of the two fractions in the original oil. As shown in Figure 2-2, the asphaltene content increased in the CC runs compared to the DB1 tests, while the maltenes content decreased in the CC runs more than in the DB1 runs. These fractions were then further analyzed for their elemental composition (carbon, hydrogen, sulfur, nitrogen and oxygen) and boiling point distributions. The boiling point distributions for the maltenes and asphaltenes for the CC and DB1 tests are shown in Figure 2-3 and Figure 2-4, respectively.

In Figure 2-3a and Figure 2-4a, there were no high temperature simulated distillation data available for either original oil maltenes fractions.

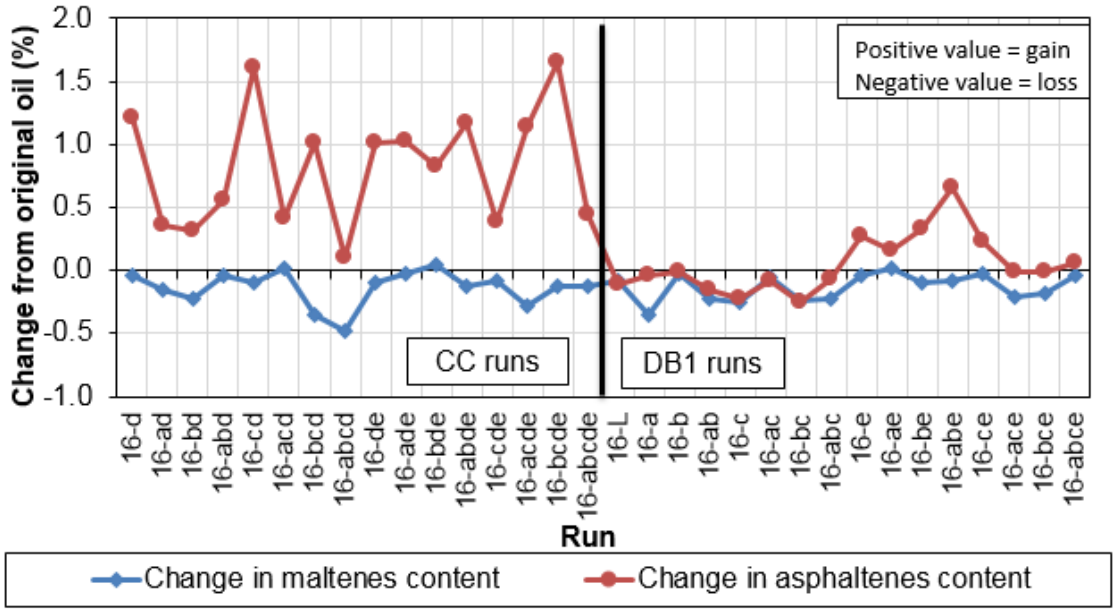

Figure 2-2: Change in +204ºC fraction maltenes and asphaltenes content from original oil

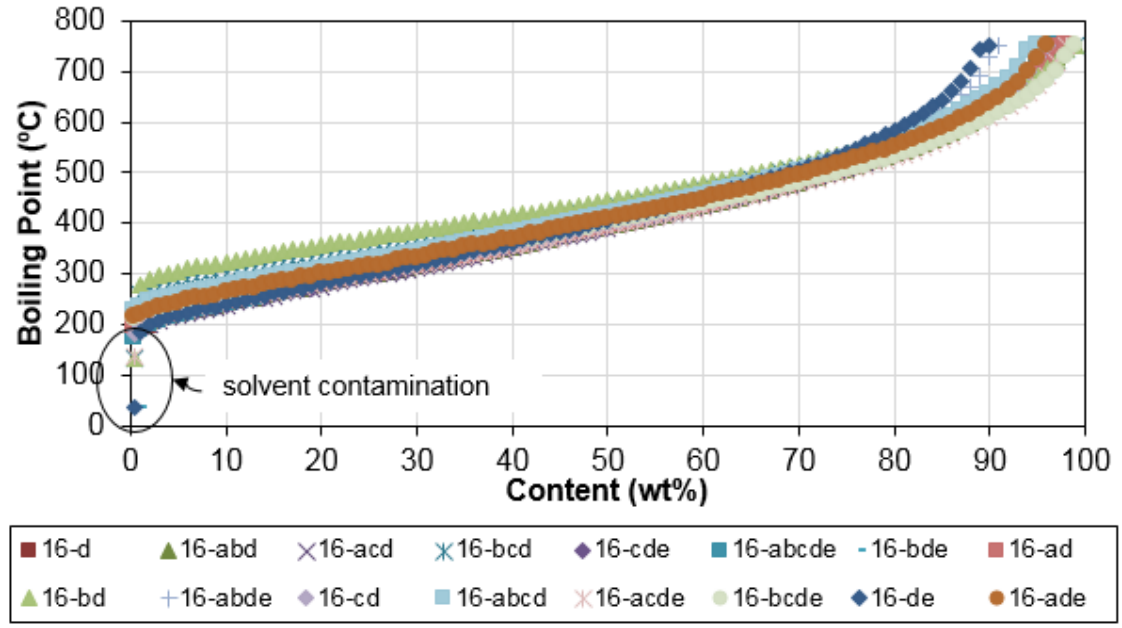

(a)

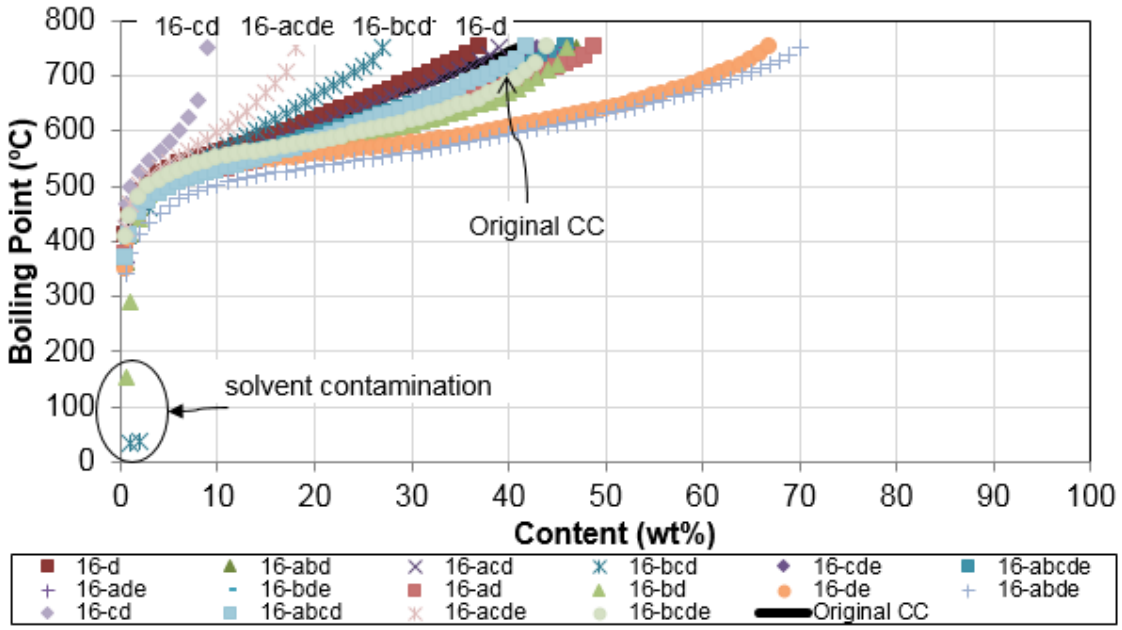

(b)

Figure 2-3: Boiling point distributions of +204ºC (a) maltenes and (b) asphaltenes fractions for CC tests

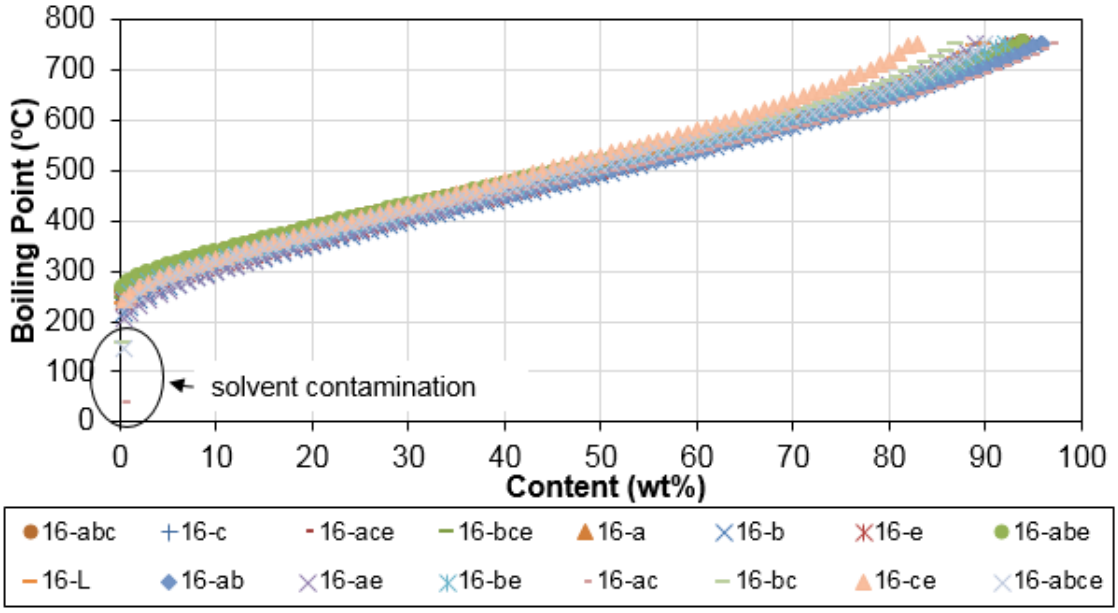

(a)

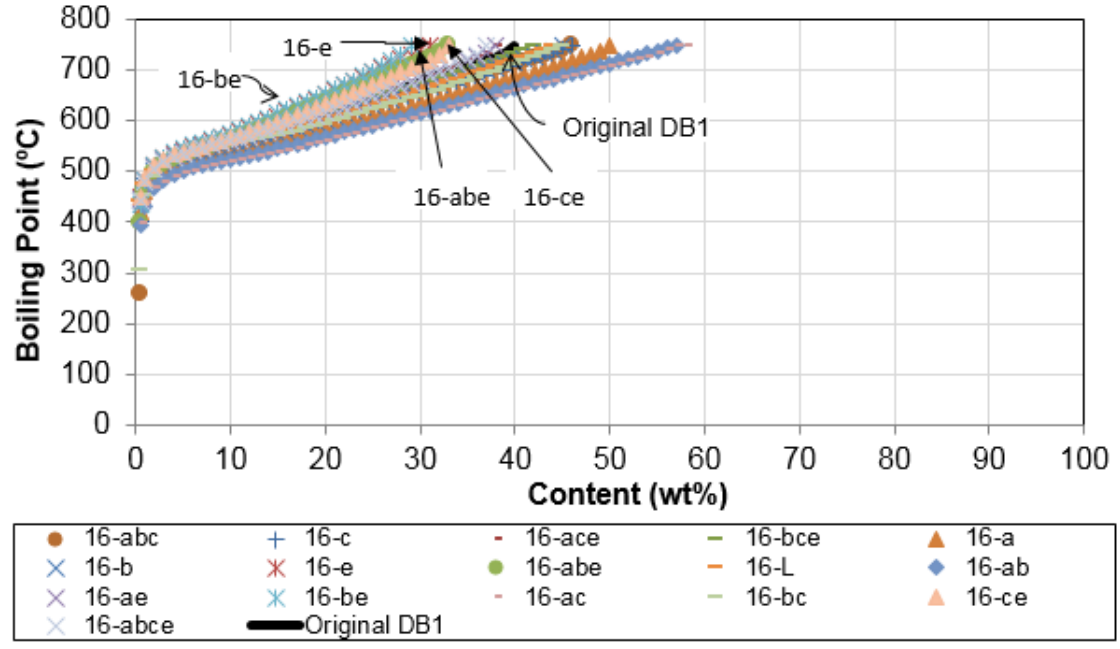

(b)

Figure 2-4: Boiling point distributions of +204ºC (a) maltenes and (b) asphaltenes fractions for DB1 tests

From the elemental analysis of the floating oil, minimal changes were observed in the carbon, hydrogen, nitrogen and sulfur contents, with most changes being found in the oxygen contents. For this reason, only the oxygen data is shown and the change in the carbon, hydrogen, nitrogen and sulfur contents can be found in Appendix C. The percent change from the original oil is calculated based on the absolute mass of the oxygen in the maltenes and asphaltenes fractions relative to the mass of the oxygen in the two fractions in the original oil. The change in the oxygen content (by mass) from the original oil for the maltenes and asphaltenes fractions is shown in Figure 2-5. There is significant increase in the oxygen content in the asphaltenes fraction for the CC runs compared to the DB1 runs, while the oxygen content in the maltenes fraction decreased for all CC runs and increased for most of the DB1 runs.

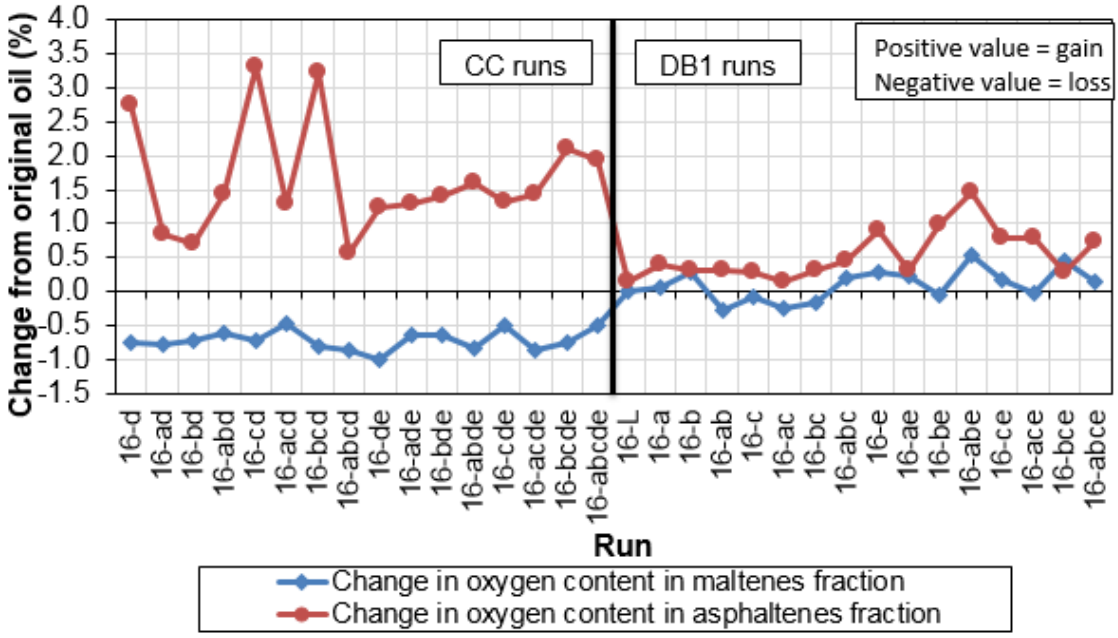

Figure 2-5: Change in oxygen content from original oil for maltenes and asphaltenes fractions

In the previous study (Section 1.5), oil losses were observed for some of the runs. As there were significant variations in the contents of material boiling greater than 750ºC (Figure 2-3 and Figure 2-4) as well as significant changes in oxygen contents (Figure

2-5), the three sets of data for the runs are plotted in Figure 2-6 for the maltenes and asphaltenes fractions, to observe whether there was a relationship between these factors. As shown in Figure 2-6, there is more variance in the asphaltene fractions for both oils, compared to the maltenes fraction.

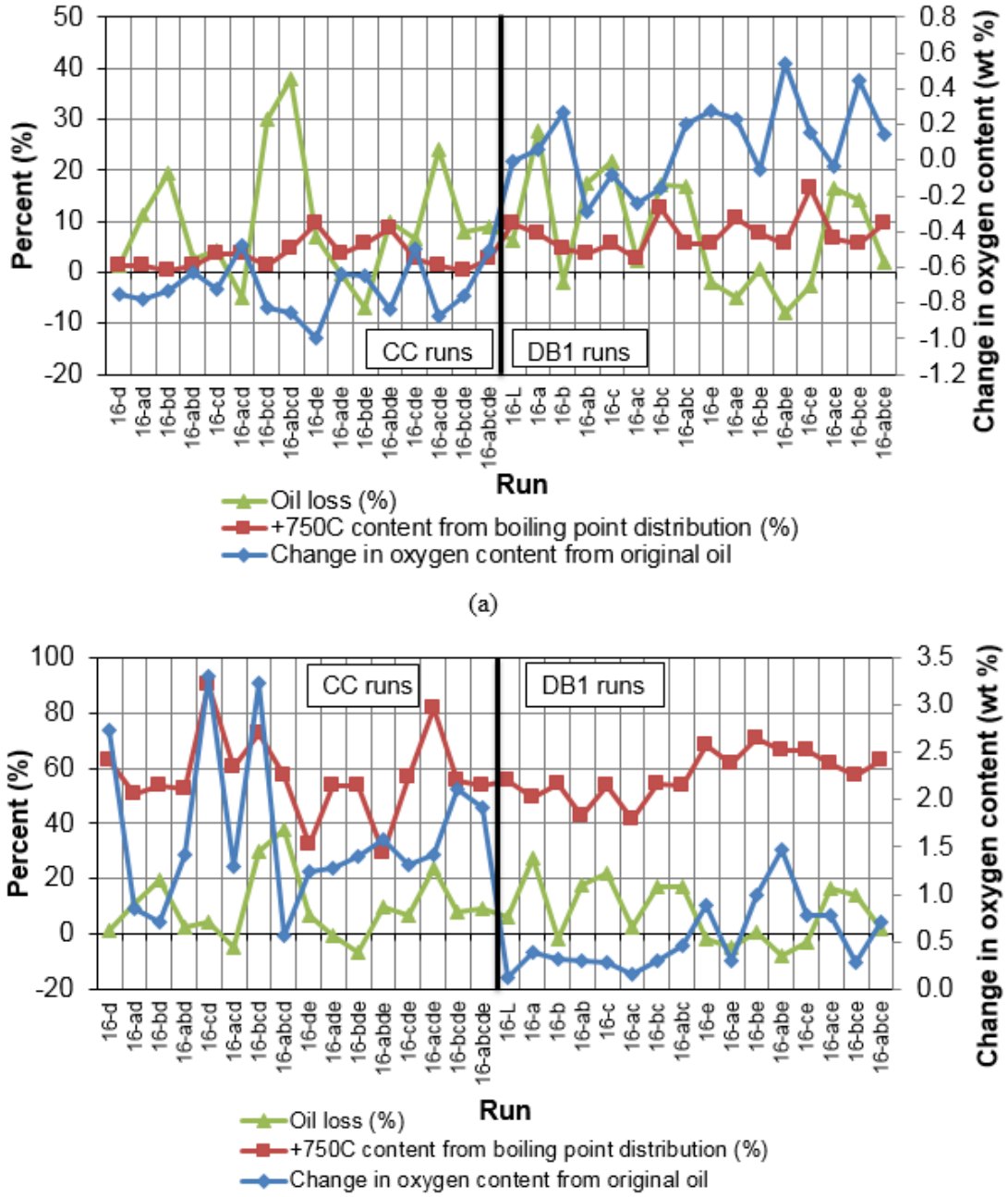

Figure 2-6: Oil loss, +750ºC content, and oxygen content in +204ºC (a) maltenes fraction and (b) asphaltenes fractions

After each mixing test, the water and sediment were separated from the floating oil. The oil dissolved and dispersed in the water phase was extracted using carbon disulfide

and then dichloromethane. The boiling point distributions for the extracted oils were then measured. Since two solvents were used for extraction, each oil sample from the water had two boiling point distributions. The two boiling point distributions were combined based on the yield of oil from each extraction. The resulting boiling point distribution curves for the oil isolated from the water phase for the CC and DB1 tests are shown in Figure 2-7. This shows us that there is greater variance in the boiling point distributions of the DB1 oil extracted from the water as compared to the CC oil.

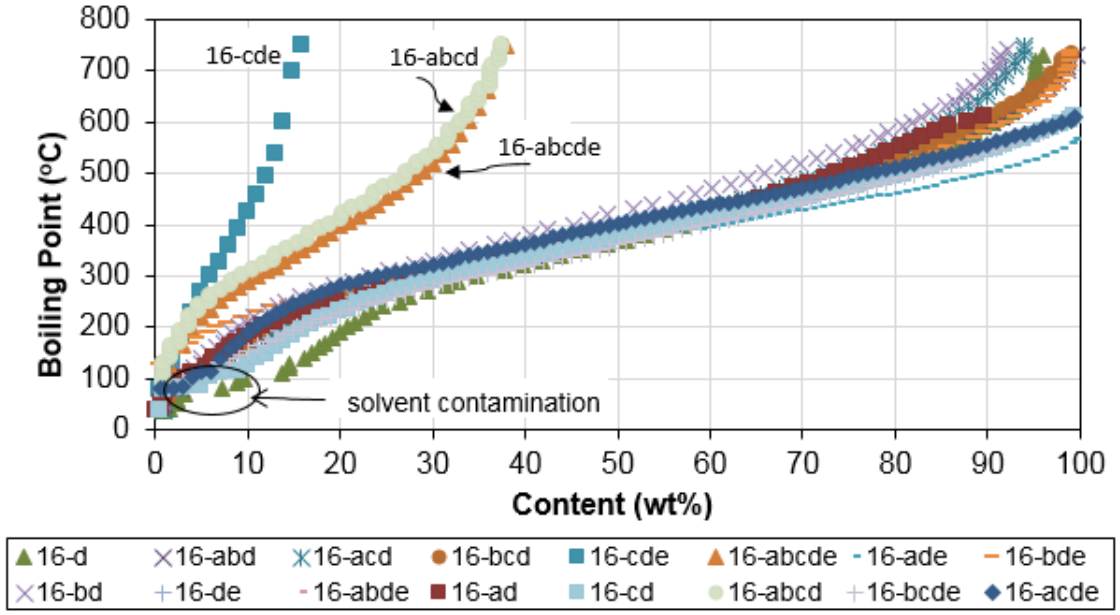

(a)

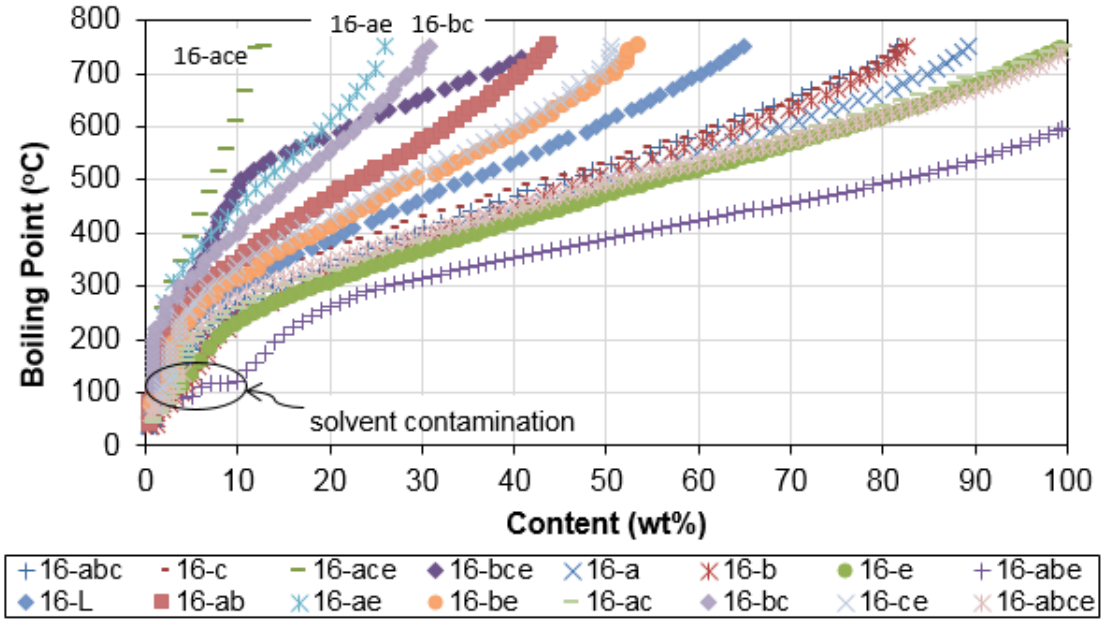

(b)

Figure 2-7: Boiling point distributions of oil extracted from the water for (a) CC and (b) DB1 tests

From the sediment samples collected, the oil on the sediment was extracted using dichloromethane. The boiling point distribution results for the oil extracted from the sediment for the CC and DB1 runs are shown in Figure 2-8. There is an increase in the >750ºC boiling material for the DB1 runs as compared to the CC runs.

Note that there was not enough oil extracted for Run 16-ace and Run 16-ae to obtain the boiling point distribution for those DB1 runs (Figure 2-8b).

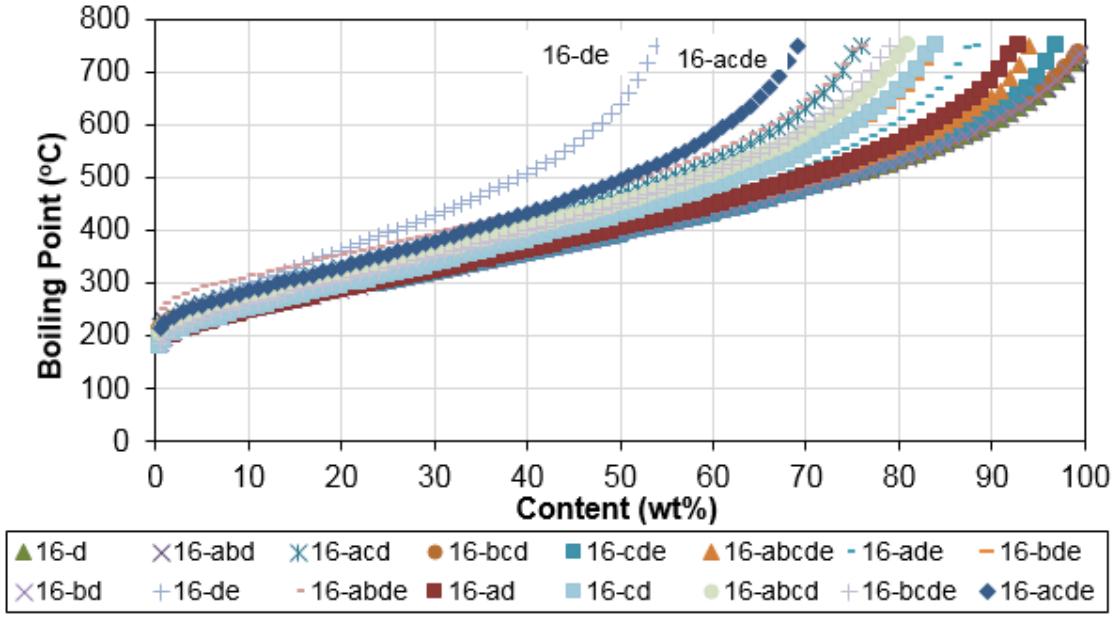

(a)

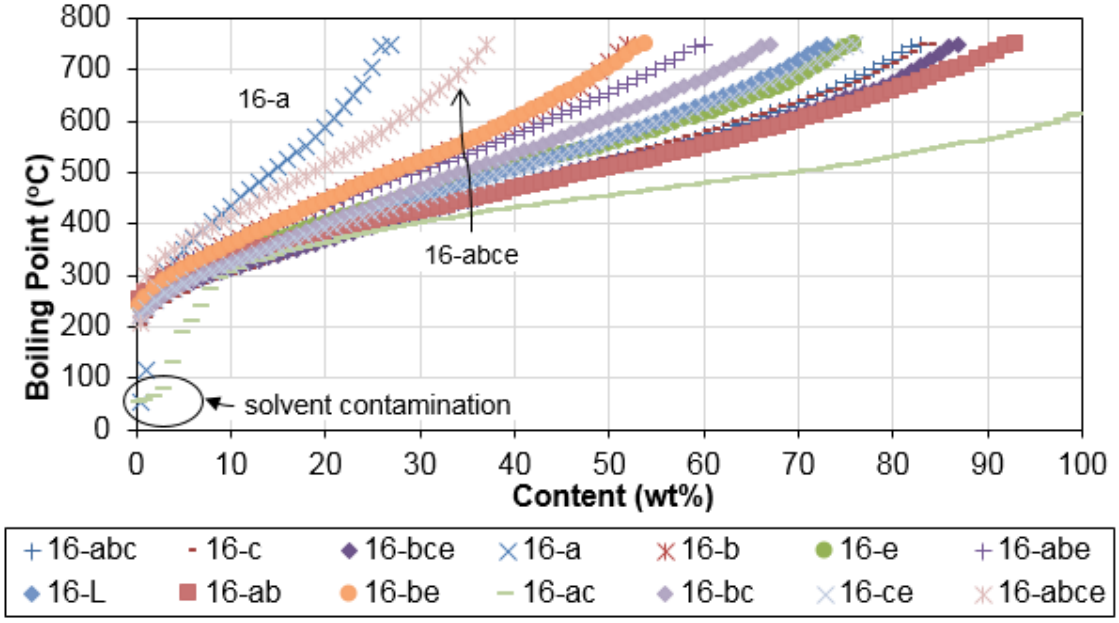

(b)

Figure 2-8: Boiling point distributions of oil extracted from sediment for (a) CC and (b) DB1 tests

To determine the effects of mixing on the boiling point distribution of the oils, the data was grouped into four boiling range fractions including initial boiling point (IBP) to 204ºC for naphtha, 204ºC-343ºC for middle distillate, 343ºC-524ºC for gas oil and 524ºC+ for residue. The mass of each boiling range fraction was calculated from the yields of the floating oil, oil in water and oil from sediment for each test. Once the total mass of each boiling fraction was determined for a test, the difference with respect to the original oil content was determined. The change in the mass of each boiling range fraction after each mixing test is shown in Figure 2-9. The residue fraction increases for most DB1 runs compared to the CC runs, while there is a decrease in the naphtha, middle distillate and gas oil fractions for both DB1 and CC.

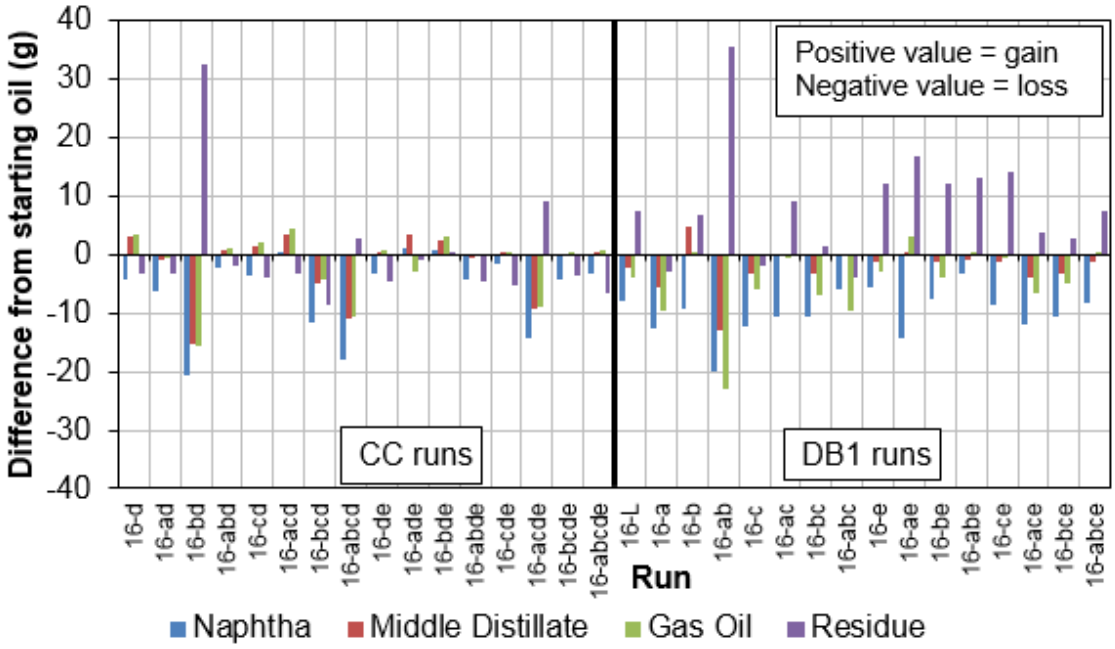

Figure 2-9: Change in boiling range fractions based on original oil content

2.5 Discussion

Mixing between oil and water in the presence of sediment is a complex phenomenon. The significant physical effects from the initial screening of the design factors were that

salt water had the greatest impact on floating oil recovery with greater recovery of DB1 than CC in salt water; DB1 dispersed more in fresh water than CC; CC interacted more with sediment than DB1; and a thicker emulsion layer was formed when mixing with DB1 (Section 1.5). The objective of this study was to analyze the chemical changes of the oil after mixing to determine if certain components of the oil preferentially dispersed into one of the three phases.

Floating oil. The conventional method of predicting the behaviour of oil when spilled on water is by relating the density and viscosity of the oil to that of water. As long as the density of the oil is less than water, it is expected to float. The density of the oils used in this study were both less than that of water (Table 2-3), and as expected, the bulk oil remained floating on the water after mixing. The viscosity of DB1 was considerably higher than that of CC (Table 2-3), and according to Stoffyn-Egli and Lee (2002), increasing the viscosity of an oil would reduce interaction with sediment. A lower viscosity oil would mix more in the water creating more surface area for the oil to interact with the sediment. This supports our findings that CC, with the lower viscosity, interacted more with sediment compared to DB1. Although DB1 was found to disperse more in fresh water than CC, due to its higher viscosity, there was less surface area of DB1 available to interact with sediment (Stoffyn-Egli & Lee, 2002). Another chemical property that is used to predict the behaviour between oil and water is the interfacial tension between the two liquids. The lower the interfacial tension, the greater the interaction between the oil and water, with the opposite holding true as well (Butt et al., 2006; Israelachvili, 2011). As shown in Table 2-3, the interfacial tension data between CC and fresh and salt water is less than that for DB1. This suggests that CC would interact more in both types of water. However, the mixing tests show that DB1 remained dispersed more into fresh water than CC, indicating that other variables can have a significant impact on the mixing. The interfacial tension data can also be used to predict the behaviour of the starting oils in salt versus fresh water. The interfacial tension for both CC and DB1 is lower in salt water compared to fresh water (Table 2-3). From this information alone, it would imply that the oils would mix in salt water more than fresh

water, which is supported by the study carried out by Omotoso et al. (2002). However, according to Hollebone (2014), the interfacial tension of oils in salt water is greater than the interfacial tension of oils in fresh water. This supports the finding from the first study where the floating oil recovery was greater in salt water than fresh water as a result of less interaction with salt water. A higher interfacial tension in salt water also supports the salting-out effect, or the effect of an ionic solution on oil-water mixing. With increased salt concentration in the water, the surface charge density of the oil particles decreases causing less oil dispersion in salt water, allowing for greater oil separation from water (Le Floch et al., 2002; Stoffyn-Egli & Lee, 2002; Trefalt & Borkovec, 2014). This phenomenon was discussed in further detail in the initial study in Section1.5. Hollebone (2014) also suggests that the error in interfacial tension measurements can be as high as ±15%, so these values and their effects should be interpreted with caution.

Another key interaction identified in the initial study was that DB1 formed a thicker emulsion layer than CC. Even though the surface tension of DB1, and the interfacial tensions of DB1 with salt and fresh water, are all greater than CC, from the mixing tests it was found that more water was entrained in DB1 causing the production of a larger emulsion volume. This could be a result of the nature of mixing a higher viscosity oil in an end-over-end style agitator, causing entrainment of pockets of water in the oil resulting in thicker emulsions. These pockets of entrained water were observed during distillation of the DB1 floating oil, causing bumping of the sample. The entrained pockets of water could also be attributed to the polarity of DB1. The presence of heteroatoms and the aromaticity of an oil influences its polarity. DB1 is more polar than CC (Table 2-3). The higher polarity would foster the mixing with fresh water, while the higher viscosity would trap pockets of water caused by the rotational mixing in the jars producing thicker emulsions with DB1. The effect of polarity on the oils mixing in the water phase is covered later in the discussion.

The high temperature simulated distillation data of the floating oils provides further information on changes that occur due to mixing. The boiling point distribution data

show how the content of the material boiling greater than 750ºC changes after mixing. The addition of oxygen to the hydrocarbons could result in the boiling points of the hydrocarbons being higher than 750ºC. However, it is also possible that oxygenated compounds may not be soluble in the carbon disulfide solvent used in the analysis. This would result in a greater proportion of material being reported as having greater than 750ºC boiling point. In Figure 2-1a, there is a diverse range of b.p.>750ºC contents for the CC compared to the DB1 tests (Figure 2-1b), where contents varied from more than 60 wt% of b.p.>750ºC boiling material to less than that of the starting oil. For DB1, there was less variance with exception of one of the tests, run 16-ab, containing ~70 wt% of b.p. >750ºC material, while the rest clustered around the same amount as the starting oil. These results indicate that there are variable quantities of either higher boiling or insoluble compounds remaining in the CC compared to the starting oil.

The reasons for the significant effects mentioned above were based on the bulk oil properties which provided partial explanation due to the heterogeneity nature of the oils. Chemical analyses of the sub-fractions of the oils (below) provided further insight to the observations.

Since in an actual oil spill scenario there would be losses of the lighter boiling material in the oil (b.p.<204ºC) (Zhou et al., 2015), it was important to understand the behaviour of the heavier oil (b.p.>204ºC) that would remain with the water. The analyses of the boiling fraction b.p.>204ºC produced by distillation of the original and floating oils, offered information about changes in molecular composition due to conversion to another fraction or losses from the oil, the presence of biodegradation and interaction with sediment. As shown in Figure 2-2, there is greater variance in the asphaltenes contents after mixing, with minimal change in the maltenes contents for the CC tests. For the DB1 tests there was minimal variance in both the maltenes and asphaltenes contents. With CC being a lighter oil than DB1, the starting oil will contain more maltenes and less asphaltenes than DB1 (Gray, 1994), which is consistent with results presented in Table 2-3. An increase in oxygen content in the floating oil could cause the asphaltenes content

to increase at the expense of the maltenes fraction. Similar information is also shown in Figure 2-3a and Figure 2-3b for CC, where there was minimal change in the maltenes boiling point distributions, but a wider range of b.p.>750ºC contents for the asphaltenes. The curves to the right of the original CC asphaltenes sample indicate the amount of material that boils at temperatures greater than 750ºC in the floating oil had reduced after mixing. Each of these runs were conducted at the warmer mixing temperature, except for Run 16-d. This implies that mixing at higher temperatures increases the amount of heavier boiling material (at the expense of the lighter boiling material). The initial boiling point for Run 16-bd shows the presence of oxygen containing lower boiling compounds that may have shifted into the asphaltenes after the maltenes were oxidized. A few DB1 tests saw a slight increase in the asphaltene content: runs 16-e, 16-be, 16-abe and 16-ce (Figure 2-2), along with an increase in the b.p.>750ºC boiling material ranging from 30%-60% (Figure 2-4b). The smaller changes for the diluted bitumen are consistent with the effects seen for CC due to biodegradation as there are greater contents of susceptible hydrocarbons present in CC compared to the DB1. Bitumen is the result of biodegradation of crude oil in the reservoir so the most susceptible hydrocarbons for biodegradation are no longer present.

Changes in the oxygen content in the floating oil could be the result of oxidation of the hydrocarbons, possibly by biodegradation and/or interaction with the silicon oxide and aluminum oxide from the sediment. The greatest increase in oxygen occurs in the asphaltene fractions of the CC tests in runs 16-d, 16-cd and 16-bcd (Figure 2-5). These three runs were mixed in the presence of diatomaceous earth in fresh water. Runs 16-cd and 16-bcd were both carried out at the warmer mixing temperature. Warmer mixing temperatures would encourage biodegradation of the oil. The decrease in the oxygen content in the maltenes fraction was ~1% and was consistent for all of the CC tests. As shown in Figure 2-5, the increase in the oxygen content was minimal when mixing DB1 in fresh water (~0.5%) for both the maltenes and asphaltenes fractions, while the oxygen content increases for runs in salt water in both fractions (up to 1.5%). Oxygen increase caused by the interaction with sediment would yield an elemental mass balance (carbon,

hydrogen, nitrogen, sulfur and oxygen) less than 100% due to the silicon and aluminum not being measured. This was observed in the asphaltenes fraction for some of the CC and DB1 tests. Runs 16-cd, 16-acde 16-bcd and 16-d had the greatest increase in asphaltenes (Figure 2-2), the greatest amount of >750ºC boiling material in the asphaltene fraction (Figure 2-3b), and also the greatest increase in oxygen content for the CC tests (Figure 2-5). Interaction with the silicon oxide and alumina oxide in both the diatomaceous earth (Run 16-cd, Run 16-bcd and Run 16-d) and sand (16-acde) could cause an increase in oxygen content for these runs as shown in Figure 2-5. All of these runs had elemental mass balances ranging between 70-85%. This suggests interaction with sediment could be significant. Metals analyses of these oil samples would provide more information on the extent of interaction with sediment.

When comparing the oil loss, b.p.>750ºC content, and change in oxygen from original oil, there is a decrease in the oxygen content in the maltenes fraction for the CC tests with higher oil loss per run, while the oxygen content increases for the DB1 tests with lower oil loss in the salt water runs (Figure 2-6a). The amount of material boiling greater than 750ºC ranges between 0-10% for the CC runs and 2-16% for the DB1 tests. The increase in oxygen content in the maltenes fractions for the DB1 tests also show an increase in material boiling greater than 750ºC. Since the range for the axis representing the change is oxygen content in the maltenes is so narrow (±1%), the observable change could be within the error of the analysis. The notable increase in oil loss for runs 16-bcd and 16-abcd was due to oil losses encountered during the mixing tests (leaking jars), so these results do not represent actual oil loss caused by the mixing condition. As for the asphaltenes fractions (Figure 2-6b), an increase in oxygen content results in an increase in the b.p.>750ºC material in the CC oil. This may be a result of the solubility effect of oxygenated compounds that show up as material boiling >750ºC. The change in oxygen content varies more in fresh water runs compared to the salt water runs, and is more pronounced with CC than DB1. This is consistent with CC being more biodegradable than DB1 (more susceptible hydrocarbons for biodegradation are present). The opposite can be seen in the DB1 runs; the change in oxygen in the asphaltenes fraction is quite

steady around 0.3% in fresh water runs, while the increase in oxygen in the salt water runs varies between 0.3-1.5% due to the different microbes that exist in fresh versus salt water. The amount of material that boils >750ºC is greater in the salt water runs with DB1 compared to the fresh water runs. Less variance was observed with the DB1 tests, since DB1 contains less available hydrocarbons to undergo biodegradation at the same rate as CC. The relationship with the amount of oil loss per run is inconclusive as the results show no obvious trend.

Oil in water and sediment. As shown in Figure 2-7a, most of the CC oil extracted from the water has less than 10% material boiling greater than 750ºC with the exception of Runs 16-cde (85%), 16-abcd (65%), and 16-abcde (65%). The runs with the greatest amount of heavier boiling material in Figure 2-7a were all carried out at the higher mixing temperature. This implies greater biodegradation at the higher mixing temperature which then shows up as material boiling greater than 750ºC. It is interesting to note that runs 16-cde and 16-abcde were both mixed with salt water, yet exhibited the greatest content of b.p.>750ºC. This implies the effects of other variables may have greater impact. There is greater variance in the boiling point distributions for DB1 tests extracted from the water phase (Figure 2-7b). Run 16-ace has almost 85% material that boils greater than 750ºC while for runs 16-ae, 16-bc and 16-ab the content of the heavier boiling material is greater than 75%. The greatest content of heavy boiling material for the CC tests (85%) was when mixed with diatomaceous earth (Figure 2-7a), while the greatest content of heavy boiling material for the DB1 tests (87%) was when mixed with sand (Figure 2-7b). From Figure 2-7, it is clear that there is greater variance in the boiling point distribution results for the DB1 tests than CC tests; this would suggest presence of oxygenated compounds from biodegradation and/or interaction with sediment. Additional elemental and metals analyses of the oil isolated from the water phase would provide more information to further explain the trends of the boiling point distribution curves.

As shown in Figure 2-8a, the oil extracted from the sediment from the CC tests in Run 16-de had the greatest amount of heavier boiling material (45%) followed by Run 16-acde (30%). Both of these runs were mixed in salt water with the two different sediments (16-de was mixed with diatomaceous earth and 16-acde mixed with sand). The content of the material boiling >750ºC for the DB1 oil extracted from the sediment is greatest for Run 16-a (75%) as shown in Figure 2-8b. It can be seen that DB1 extracted from the sand in fresh water (Run 16-a) and sand in salt water (Run16-abce) both contain the greatest amount of material boiling greater than 750ºC, with the difference being the mixing speed and temperature. The oil for Run 16-ac was extracted using carbon disulfide, instead of dichloromethane, which is the reason for the low initial and final boiling points shown in Figure 2-8b as the higher boiling material in the oil was not extracted from the oil-sediment sample. DB1 tests contain a wider range of b.p. >750ºC material than the CC tests. Even though greater quantities of CC were extracted from the sediment in the initial study, the CC oil recovered has less material that boils >750ºC compared to the DB1 tests. As with the oil extracted from the water, elemental and metals analyses of the oil from the sediment would provide more information about the causes for the differences in boiling point curves from the CC and DB1 tests.

The polarity of an oil provides information on the behaviour of the oil when it enters the water column and interacts with sediment. DB1 is more polar than CC due to the higher heteroatom content and lower hydrogen to carbon ratio (H/C ratio) in the b.p.>204ºC fraction as shown in Table 2-3. The higher polarity of DB1 would lead to greater recovery in salt water because of the ionic effect at the oil-water interface. This further supports the significant effect observed that there was greater oil recovery in salt water, with the recovery of DB1 being greater than CC. Subsequently, in fresh water, the higher polarity of DB1 would cause it to disperse more in fresh water, as was observed as a significant effect in the mixing tests. On the other hand, CC is less polar than DB1 since it has greater H/C ratio and lower heteroatom content (Table 2-3). As CC is mixed with the water, smaller oil droplets are formed (due to lower viscosity) allowing for a greater surface area for the microbes in the water to work at the oil-water interface. This

creates a greater opportunity for biodegradation causing a larger increase in oxygen content (Figure 2-5) and increase in its polarity. The smaller oil droplets would lead to more interaction with sediment as well. This was observed in the mixing tests (identified as a significant effect). Based on the effect of the polarity of the two oils, there is greatest recovery of DB1 in salt water and most dispersion of DB1 in fresh water. This behaviour is further illustrated in Figure 2-10.

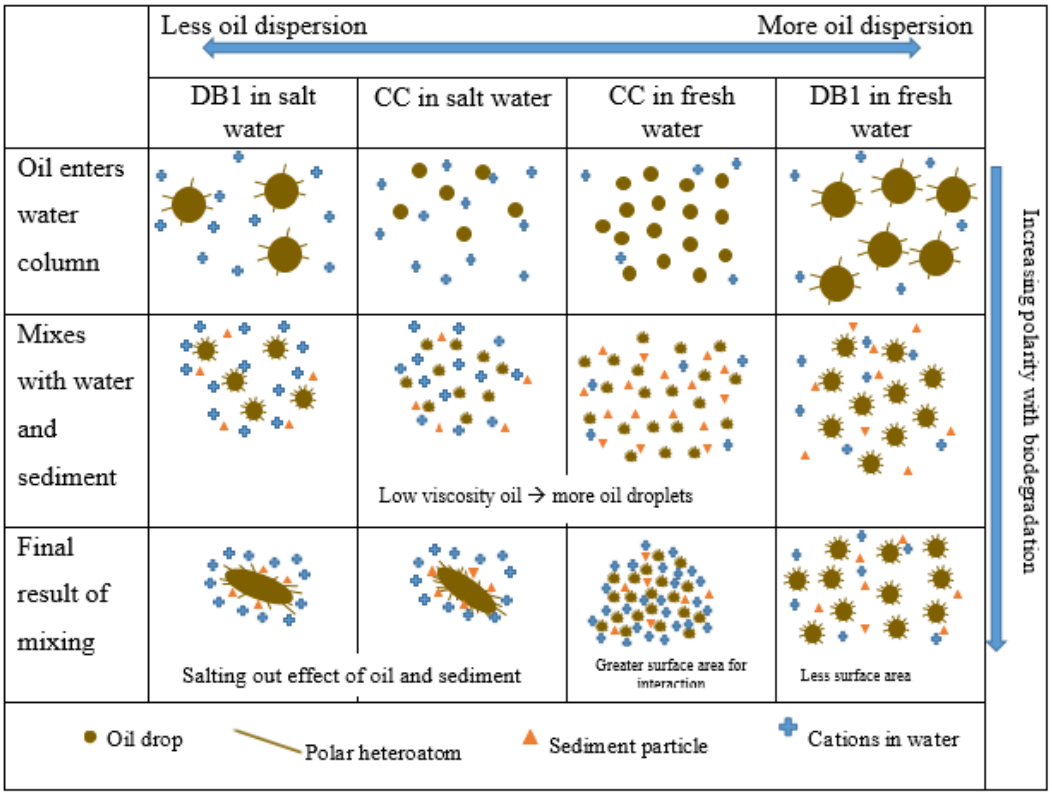

Figure 2-10: Polarity effect on mixing CC and DB1 in water with sediment

Full oil distribution. The mass of each boiling fraction from the floating oil, oil in water and oil on sediment were combined and then compared to the mass of the boiling fractions in the original oil (Figure 2-9). Even in a closed system, the naphtha content for the runs decreased after mixing and was most prominent for the DB1 tests. Since the

initial boiling points remained similar for both oils (Figure 2-1), the loss was not primarily due to evaporation, except for the two DB1 samples that did lose the lightest hydrocarbons (runs 16-ae and 16-b, Figure 2-1b), which correlate to the losses shown in Figure 2-9 for the same runs. There is a slight increase in the middle distillate and gas oil fractions in the CC with fresh water runs, and then decreases with the salt water runs. This may be a result of partial biodegradation of the residue fraction creating more middle distillate and gas oil fractions. The greatest amount of residue is found in Run 16-bd when mixing with CC. Most of the runs with DB1 show an increase in the amount of residue in the resulting oil, which is not biodegradable. The loss of the naphtha, middle distillate and gas oil fractions is also greater with the DB1 runs. Interestingly, changes due to the polarity of the oils, as discussed previously, are not reflected in the overall boiling point distributions.

2.6 Conclusions

This work focussed on the analysis of the original oil, floating oil and oil from the water and sediment to understand the causes of the significant physical effects identified in the first study (Section 1.5). The significant physical effects from the initial screening of the design factors were that salt water had the greatest impact on floating oil recovery with greater recovery of DB1 than CC in salt water; DB1 dispersed more in fresh water than CC; CC interacted more with sediment than DB1; and, a thicker emulsion layer was formed when mixing with DB1.

The bulk oil properties provided the necessary information to explain the key interactions during mixing, and analyses of the sub-fractions of the oils identified the significance of polarity of the oils during mixing. It was found that the floating oil recovery in salt water was greater than in fresh water, due to the decrease in electrostatic repulsion between the oil particles caused by the ionic effect in salt water. The interfacial tension results measured for the bulk oils could not be interpreted according to the

literature, possibly due to the heterogeneity of the oils. According to literature, the interfacial tension of oils in fresh water is less than that in salt water (Hollebone, 2014), which explains why this behaviour was observed in the initial study. As for the reason behind thicker emulsions forming with DB1, it was concluded that the density and viscosity were important factors. With a higher density and viscosity than CC, DB1 did not mix in to the bulk water as easily and the mixing method (rotary agitation) caused entrainment of water pockets in the oil. It was also identified from the mixing tests that DB1 dispersed more in fresh water compared to salt water. The higher viscosity of DB1 compared to that of CC could be the reason why DB1 remained dispersed in the water column and did not resurface as was observed for CC. Further analyses of the sub-fractions of the oils revealed that the polarity of the oils, along with the bulk oil properties, also influenced the extent of interaction with water and sediment. Although DB1 interacted more with water, CC was found to interact most with sediment due to its lower viscosity, which is also supported by literature (Stoffyn-Egli & Lee, 2002). It was found that the changes in the boiling point distributions were most significant when mixing with CC than DB1. There was also greater increase in the asphaltenes content after mixing with CC along with a greater increase in oxygen content in the asphaltenes fraction for CC. This behaviour suggests interaction with sediment and the presence of bioactivity with CC. Further analyses of the metals content in the asphaltenes fraction, along with analysis of nuclear magnetic resonance (NMR) and Fourier transform infrared spectroscopy (FTIR) data would provide insight to the source of oxygen.

More change occurred in the naphtha, middle distillate, gas oil and residue fractions when mixing with DB1 compared to CC. Mixing DB1 and salt water resulted in more loss of the naphtha fraction with an increase in the residue fraction.

The results from this work provide further information to the findings from the first study. The effect of salt water and interaction with sediment have shown to be significant factors in changes to the oil after mixing. The knowledge of the physical and chemical changes that occur after oil is spilled on water is beneficial from an oil spill remediation

perspective. However, the impact of an oil spill on water varies greatly depending on the unique chemical composition of the oil, and the dynamic water and environment conditions.

2.7 Acknowledgments

The authors would like to thank NRCan Program of Energy Research and Development (PERD) and the Interdepartmental Tanker Safety Program for funding this study, and the CanmetENERGY Environmental Impacts Team for the water analyses and the Analytical Team for the hydrocarbon analyses. We would like to recognize the efforts of Dr. Aleksey Baldygin and his supervisor Dr. Prashant Waghmare, from the University of Alberta Mechanical Engineering Department, for analyzing the surface tensions and interfacial tensions of the oil and water samples. We would also like to acknowledge the Canadian Association of Petroleum Producers (CAPP) for providing the two oils for this study.

2.8 Nomenclature

A	sediment (input variable)
B	mixing speed (input variable)
b.p.	boiling point
C	temperature (input variable)
CC	conventional crude
D	oil (input variable)
DB1	diluted bitumen
E	water (input variable)
FTIR	Fourier Transform Infrared Spectroscopy

NMR Nuclear Magnetic Resonance

2.9 References

Abdel-Rauf, M. E. (2012). Emulsions- composition stability and characterization chapter 10. Retrieved from http://www.intechopen.com/books/crude-oil-emulsions-composition-stability-and-characterization/factors-affecting-the-stability-of-crude-oil-emulsions

Bragg, J. R., & Owens, E. H. (1994). Clay-oil flocculation as a natural cleansing process following oil spills: Part 1. Studies of shoreline sediments and residues from past spills. Environment Canada, Ottawa, ON. (Canada). 1, 1-23.

Butt, H., Graf, K., & Kappl, M. (2006). Physics and chemistry of interfaces John Wiley & Sons.

Czarnecki, J., Tchoukov, P., & Dabros, T. (2012). Possible role of asphaltenes in the stabilization of water-in-crude oil emulsions. Energy & Fuels, 26(9), 5782-5786.

Fingas, M., & Fieldhouse, B. (2004). Formation of water-in-oil emulsions and application to oil spill modelling. Journal of Hazardous Materials, 107(1-2), 37-50.

Fingas, M., & Fieldhouse, B. (2005). How to model water-in-oil emulsions. Paper presented at the 2005 International Oil Spill Conference, IOSC 2005, May 15, 2005 - May 19, 11354-11361.

Fingas, M., & Fieldhouse, B. (2009). Studies on crude oil and petroleum product emulsions: Water resolution and rheology. Colloids and Surfaces A: Physicochemical and Engineering Aspects, 333(1-3), 67-81.

Fingas, M., & Fieldhouse, B. (2012). Studies on water-in-oil products from crude oils and petroleum products. Marine Pollution Bulletin, 64(2), 272-283.

Gray, R. M. (1994). Upgrading petroleum residues and heavy oils CRC press.

Gundlach, E. R., & Hayes, M. O. (1978). Vulnerability of coastal environments to oil spill impacts. Marine Technology Society Journal, 12(4), 18-27.

Hollebone, B. P. (2014). Oil physical properties. Handbook of oil spill science and technology (pp. 37-50) John Wiley & Sons, Inc.

Israelachvili, J. N. (2011). Intermolecular and surface forces Academic press.

Le Floch, S., Guyomarch, J., Merlin, F. X., Stoffyn-Egli, P., Dixon, J., & Lee, K. (2002). The influence of salinity on oil-mineral aggregate formation. Spill Science & Technology Bulletin, 8(1), 65-71. 10.1016/S1353-2561(02)00124-X

Lee, K. (2002). Oil-particle interactions in aquatic environments: Influence on the transport, fate, effect and remediation of oil spills. Spill Science & Technology Bulletin, 8(1), 3-8. 10.1016/S1353-2561(03)00006-9

Lee, R. F., & Page, D. S. (1997). Petroleum hydrocarbons and their effects in subtidal regions after major oil spills. Marine Pollution Bulletin, 34(11), 928-940. 10.1016/S0025-326X(97)00078-7

McLean, J. D., & Kilpatrick, P. K. (1997). Effects of asphaltene solvency on stability of water-in-crude-oil emulsions. Journal of Colloid and Interface Science, 189(2), 242-253. 10.1006/jcis.1997.4807

National Research Council. (2003). Oil in the sea III: Inputs, fates, and effects National Academies Press.

Omotoso, O. E., Munoz, V. A., & Mikula, R. J. (2002). Mechanisms of crude oil-mineral interactions. Spill Science & Technology Bulletin, 8(1), 45-54. 10.1016/S1353-2561(02)00116-0

Sjoblom, J., Aske, N., Auflem, I. H., Brandal, O., Havre, T. E., Sther, O., Kallevik, H. (2003). Our current understanding of water-in-crude oil emulsions. Recent characterization techniques and high pressure performance. Advances in Colloid and Interface Science, 100-102, 399-473.

Stoffyn-Egli, P., & Lee, K. (2002). Formation and characterization of oil–mineral aggregates. Spill Science & Technology Bulletin, 8(1), 31-44.

Tadros, T. F. (2013). Emulsion formation and stability John Wiley & Sons.

Tambe, D. E., & Sharma, M. M. (1994). The effect of colloidal particles on fluid-fluid interfacial properties and emulsion stability. Advances in Colloid and Interface Science, 52, 1-63.

Tchoukov, P., Yang, F., Xu, Z., Dabros, T., Czarnecki, J., & Sjoblom, J. (2014). Role of asphaltenes in stabilizing thin liquid emulsion films. Langmuir, 30(11), 3024-3033.

Trefalt, G., & Borkovec, M. (2014). Overview of DLVO theory

Wang, Z., Hollebone, B. P., Fingas, M., Fieldhouse, B., Sigouin, L., Landriault, M., Weaver, J. W. (2003). Characteristics of Spilled Oils, Fuels, and Petroleum Products: 1. Composition and Properties of Selected Oils. US EPA Report EPA/600-R/03, 72

Zhou, J., Dettman, H., & Bundred, M. (2015). A comparative analysis of environmental behaviour of diluted bitumen and conventional crudes. Paper presented at the AMOP, 495-516.

Chapter 3: Conclusions, Implications and Recommendations for Future Work

From the first part of the study it was found that mixing with salt water and the presence of sediment have significant influence the oil distribution after mixing. The significant physical effects from the initial screening of the design factors were that salt water had the greatest impact on floating oil recovery with greater recovery of DB1 than CC in salt water; DB1 dispersed more in fresh water than CC; CC interacted more with sediment than DB1; and, a thicker emulsion layer was formed when mixing with DB1. From the second part of the study, the bulk oil properties provided the necessary information to explain the key interactions during mixing, and analyses of the sub-fractions of the oils identified the significance of polarity of the oils during mixing. The effect of viscosity and interfacial tension allowed for greater mixing of conventional crude into the water increasing interaction with sediment. The most change in elemental composition after mixing was observed in the conventional crude mixing tests, with the greatest change occurring in the oxygen content for the maltenes and asphaltene fractions. Conventional crude oil has a higher hydrogen-to-carbon ration allowing for more substrate which contains the necessary hydrocarbon chains for biodegradation. Interaction with sediment and biodegradation of the conventional crude oil would cause a change in the oxygen content of the floating oil after mixing. Further analyses of the oxygen containing hydrocarbons (metals content and NMR with FTIR analyses) would provide more information on the source of the oxygen.

The results from this study are useful not only for reclamation and the effects on marine life, but also for oil spill responders so they can make a more informed decision on appropriate oil spill response options and strategies. As shown from the mixing tests, diluted bitumen and conventional crude oil exhibit quite different mixing behaviours in a

water environment. Information on the significant effects on mixing behaviour after an oil spill would provide valuable information for modelling oil spill behaviour. Understanding the fate of the oil, would fill key knowledge gaps that currently exist.

More information is required to fully understand the fate and behaviour of oil after an oil spill under varying environmental conditions. Recommendations for future studies:

- Conduct similar mixing tests at cooler temperatures (similar to winter or arctic conditions) would increase the range between the positive and negative levels in a factorial design for the temperature variable and provide an insight on the fate of on oil spills in cooler waters.
- Study similar mixing tests on weathered oils since the composition of weathered and fresh oils differ in their heavier fractions. Accounting for evaporation will be more representative of spills in open waters.
- Studying the effect of water pH on the mixing of oil, water and sediment will allow for a better understanding on how the varying pH of different bodies of water will affect oil-water-sediment interaction.

References (all)

Abdel-Rauf, M. E. (2012). Emulsions- composition stability and characterization chapter 10. http://www.intechopen.com/books/crude-oil-emulsions-composition-stability-and-characterization/factors-affecting-the-stability-of-crude-oil-emulsions

Andale Publishing. (2013). Normal probability plots.

Boglaienko, D., & Tansel, B. (2015). Instantaneous stabilization of floating oils by surface application of natural granular materials (beach sand and limestone). Marine Pollution Bulletin, 91(1), 107-112.

Boglaienko, D., & Tansel, B. (2016). Partitioning of fresh crude oil between floating, dispersed and sediment phases: Effect of exposure order to dispersant and granular materials. Journal of Environmental Management, 175, 40-45.

Boglaienko, D., & Tansel, B. (2017). Submergence patterns of floating crude oil by granular particles. Chemical Engineering Journal, 314, 548-553.

Bradley, R. W., Venditti, J. G., Kostaschuk, R. A., Church, M., Hendershot, M., & Allison, M. A. (2013). Flow and sediment suspension events over low-angle dunes: Fraser estuary, Canada. Journal of Geophysical Research: Earth Surface, 118(3), 1693-1709.

Bragg, J. R., & Owens, E. H. (1994). Clay-oil flocculation as a natural cleansing process following oil spills: Part 1. Studies of shoreline sediments and residues from past spills. Environment Canada, Ottawa, ON. (Canada).1, 1-23.

Bridie, A. L., Wanders, T. H., Zegveld, W., & Van der Heijde, H B. (1980). Formation, prevention and breaking of seawater in crude oil emulsions 'chocolate mousses'. Marine Pollution Bulletin, 11(12), 343-348.

Butt, H., Graf, K., & Kappl, M. (2006). Physics and chemistry of interfaces John Wiley & Sons.

Calvert, R. (1930). Diatomaceous earth. J.Chem.Educ, 7(12), 2829.

Crude Quality Inc. (2017). Crude monitor. http://www.crudemonitor.ca/home.php

Czarnecki, J., Tchoukov, P., & Dabros, T. (2012). Possible role of asphaltenes in the stabilization of water-in-crude oil emulsions. Energy & Fuels, 26(9), 5782-5786.

Dapkunas, S. J., Jillavenkatesa, A., & Lum, L. H. (2001). Particle size characterization.

Fingas, M. (1995). Water-in-oil emulsion formation - a review of physics and mathematical-modeling. Spill Science & Technology Bulletin, 2(1), 55-59.

Fingas, M. (2014). Oil physical properties. Handbook of oil spill science and technology (Chapter 20) John Wiley & Sons, Inc.

Fingas, M. (2015). Diluted bitumen (dilbit): A future high risk spilled material. Proceedings of Interspill. Edmonton, Alberta, Canada. Spill Science, 24

Fingas, M., & Fieldhouse, B. (2003). Studies of the formation process of water-in-oil emulsions. 47(9-12), 369-396. http://dx.doi.org/10.1016/S0025-326X(03)00212-1

Fingas, M., & Fieldhouse, B. (2005). How to model water-in-oil emulsions. Paper presented at the 2005 International Oil Spill Conference, IOSC 2005, May 15, 2005 - May 19, 11354-11361.

Fingas, M., & Fieldhouse, B. (2008). Water-in-oil emulsions: Studies on water resolution and rheology over time. Paper presented at the 31st AMOP Technical Seminar on Environmental Contamination and Response, June 3, 2008 - June 5, 1 1-34.

Fingas, M., & Fieldhouse, B. (2012). Studies on water-in-oil products from crude oils and petroleum products. Marine Pollution Bulletin, 64(2), 272-283. http://dx.doi.org/10.1016/j.marpolbul.2011.11.019

Fingas, M., Fieldhouse, B., & Mullin, J. (2005). Water-in-oil emulsions: How they are formed and broken. Paper presented at the 2005 International Oil Spill Conference, IOSC 2005, May 15, 2005 - May 19, 9058-9060.

Fingas, M. F., Fieldhouse, B., Lane, J., & Mullin, J. V. (2005). What causes the formation of water-in-oil emulsions? Paper presented at the 2005 International Oil Spill Conference, IOSC 2005, May 15, 2005 - May 19, 9120-9125.

Fingas, M., & Fieldhouse, B. (2004). Formation of water-in-oil emulsions and application to oil spill modelling. Journal of Hazardous Materials, 107(1-2), 37-50.

Fingas, M., & Fieldhouse, B. (2009). Studies on crude oil and petroleum product emulsions: Water resolution and rheology. Colloids and Surfaces A: Physicochemical and Engineering Aspects, 333(1-3), 67-81.

Gong, Y., Zhao, X., Cai, Z., O'Reilly, S. E., Hao, X., & Zhao, D. (2014). A review of oil, dispersed oil and sediment interactions in the aquatic environment: Influence on the fate, transport and remediation of oil spills. Marine Pollution Bulletin, 79(1-2), 16-33. 10.1016/j.marpolbul.2013.12.024

Government of Canada. (2013a). Federal government technical report: Properties, composition and marine spill behaviour, fate and transport of two diluted bitumen products from the Canadian oil sands. http://www.ec.gc.ca/Publications/default.asp?lang=En&xml=D6AB8B67-73F5-48B6-B3D1-AAE1B06FF9A2

Government of Canada. (2013b). Properties, composition and marine spill behaviour, fate and transport of two diluted bitumen products from the Canadian oil sands. (Canadian Federal Government Technical Report No. Cat. No.: En84-96/2013E-PDF). ISBN 978-1-100-23004-7

Gray, R. M. (1994). Upgrading petroleum residues and heavy oils. CRC press.

Gros, J., Nabi, D., Würz, B., Wick, L. Y., Brussaard, C. P., Huisman, J., Arey, J. S. (2014). First day of an oil spill on the open sea: Early mass transfers of hydrocarbons to air and water. Environmental Science & Technology, 48(16), 9400-9411.

Gundlach, E. R., & Hayes, M. O. (1978). Vulnerability of coastal environments to oil spill impacts. Marine Technology Society Journal, 12(4), 18-27.

Halboose, A. T. (2010). Effect of pH and salinity on stability of crude oil water emulsions. Misan Journal for Academic Studies, 9(17)

Hollebone, B. P. (2014). Oil physical properties. Handbook of oil spill science and technology (pp. 37-50) John Wiley & Sons, Inc.

Huang, C. P., & Elliott, H. A. (1977). The stability of emulsified crude oils as affected by suspended particles. Fate and Effects of Petroleum Hydrocarbons in Marine Organisms and Ecosystems. D.A.Wolfe, Ed., Pergammon Press, 413-420.

Huang, L., Fang, H., & Chen, M. (2012). Experiment on surface charge distribution of fine sediment. Science China Technological Sciences, 55(4), 1146-1152.

Hutchinson Environmental Sciences Ltd. (2014). North Saskatchewan River: Water quality and related studies (2007-2012) final report.

International Maritime Organization. (2005). Spills of heavy fuel oils - features and countermeasures. Manual on oil pollution: Combating oil spills (pp. 195). UK: Polestar Wheatons, Exeter.

International Towing Tank Conference. (2011). Fresh water and seawater properties. (No. 7.5-02-01-03).

Israelachvili, J. N. (2011). Intermolecular and surface forces. Academic press.

Jenkins, R. H., Grigson, S. J. W., & McDougall, J. (1991). Formation of emulsions at marine oil spills and the implications for response strategies. Paper presented at the Proceedings of the First International Conference on Health, Safety and Environment in Oil and Gas Exploration and Production Part 2 (of 2), November 11, 1991 - November 14, 437-443.

Kaku, V. J., Boufadel, M. C., Venosa, A. D., & Weaver, J. (2006). Flow dynamics in eccentrically rotating flasks used for dispersant effectiveness testing. Environmental Fluid Mechanics, 6(4), 385-406. 10.1007/s10652-006-0003-3

Kanicky, J. R., Lopez-Montilla, J., Pandey, S., & Shah, D. (2001). Surface chemistry in the petroleum industry. Handbook of applied surface and colloid chemistry (pp. 251-267) John Wiley and Sons Ltd New York.

Kester, D. R., & Pytkowicx, R. M. (1967). Determination of the apparent dissociation constants of phosphoric acid in seawater. Limnology and Oceanography, 12(2), 243-252.

Khelifa, A., Stoffyn-Egli, P., Hill, P. S., & Lee, K. (2002). Characteristics of oil droplets stabilized by mineral particles: Effects of oil type and temperature. Spill Science and Technology Bulletin, 8(1), 19-30. http://www.sciencedirect.com/science/article/pii/S1353256102001172

Khelifa, A., Stoffyn-Egli, P., Hill, P. S., & Lee, K. (2005). Effects of salinity and clay type on oil–mineral aggregation. Marine Environmental Research, 59(3), 235-254. http://www.sciencedirect.com/science/article/pii/S0141113604001680

King, T. L., Robinson, B., Boufadel, M., & Lee, K. (2014). Flume tank studies to elucidate the fate and behavior of diluted bitumen spilled at sea. Marine Pollution Bulletin, 83(1), 32-37.

Kingston, P. F. (2002). Long-term environmental impact of oil spills. Spill Science & Technology Bulletin, 7(1-2), 53-61. 10.1016/S1353-2561(02)00051-8

LaFargue, E., & Barker, C. (1988). Effect of water washing on crude oil compositions. AAPG Bulletin, 72(3), 263-276.

Le Floch, S., Guyomarch, J., Merlin, F. X., Stoffyn-Egli, P., Dixon, J., & Lee, K. (2002). The influence of salinity on oil-mineral aggregate formation. Spill Science & Technology Bulletin, 8(1), 65-71. 10.1016/S1353-2561(02)00124-X

Lee, R. F., & Page, D. S. (1997). Petroleum hydrocarbons and their effects in subtidal regions after major oil spills. Marine Pollution Bulletin, 34(11), 928-940. 10.1016/S0025-326X(97)00078-7

Lee, K. (2002). Oil-particle interactions in aquatic environments: Influence on the transport, fate, effect and remediation of oil spills. Spill Science & Technology Bulletin, 8(1), 3-8. 10.1016/S1353-2561(03)00006-9

Lima, E. R., De Melo, B. M., Baptista, L. T., & Paredes, M. (2013). Specific ion effects on the interfacial tension of water/hydrocarbon systems. Brazilian Journal of Chemical Engineering, 30(1), 55-62.

McLean, J. D., & Kilpatrick, P. K. (1997). Effects of asphaltene solvency on stability of water-in-crude-oil emulsions. Journal of Colloid and Interface Science, 189(2), 242-253. 10.1006/jcis.1997.4807

Memarian, R., & Dettman, H. D. Energy scaling for understanding the effect of sand particles on aggregate size of crude oils (unpublished)

Montgomery, D. C. (2013). Design and analysis of experiments (Eighth ed.). Hoboken, NJ: John Wiley & Sons, Inc. http://catdir.loc.gov/catdir/enhancements/fy1206/2012000877-t.html

Montgomery, D. C., & Runger, G. C. (2010). Applied statistics and probability for engineers John Wiley & Sons.

Muschenheim, D. K., & Lee, K. (2002). Removal of oil from the sea surface through particulate interactions: Review and prospectus. Spill Science & Technology Bulletin, 8(1), 9-18.

National Oceanic and Atmospheric Administration. (2015). Why is the ocean salty? Salinity data. http://oceanservice.noaa.gov/facts/whysalty.html

National Research Council. (2003). Oil in the sea III: Inputs, fates, and effects National Academies Press.

Nordvik, A. B., Simmons, J. L., Bitting, K. R., Lewis, A., & Strm-Kristiansen, T. (1996). Oil and water separation in marine oil spill clean-up operations. Spill Science & Technology Bulletin, 3(3), 107-122.

Omotoso, O. E., Munoz, V. A., & Mikula, R. J. (2002). Mechanisms of crude oil-mineral interactions. Spill Science & Technology Bulletin, 8(1), 45-54. 10.1016/S1353-2561(02)00116-0

Özen, İ, Şimşek, S., & Okyay, G. (2015). Manipulating surface wettability and oil absorbency of diatomite depending on processing and ambient conditions. Applied Surface Science, 332, 22-31.

Poindexter, M. K., Chuai, S., Marble, R. A., & Marsh, S. C. (2005). Solid content dominates emulsion stability predictions. Energy & Fuels, 19(4), 1346-1352.

Sjoblom, J., Aske, N., Auflem, I. H., Brandal, O., Havre, T. E., Sther, O., Kallevik, H. (2003). Our current understanding of water-in-crude oil emulsions. Recent characterization techniques and high pressure performance. Advances in Colloid and Interface Science, 100-102, 399-473. http://dx.doi.org/10.1016/S0001-8686(02)00066-0

Stewart, P. L. (2010). Oceanographic measurements - salinity, temperature, suspended sediment, turbidity, minas passage study Site.

Stoffyn-Egli, P., & Lee, K. (2002). Formation and characterization of oil–mineral aggregates. Spill Science & Technology Bulletin, 8(1), 31-44.

Tadros, T. F. (2013). Emulsion formation and stability John Wiley & Sons.

Tambe, D. E., & Sharma, M. M. (1994). The effect of colloidal particles on fluid-fluid interfacial properties and emulsion stability. Advances in Colloid and Interface Science, 52, 1-63.

Tchoukov, P., Yang, F., Xu, Z., Dabros, T., Czarnecki, J., & Sjoblom, J. (2014). Role of asphaltenes in stabilizing thin liquid emulsion films. Langmuir, 30(11), 3024-3033.

Teal, J. M., Farrington, J. W., Burns, K. A., Stegeman, J. J., Tripp, B. W., Woodin, B., & Phinney, C. (1992). The west Falmouth oil spill after 20 years: Fate of fuel oil compounds and effects on animals. Marine Pollution Bulletin, 24(12), 607-614.

Trefalt, G., & Borkovec, M. (2014). Overview of DLVO theory www.colloid.ch/dlvo

Tsai, W., Lai, C., & Hsien, K. (2006). Characterization and adsorption properties of diatomaceous earth modified by hydrofluoric acid etching. Journal of Colloid and Interface Science, 297(2), 749-754.

Venosa, A. D., & Holder, E. (2011). Laboratory-scale testing of dispersant effectiveness of 20 oils using the baffled flask test. US Environmental Protection Agency, 600-699.

Wang, Z., Hollebone, B. P., Fingas, M., Fieldhouse, B., Sigouin, L., Landriault, M., Weaver, J. W. (2003). Characteristics of Spilled Oils, Fuels, and Petroleum Products: 1. Composition and Properties of Selected Oils. US EPA Report EPA/600-R/03, 72

Wei, Q., Mather, R. R., Fotheringham, A. F., & Yang, R. D. (2003). Characterization of water-in-crude oil emulsions in oil spill response. Journal of Environmental Sciences, 15(4), 506-509.

Zhou, J., Dettman, H., & Bundred, M. (2015). A comparative analysis of environmental behaviour of diluted bitumen and conventional crudes. Paper presented at the AMOP, 495-516.

Appendix A: Energy Scaling Paper

Energy Scaling for Understanding the Effect of Sand Particles on Aggregate Size of Crude Oils

Ramin Memarian, Heather D. Dettman

Canmet ENERGY, Natural Resources Canada

Devon, Alberta, Canada

Abstract

The objectives of this study were to identify the variations of energy dissipations in the jar tests for the rapid mixing of crude oils and to determine whether sand –oil aggration for conventioal crude oil (CC) are similar to diluted biutmen (DB) derived from the Alberta oil sands mines. Energy disspation rates were quantified by a predictive model, defined as a finction of amplitude measure corresponding to the speed quantity.The comparable rates of energy including 1.1×10^{-2} m^2s^{-3}, 1.4 $m^2s^{-3}$and 10.6 m^2s^{-3},which are made up of breaking waves, were used for assessing the role of sand particles on the agreggation proceses. In the case of CC, sand–CC agreggation appears to be less affected by varying of energy dissipation. In contrast, the DB is very sensitve to the change of energy in the test jars. For the DB, high energy dissipation rate yields low agreggation result even in the percence of increased bulk sand while increasing dispersion. Hence, the sand-DB agreggation rate should be largely controlled by its physico-chemical properties not the rate of the energy. A dissipation rate of 1.1×10^{-2} m^2s^{-}

^{3} simulating the field scale energy was found to be effective and optimal to form sand-oil aggregation for both crude oils tested.

Keywords Energy modeling, amplitude simulation, breaking and non-breaking waves, oscillatory Reynolds number

1.Introducation

After a spill of crude oil into water, wave action can cause the transport and fate processes such as oil–sediment aggrgation, settling, emulsion formation and resuspension To undersatnd the variability in behavior of different crude oils, lab-scale and test tank studies are being performed. For the lab-scale rotary agitator being used at CanmetENERGY, the rotation speed, jar geometry, and liquid volume were all found to influnce the energy dissipation. Fingas (2005) calculated energy dissipations in a swirling flask and a large 300 L tank and noted that vertical mixing is much lower in the swirling flask than in the large tank. It is well known that fluid energy plays a significant role in many chemical - physical processes. Modeling of flow regime will differ based on the liquid properties and vessel geometry and experiment setting. Also, models can be useful tools to be able to compare results between different types of test equipment, or conditions found in open water. Sand–oil aggregates are known to possibly form when the energy of the water-oil system is high enough. Consequently, it is important for experiments with rotary agitator equipment, a lab-scale status, to understand when the conditions of the experiment are in breaking waves. Reynolds number counts have been applied commonly to integrate three main properties (density, viscosity and speed) of a flow for identifying its regime. In this way, scientists have developed the distinctive types of equations to calculate Reynolds number. Ni et al., (2003) suggests that the oscillation behaviour of fluid in a closed system is defined by the oscillatory Reynolds number, Eq. (1), as follows

$$Re = \frac{2\pi\, f\, A\, pD}{\mu} \quad (1)$$

Where, D = column diameter, m; p = density, kg/m^3; μ = viscosity, kg/ms; f = oscillation frequency, Hz ; A = amplitude length, m. The later describes the wave behaviour traveling in the jar during rotation. The oscillatory Reynolds number may characterize the mixing intensity (Ni and Gough, 1997). For laboratory scales, Bache and Rasool (1996) presented Reynolds number in a form of, $Re = Ud/\nu$ where U is the speed and d is the cylinder diameter and ν represents the kinematic viscosity. Thus, they obtained a wide range of *Re* up to 10 000 and flow has been considered as a laminar status for $Re < 200$. In a given test pipe, for Reynolds number greater than 1000, flow considers to be a turbulent regime (Cartland and Fitzpatrick, 2007) while at low rate $Re <$ 1000 corresponds to laminar flow (Ni et al., 2003). Earlier, Spriggs (1973) suggests that laminar flow exists if $Re < 2000$ and also *Re* between 2000 and 3000 should be considered as transient regime. The oscillatory Reynolds number will also specify that for a system where the oscillation amplitude is zero, no turbulent flow is expected so the resulting energy dissipation negligible. A rise in the jar volume would result in improved mixing because it strengthens more corresponding flow in axial and radial directions. However, the effects of energy dissipation on mineral partials-oil interaction have not yet been fully evaluated. For instance, under what level of energy is the effect of mixing likely to be important?

Extensive laboratory attempts have been dedicated for investigating the oil–sediment aggregation based on their devices, generating different levels of energies and often in short-time periods. In general, results obtained in laboratory scales are more stable than that in field scales because of control conditions. However, energy may not predict accurately oil– mineral particles aggregate rates that, in part, depend on the water chemistry, oil properties and time. For instance, as the degree of solubility of the oil components decreases from resins to asphaltenes, thereby stable emulsions are expected

to contain more asphaltenes and less resin (Hoshyargar and Ashrafizadeh, 2013). In response to physical forcing, the rate of turbulent kinetic energy will differ quickly in time and space by up to several orders of magnitude (Skyllingstad et al., 1999). Homogenous turbulent is then defined as a flow that statically tends to be unchanging in time, uniform in space without having preferential direction. The lack of a general solution to the governing Navier–Stokes equations means that there is no fundamental theory of turbulent (Bradley et al., 2011). Navier-Stokes equations are known as basic governing equations for turbulent flow modelling. Energy in terms of kinetic energy is well known by

$$E_k = \frac{1}{2} mv^2 \tag{2}$$

As seen, the kinetic energy is equal to the half of mass m, kg, multiplied by the square of speed v, m/s. To estimate the energy dissipation, the energy dissipation could be proportional to the angular frequency and amplitude length (D'Asaro and Lien, 2007) according to

$$\in \sim \omega^3 A^2 \tag{3}$$

Where $\in$ = energy dissipation, m^2/s^{-3}; ω = angular frequency, 1/s; A= amplitude length, m. The above equation was applied to approximate the energy dissipations over a desired region in this study.

2. Experiment setup

The experiment setup consists of 2.45 ± 0.05 L jars and a rotary agitator (Fig.1). Each jar contained 600 mL of water and 28 ± 2 mL of crude oil, a liquid to liquid weight ratio of 20:1. Two types of fresh crude oils; Mixed Sweet Blend and Cold Lake Blend,

were chosen for the assessment because of their highest volume of transportation across Canada. Mixed sweet blend is a conventional crude oil (CC) and Cold Lake Bend is classified as diluted bitumen (DB), their density and viscosity are listed in Table 1.

Table 1 Densities and viscosities of fresh crude oils at 25° C*

Name of crude oil	Density (g/mL)	Viscosity (cSt)
MSB, CC	0.8212	5
CLB, DB	0.9247	219

*Zhou et al., 2015

Sand 50-70 mesh practical size was purchased from Sigma-Aldrich and used in the amounts of 2000 ppm and 5000 ppm for assessing its aggregation with CC and DB. After adding the crude oils to the jars, which previously contained the water and arbitrary chosen sand rates, the samples were agitated using an orbital agitator for a period of 12 hours at room temperature. The agitator is capable of generating the speeds in the range of from 2.3 to 55.6 rpm. Three constant speeds chosen for study were 16.4, 33.1 and 55.6 rpm to examine the advantage of breaking waves on the aggregation of sand-crude oil. As suggested by Kaku et al. (2006), density 998.2 kg/ m^3 and viscosity 0.001 kg/ ms of water were taken to account for the Reynolds numbers and to estimate for energy dissipation as well.

After 12 hours of agitation, the jars were placed on a bench top and remained undisturbed. The formation of sand- crude oil aggregates was observed and their status were recoded using a high resolution camera over the course of the test.

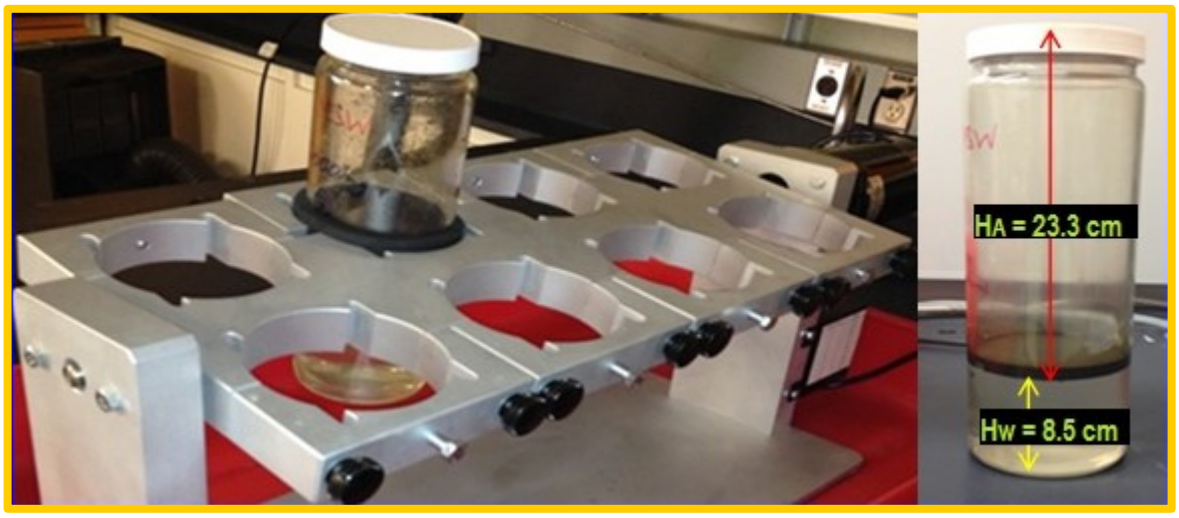

Fig. 1. Experiment setup, an orbital agitator and a jar sample

3. Results and discussion

3.1. Jar Test as Closed System and Kinetic Energy

First it is required to know how kinetic energy changes during the jar rotation. Here, as we have a closed system so the water has a reciprocal role in the generation of kinetic energy, increasing and decreasing with different water volumes in the jar. Although the water speed in the jar is a function of the speed of the agitator, but decreasing when the water exceeds a certain height of the jar. At a specific point shown in Fig. 2, adding water to the jar will have a reverse effect on kinetic energy as there is less space available for water turnover in the jar. Sufficient speed must be available for turnover of the oil and water due to agitations of flow and sand loading.

As noted earlier, the water properties are substituted for the density and viscosity of the fluid mixture to calculate kinetic energy and the resulting dissipation of energy. The

total kinetic energy of the water traveling at a distance l (available length in the jar) from the y- axis can be determined by Eq.(4) is:

$$K = \tfrac{1}{2}\, mv^2 = \tfrac{1}{2}\, m\, (l\omega)^2 = \tfrac{1}{2}\, (m\, l^2)\, \omega^2 \qquad (4)$$

Where $\theta = m\, l^2$ is the moment of the water mass with respect to the y- axis and ω is the angular frequency and m is the water mass. To achieve the efficiency maxing maximum, therefore, we conclude the variables m and l optimized so that the θ output is enlarged.

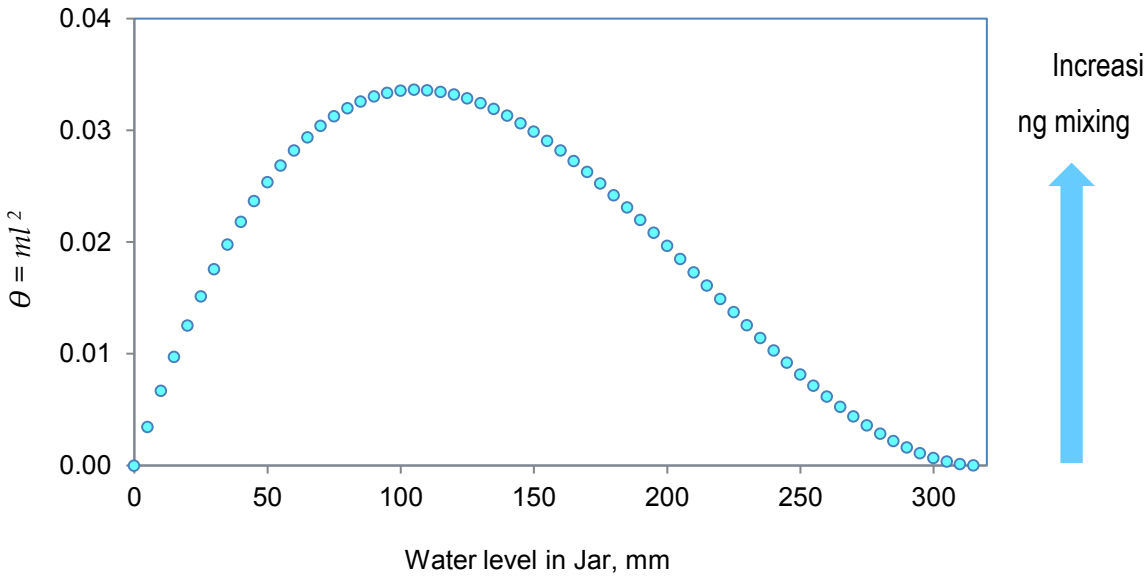

Fig. 2. Relation between θ and water level in jar reflecting mixing efficiency

The arrangement of the θ variable results in a very obvious and characteristic behavior shown in Fig. 2. As can be seen, the profile of θ through a cross segment of the water has a nearly parabolic shape. The water level 105 mm having a peak value of θ = 0.03363 is noted which results in a maximum efficiency of the mixing. If H_A and H_w

were chosen equal, generation of the kinetic energy as a result could have a lower value based on the θ analysis. However, in our case Hw = 85 mm, the θ measures a comparable value of 0.03257.

The indication of θ provides the potential for generating the kinetic energy, computed on basis of the different distance plus corresponding mass at which the latter limits the speed when Hw > 110 cm. In this case, the profile of the speeds begins to lower and should follow a trend as the θ, similar to that shown in Fig. 2. Hence, the greater the θ value, the higher the kinetic energy in the jar at highest speed set. In the next part, we can see l given in Eq. (5) is then defined as maximum possible amplitude in our system.

3.2. Analysis of Amplitudes and Modeling

Through knowledge of the amplitudes, it is possible to afford Eq. (3). Because of difficulty in measuring the amplitudes for the breaking waves, the models proposed Eq. (6) and (7) were needed to simulate the amplitudes corresponding to the agitator speeds.

The key observation of the tests was that no change in the patterns of the flows occurred for speeds higher than 45 rpm. Fig. 3 illustrates these situations and indicates the internal flow patterns are not amplitude limited. To explore the trend, the proposed model was to correlate the observed amplitudes with their velocities and then estimating the quantities of the unknown amplitudes for the other cases (Fig. 4.). In all situations, the amplitudes tend to enlarge as speed is increased. In practice, the largest waves in the test jars are these that raise the largest amplitude defined by Eq. (5)

$$A_{max} = l = H_A \tag{5}$$

H_A is the jar height that is empty. The maximum amplitude A_{max} is equal to H_A value. Hence, that maximum excursion is the approximate distance a droplet will travel along the main axis of the jar in going from the top of the water to the top of the jar or vice-versa. As a consequence, for the three flow patterns linked to the 46.9, 54.1 and 55.6 rpm, a maximum amplitude of A_{max} = 23.3 cm seems to have been reached and presents itself being responsible for these cases. Low velocities of 2.3 and 8.2 rpm generate identical amplitudes which measure about 0.4 and 2 cm, respectively (Fig. 3.a and 3.b). For simplicity, assuming that the components of the velocities (*u, v, w*) are essentially the same restricted to homogeneous flows in all situations. Alternatively, the quantity H_A may be defined as the maximum capacity of the jar that the highest energy dissipation can occur. Since $H_A > H_w$, water in the jar should move at the similar speed as the agitator. The quantitative model then for amplitude analysis in the jar is one in which the amplitude of the different speeds is less than A_{max} value. Therefore, we expect that Eq. (6) serving as the amplitude model can reasonably describe the variation in the amplitude

$$A = \frac{Amax}{1+exp[\,-(\,aS-b\,)\,]} \tag{6}$$

Where A is the amplitude in cm and A_{max} is the ultimate amplitude, defined by Eq. (5) and the letter *a* and *b* are the coefficients to the equation. For this model, the driving force for generation of the amplitude condition is given by the difference of the ultimate value and amount that can

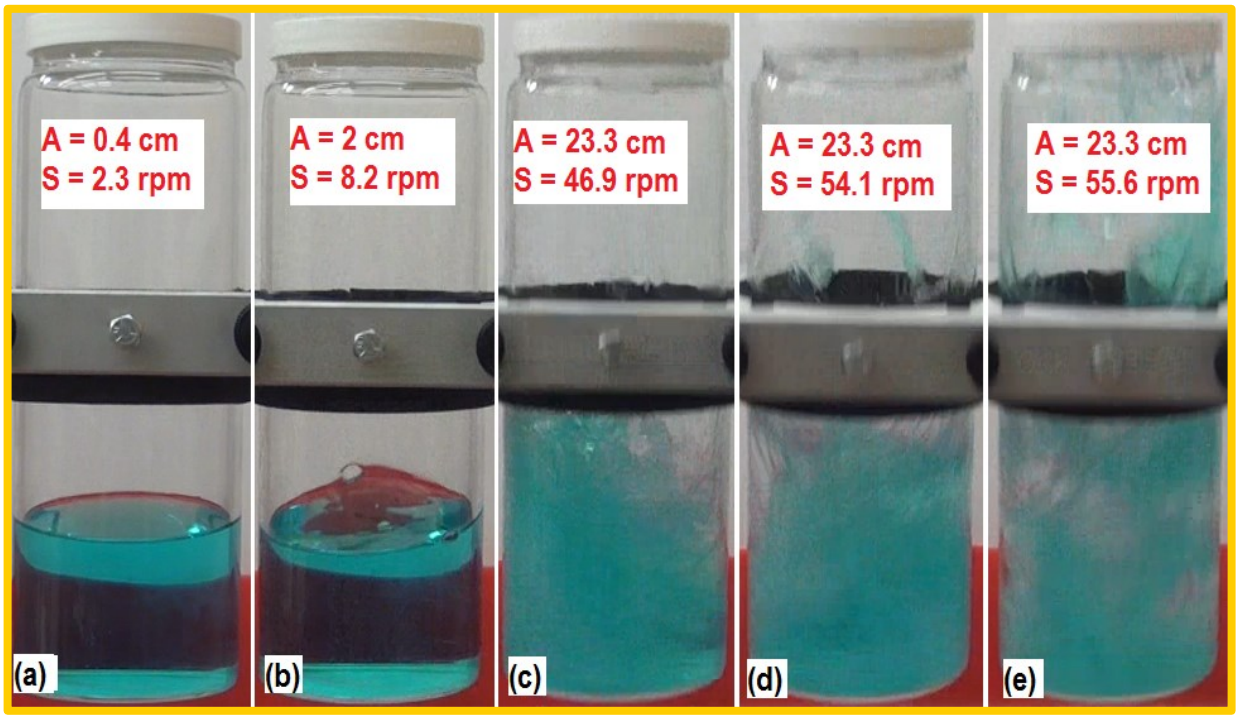

Fig. 3. Key observations taken as inputs to the model. (a) Wave with A = 0.4 cm for S = 2.3 rpm. (b) Wave with A = 2 cm for S = 8.2 rpm. Images (c), (d) and (e) show visually similar patterns, assuming their amplitude being the maximum possible value, A_{max} = 23.3 cm

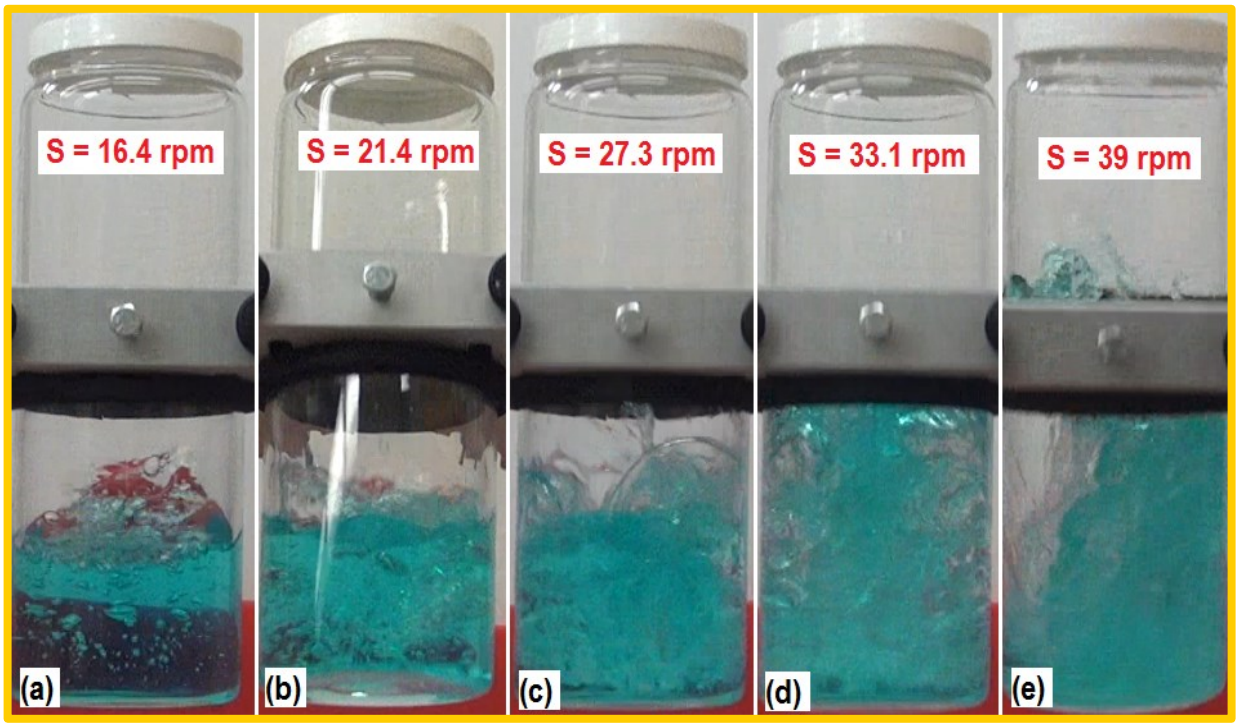

Fig. 4. Flow patterns of remaining velocities from the breaking waves aimed at finding their unknown amplitude

exist in the jar. The rate of change of the amplitude with respect to the speed can then be considered to be proportional to this difference. To assess the proposed model, modeling efficiency (*EF*) was applied as suggested by (Bensadoun et al., 2013; Golmohammadi et al., 2014) that is

$$EF = \frac{\sum_{i=1}^{n}(x_i-\bar{x})^2-\sum_{i=1}^{n}(y_i-x_i)^2}{\sum_{i=1}^{n}(x_i-\bar{x})^2} \quad (7)$$

Where, x_i and y_i denote measured and modeled values, $\bar{x}$ is the mean of measured values and n is the number of values considered. If modeled values perfectly match the measured ones then *EF* could be equal to unity. Typical values of the unknown

amplitudes were obtained to be in the range from 16.4 to 55.6 rpm enclosing the domain of the breaking waves. Successful application of the sigmoidal model can be proved by *EF* = 0.99, implies it has excellent predictability for the five known amplitudes as shown in Fig. 5. Therefore, this geometry-based model is promising in sizing of the unknown amplitudes relative to the remaining speeds ranging from 16.4 up to 39 rpm.

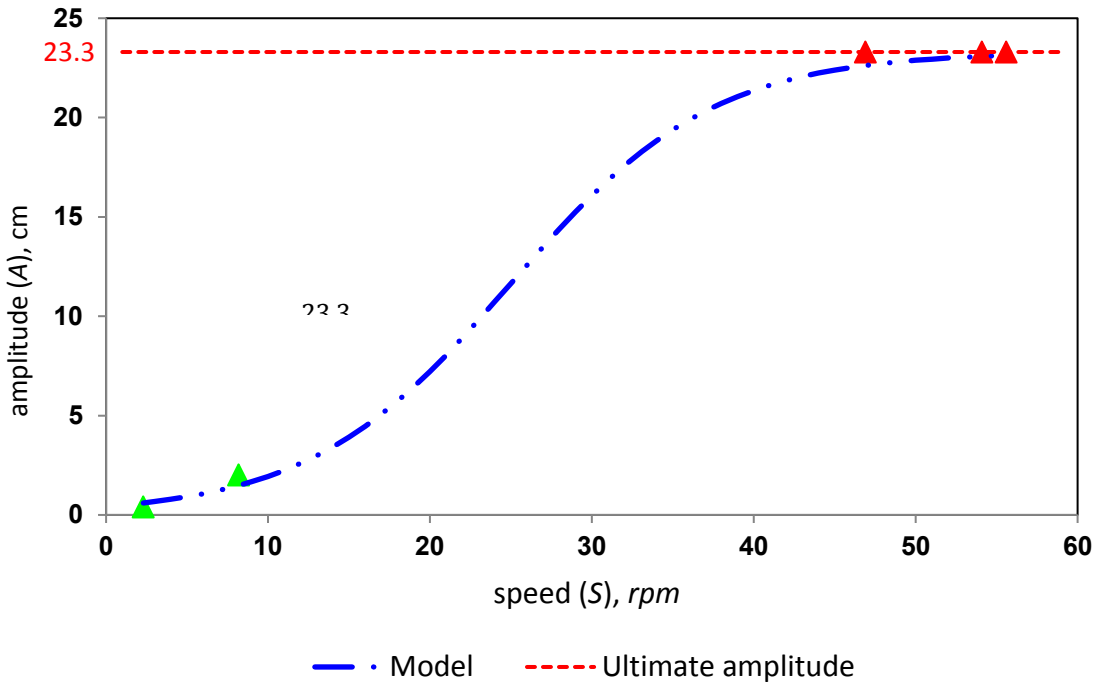

Fig. 5. Modeled amplitudes as function of speed. Measured amplitudes and flow pattern amplitudes analyzed are shown in green and red triangles, respectively.

3.3. Estimate of Energy Dissipation from Kinetic Energy

The value of the energy dissipation is attributable once Reynolds number has occurred for some time. Of course, it takes more time for non- breaking waves to fully

develop along the jar. As seen in Table 2, the two major parameters studied here namely the amplitudes and their oscillatory Reynolds numbers. Clearly, Reynolds values for the situation of non-breaking waves are much lower than that for the breaking waves. This is known as solid body motion, where shear flow or speed gradient is essentially absent (Venosa et al., 2005). The unknown amplitudes were explored by using the proposed model and its high *EF* indicated the level of acceptance.

Table 2 Characterized amplitudes and resulting dissipation of energies

Speed of agitation		Amplitude (cm)	Amplitude modeled (cm)	Oscillatory Reynolds number	Flow regimes, observed	Kinetic energy (J)	Dissipation of energy (m^2/s^3)
rpm	1/s*						
2.3	0.04	0.4**	0.6	96.29	Non-breaking waves	0.0002	n.a
8.2	0.14	2**	1.48	1,716		0.004	n.a
16.4	0.27	Unknown	4.7	19,568	Breaking waves	0.018	1.1×10^{-2}
21.4	0.36		8.38	31,806		0.036	7.8×10^{-2}
27.3	0.46		13.77	47,719		0.064	4.4×10^{-1}
33.1	0.55		18.30	64,093		0.1	1.4
39	0.65		21.06	80,415		0.14	3
46.9	0.78	23.3 analyzed	22.62	104,068		0.24	6.1
54.1	0.90		23.08	122,309		0.277	9.7
55.6	0.93		23.14	125,700		0.281	10.6

* angular frequency

** measured

Table 2 illustrates the characteristics of the kinetic energies and resultant energy dissipations obtained by applying equation 2 and 3, respectively. For breaking waves when aggregation is believed to be formed, the energy dissipation is more efficient with a value starting at 4.4×10^{-1} m^2/s^3 and increasing to 10. 6 m^2/s^3. Such wide range of powerful energies makes the agitator capable of generating various types of aggregates and also their possible mixtures with fine minerals. With increasing dissipation, the aggregates formation is believed to be enhanced by speed gradient due to the wave action. There are significant changes in the dissipation rates of the breaking waves, suggests that sand-oil aggregation may be regulated by changing of the mixing energy.

In spite of such variability, change in the aggregation process between the two first speeds set (2.3 and 8.2 rpm) may be less pronounced. High energy by itself often is not sufficient to achieve a desired rate of aggregates. In this regard, longer mixing time involving higher energies will be required for increasing homogeneity of the mixture to achieve more the aggregates formation. In ambient conditions, if energy becomes more strongly increasing such that aggregates are formed, it may be characterized as an energetic environment such as tidal fronts.

It been has observed that non-breaking waves devoid of turbulence fail to effectively transport the mixture within the jar. If solvent and solute have the same properties, non-breaking waves should be practical approach to influence on the mixing results. At an oceanic scale, different areas of water exhibit characteristic levels of $\in$, not uniform in terms of energy distribution.

Table 3 Some work for energy dissipation recorded in nature

Water body and location	Dissipation rate (m^2/s^3)	Reference
Windermere Lake, U. K	~ 10^{-5}	*Simpson et al., 2015*
Columbia River, Washington State	$10^{-6} - 10^{-2}$	*Thomson et al., 2014*
Chukchi Sea, Alaska	$4.4 \times 10^{-9} - 5 \times 10^{-7}$	*Shroyer , 2012*
Snohomish River, Washington State	$3\times10^{-6} - 2\times10^{-4}$	*Chickadel et al.,2011*
Atlantic Ocean, North Carolina coast	$10^{-5} - 10^{-4}$	*Feddersen et al., 2007*

Alpnach Lake, Switzerland	$10^{-8} - 10^{-6}$	*Wuest et al., 2000*
Atlantic Ocean, Maryland coast	$10^{-4} - 5\times10^{-4}$	*Drennan et al., 1996*

These areas can be classified into four regions namely (i) open ocean (ii) shelf seas (iii) costal zones (iv) tidal fronts, ranging from the lowest dissipation to the highest (Kiørboe and Saiz, 1995). In comparison, the non-breaking cases in Table 2 could be subject to the ocean where waves mostly are in non-breaking status with negligible energy at the surface. Inspection of Table 3 shows energy dissipation in nature vary depending on hydrological conditions, with an overall average of about 10^{-5} m^2/s^3. Li et al. (2008) have estimated an energy rate of 0.05 m^2/s^3 of the breaking wave under a wave tank condition. To compare that rate with a marine scale, Terray et al. 1996 reported that energy dissipation varies between 10^{-5} and 10^{-2} m^2/s^3 at a wave height of 0.25 m in Lake Ontario, which is a more close value to that computed for 16.4 rpm. Examination of performance features of various devices given by Paul et al. (2004) indicates that most of our energy results fall within the agitated vessel device, whose energy dissipations ranged from 0.1 up to 100 m^2/s^3.

3.4. Visualization of sand- oil aggregates and differences

3.4.1. Phase I: test at energy dissipation of 1.1×10^{-2}

As seen from Fig.6, the aggregates in the jars containing conventional crude are considerably larger compared to the jars contain diluted bitumen. Increasing the sand amount increases aggregates formation with less turbidity. At this rate of energy which breaking waves are initiated, adhesion of the oil products to the jar surface having a height of 8.5 cm is noticeable. Given the experimental conditions, the result of this

dissipation rate which normally found in the water environment could correspond to the oil spill occurring in nature. Therefore, this phase of the study could be representation of what occurs in the oil - affected area, specifically in cold waters where volatilization is slow due to the temperature effect. However, high turbidity is obtained for the jar having CC with 2000 ppm sand (Fig. 6a) in comparison to the same oil with 5000 ppm sand. Because the high rate of the sand produces a higher amount of sand- oil aggregates, resulting in less dispersion. Comparison of this situation with the DB suggests that chemical products of the CC have entered the water more rapidly because of higher turbidity seen and if turbidity is an indication in this regard. However, this difference strongly depends on the viscosity of the crude oils so DB products have tended to flow and turnover much slower. Oil viscosity alone should be a partial barrier to re-coalescence of water droplets (Fingas and Fieldhouse, 2006).

For both the crude oils, low turbid results are yielded when the bulk sand was high. Therefore, the sand particles decreased rather than increased the levels of turbidity in the test jars. If mineral testing was clay particles that largely differ in its properties, mineral – oil aggregates and resulting turbidity were different. In this case, effectiveness of clay particles to decrease water turbidity or increase the aggregation could be questionable to use for water remediation. Despite the relatively high turbidity observed for CC test, no considerable difference between the performances of CC vs DB in terms of sand- oil aggregates exist, specifically when the high rate of the sand is applied (Fig. b and Fig. d). Changing sand particles from 2000 ppm to 5000 ppm resulted in a higher amount of spherical aggregation to be formed, which possibly indicates the formation of the stable species of the aggregates.

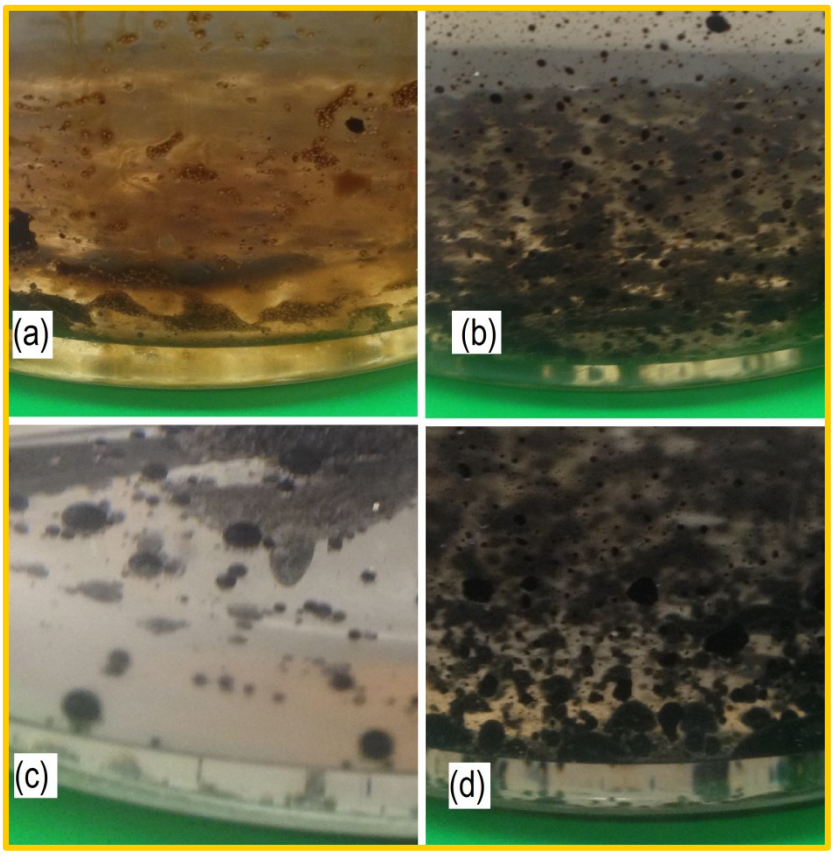

Fig. 6. Detection of sand- oil aggregates observed at energy dissipation of 1.1×10^{-2} m^2s^{-3} CC with 2000 ppm sand (b) CC with 5000 ppm (c) DB with 2000 ppm and (d) DB with 5000 ppm sand

Therefore, a possible solution for remediation of shallow and quiescent waters to lower dispersed oil and turbidity when dealing with oil spill, is that sand particles should be not only applied to the spill-affected area but properly adjusted to the spill dimensions. Sedimentation process will be involved further with its drawbacks because of sediment accumulation that may interfere with hydrologic cycle.

3.4.2. Phase II: test at energy dissipation of 1.4

With applying the energy dissipation of 1.4 m^2s^{-3}, the results are quite complicated. Figure 6 illustrates the distribution pattern of sand-oil aggregates varying depending upon the rate of sand particles. In the absence of the sand, no CC aggregates were observed; hence CC itself could not sink over the course of this study. The sand-CC aggregate for the jar containing 2000 ppm sand particles occurred highly variable in size, in which all of the sand gains had undergone the aggregation process. With 5000 ppm sand, the size of the sand-CC aggregate increases but more uniform and spherical compared to the prior case having the concentration 2000 ppm (Fig. 7.a).

For diluted bitumen (DB), the observed effect is less quantifiable and different, causing most of the sand gains are unaffected. The sand-DB aggregation contains fewer aggregates as a result of using 2000 ppm sand, which the produced aggregates have relatively the same size as the sand particles. Small-sized aggregates remain separated from each other and no longer tend to growth into larger sizes compared to the phase I. This process of the aggregation makes the oiled particles to have low vertical velocities for removal in an actual spill. Exposure of DB to 5000 ppm sand did not significantly affect the sand-DB aggregate size which suggested that there is a large threshold effect of DB on the aggregation process. The profile of sand-CC aggregates displayed in Figure 6.a is visually comparable to that of dilbit shown in Figure 6.b.

For both cases, there is no submergence of oil products in the absence of the sand sediment. It is reasonable that the first step to initiate the aggregates to be formed requires to oil slick breaks up and then generate and raise the dispersion to increasing the probability of the interaction with sand particles. Second step is that it should have affinity to adhere to the sand particles, resulting in more stable aggregates. Even though, the two steps are identical here in our system, but diluted bitumen undergoes a surprising interaction at high energy applied. The DB aggregation with sand particles is inappreciable and is limited to the small size of the spherical shaped aggregates and unlikely to be amorphous (Silva et al., 2015). Also, it could be inferred that flocs

experinced a breakage process(Nan et al., 2016). However, the DB results may not be in agreement with results that showed fine oil droplets facilites formation of more marine oil snow (MOS) together with a much higher oil content in the resulting MOS (Fu et al., 2014).

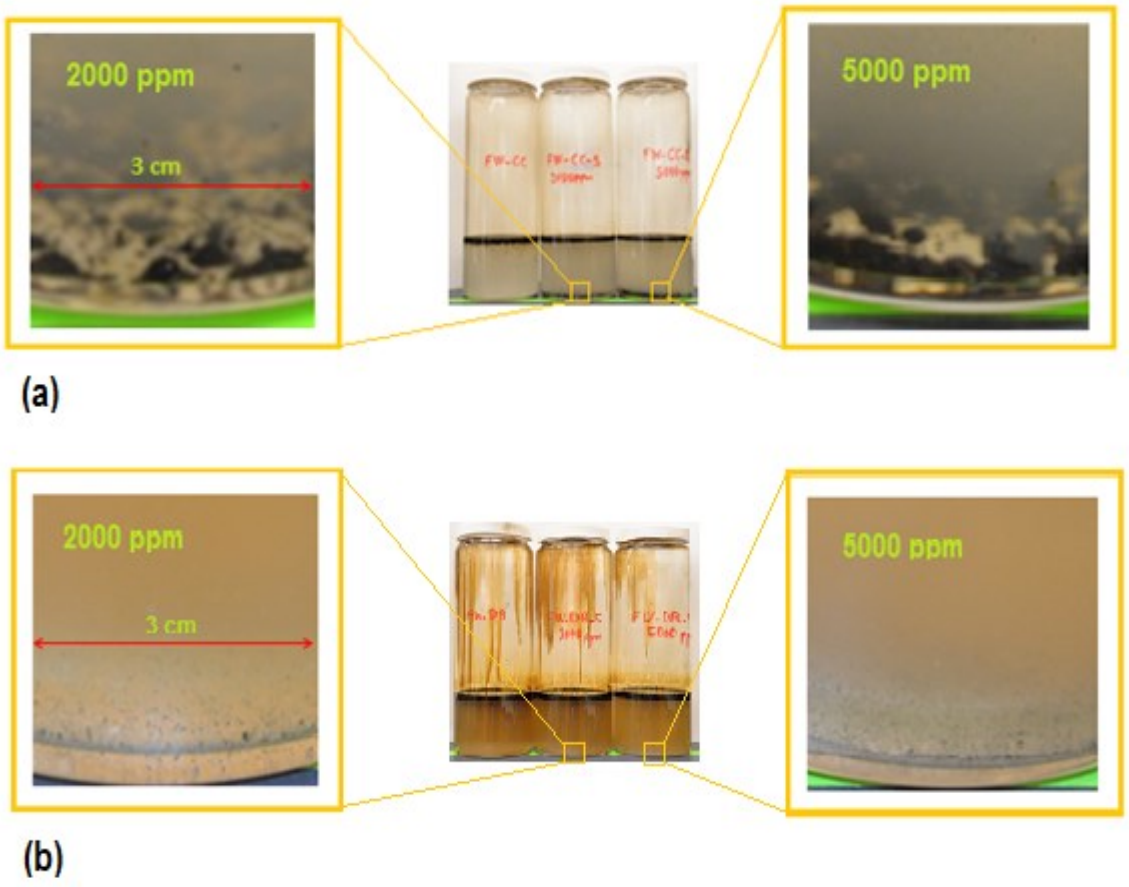

Fig. 7. Detection of sand- oil aggregates observed at energy dissipation of 1.4 m^2s^{-3}. (a) Image of CC- sand aggregates, large spherical shaped aggregates, caused aggregation of all sand particles. (b) Images of sand-DB aggregates. Black points represent aggregates which are relatively similar in size as sand particles. In the case of DB, most sand particles remained unaffected.

The prevalence of DB aggregates over the test is due to this fact that less asphaltenes could be mixed as opposed to resins, and corresponds to the level of the energy applied. The situation observed for DB should be linked to high contents of resins associated with less asphaltenes. During the breaking waves known turbulence cascade, DB has formed two distinct phases; first phase is in the mixing zone and the next phase strongly attached to the surface of the jar, acts as a stationary media, where it would equilibrate with the water over the time. Due to high viscosity, about 30 % dilbit has prevented itself from being mixed and thus did not contribute to the dispersion. However, the mass shearing between those phases is a kinetic energy rate – response relationship. Given the crucial role of energy rate in mixing, the qualitative behavior of diluted bitumen tends to be less affected by increasing sediment than what is seen for conventional crude test.

3.4.3. Phase III: test at energy dissipation of 10.6

At this dissipation of energy 10.6 m^2s^{-3} corresponding to the velocity of 55.6 rpm, conventional crude oil keeps its tendency to produce more oil-sand aggregates in comparison to dilbit. Nevertheless, higher water turbidity obtained belongs to the dilbit rather than conventional crude, different than seen in the two previous tests, phase I and II. The CC tests have shown a transparent white color and were relatively stable during the 10-day observation. However it doesn't constitute a criterion for its toxicity assessment which significantly varies with PAHs (polycyclic aromatic hydrocarbons) contents of oil. A full analysis of the chemical compositions of the oil under a given condition is needed for this propose known as an intense concern in water quality.

The increased dispersivity due to more DB products into the water did not lead to increased DB- sand aggregates in the jar tests. Not only do higher energies result in lower DB- sand aggregates, but they increase dispersion of dilbit into the water column which made the water more turbid. The energy balance then becomes more important since the sand-DB aggregation may be stimulated by excess energy input. The magnitude of energy applied, 10.6 m^2s^{-3}, could be subject to static mixer devices (Paul et. al., 2004)

which is less common in oil spill in nature. However, the residual oil products adhered to the jar surface after 12-h of agitation was insignificant for both the crude oils tested. Subtle differences in the turbidity for the DB tests had a negligible effect on their aggregation process. In Fig 8.c and 8.d, the turbidities are obvious but not identical to the aggregations of DB tests. Although, conventional crude test generated a lower water turbidity compared to DB, it had significantly higher sand-oil aggregates but seems to be less that of phase II. Increasing sand rates from 2000 ppm to 5000 had an inverse effect on the rate of the aggregates for the CC, almost visible by comparing in Fig. 8.a and 8.b.

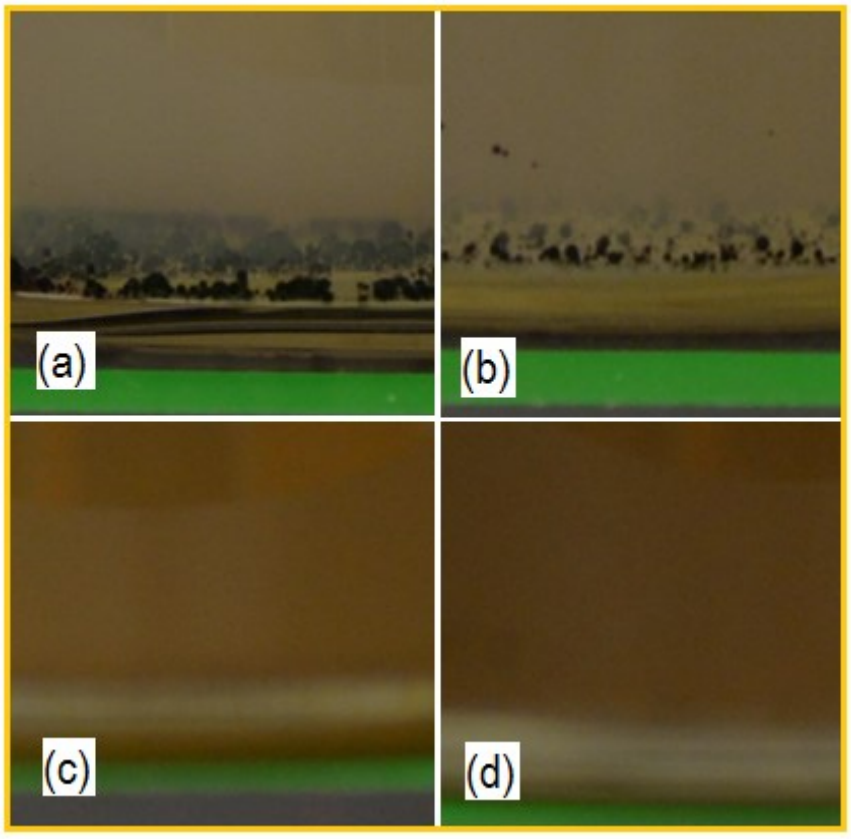

Fig. 8. Detection of sand- oil aggregates observed at energy dissipation of 10.6 m^2s^{-3} (a) CC with 2000 ppm sand (b) CC with 5000 ppm (c) DB with 2000 ppm and (d) DB with 5000 ppm sand

This complex situation should be governed by four parameters in the jars: (1) oil chemistry (2) dissipation of kinetic energy (3) ratio of oil to water and (4) ratio of oil to sand. The latter is a major that severely affected the rate of aggregates, because the other parameters were constant. This possibly indicates that the formation of sand-DB in water is unstable and highly reversible for DB. Overall and for three phases tested, if the energy was a major factor in mixing, there would be little difference between the results for CC and DB with the continuous increased dissipation of energy being applied to the jars.

4. Conclusions

The study presented here involved in determining the importance of physico-chemical properties, energy dissipation and sand-to-oil ratio on the sand-oil aggregation in the agitated vessels. A mathematical model has been developed to simulate the entire set of the unknown amplitudes, which was required for calculating of the energy dissipations due to the rotation. The typical rates of energy concern to evaluate the changes in the aggregations were applied at 1.1×10^{-2} m^2/s^3, 1.4 m^2/s^3 and 10.6 m^2/s^3. At the dissipation rate of 1.1× 10–2 m^2/s^3, the sand-DB aggregation had the same pattern as the sand-CC aggregation while has decreased dispersion because of its highly viscous products. Subsequent increase in the dissipation of the applied energy had disadvantage to sand-DB aggregation. The sand-DB aggregation drop off quickly as the mixing energy increases, even in the presence of the high- bulk sand. This indicate that the energy efficiency to promote increased aggregation beyond that of physico-chemical properties of the crude oils. Unlike, the performance of the CC appears mostly to be independent of the energy applied, and a higher rate of bulk sand caused to increase the sand-CC aggregation except for the energy rate of 10.6 m^2/s^3. Although no threshold has been detected for the optimal aggregation, observations suggest that the effective aggregation will occur in the neighborhood of 1.1×10^{-2} m^2/s^3. The simulation results showed that there exist optimum

conditions for sand-to-oil ratio and essential energy rate on the growing aggregation processes.

Acknowledgments

The authors would like to acknowledge support from the Government of Canada's Visiting Fellowship Program and Program of Energy Research and Development (PERD). We are indebted to Dr. Suzanne Kresta for her great guidance.

References

Bache, D.H., Rasool, E., 1996. Measurement of the rate of energy dissipation around an oscillating grid by an energy balance approach. Chemical Engineering Journal. 63, 105–115.

Bensadoun, A., Monod, H., Angevin, F., Makowski, D., Messéan, A., 2013. Modeling of gene flow by a Bayesian approach: A new perspective for decision support. AgBioForum. 17, 213–220.

Bradley, D.I., Fisher, S.N., Guénault, A.M., Haley, R.P., Pickett, G.R., Potts, D., Tsepelin, V., 2011. Direct measurement of the energy dissipated by quantum turbulence. Nature Physics. **7**, 473–476.

Cartland, G.M., Fitzpatrick, J.J., 2007. Modelling vortex formation in an unbaffled stirred tank reactor. Chemical Engineering Journal. 127, 11–22.

Chickadel, C.C., Talke, S.A., Horner-Devine, A.R., Jessup, A.T., 2011. Infrared – based measurements of speed, turbulent kinetic energy, and dissipation at the water surface in a tidal river. IEEE Geoscience and Remote letters. 8, 849–853.

D'Asaro, E.A; Lien, R.-C. 2007. Measurement of scalar variance dissipation from Lagrangian floats, Journal of Atmospheric and Oceanic Technology.24, 1066–1077.

Drennan, W.M., Donelan, M.A., Terray, E.A., Katsaros, K.B., 1996. Oceanic turbulence dissipation measurements in SWADE. Journal of Physical Oceanography. 26, 808–815.

Feddersen, F., Trowbridge, J.H., Williams, J.A., 2007. Vertical structure of dissipation in the nearshore. Journal of Physical Oceanography. 37, 1764–1777.

Fingas, M., 2005. Energy and work input in laboratory vessels. International oil spill conference proceedings. 1, 663–669.

Fingas, M., Fieldhouse, B., 2006. A review of knowledge of water-in-oil emulsions. Proc. 29th AMOP technical seminar. 1, 1–56.

Fu, J., Gong, Y., Zhao, X., O'Relly, S.E., Zhao, D., 2014. Effects of oil and dispersant on the formation of marine oil snow and transport of oil hydrocarbons. Environ. Sci. & Technol. 48, 14392-14399.

Golmohammadi, G., Prasher, S., Madani, A., Rudra, R., 2014. Evaluating three hydrological distributed watershed models: MIKE-SHE, APEX, SWAT. Hydrology. 1, 20–39.

Hoshyargar,V., Ashrafizadeh, S.N., 2013. Optimization of flow parameters of heavy crude oil-in-water emulsions through pipelines. Industrial & Engineering Chemistry Research. 52, 1600−1611.

Kaku, V.J., Boufadel, M.C., Venosa, A.D., 2006. Evaluation of mixing energy in laboratory flasks used for dispersant effectiveness testing. Journal of Environmental Engineering. 132, 93–101.

Kiørboe, T., Saiz, E., 1995. Planktivorous feeding in calm and turbulent environments, with emphasis on copepods. Marine Ecology Progress Series. 122, 135–145.

Li, Z., Lee. K., King, T., Boufadel, M.C., Venosa A.D., 2008. Assessment of chemical dispersant effectiveness in a wave tank under regular non-breaking and breaking wave conditions. Mar. Pollut. Bull. 56, 903–912.

Nan, J., Yao, M., Chen, T., Wang, Z.B., Li, Q, G., Zhan, D., 2016. Experimental and numerical characterization of flocmorphology: role of changing hydraulic retention time under flocculation mechanisms. Environ Sci Pollut Res. 23, 3596–3608.

Ni, X., Gough, P.,1997. On the discussion of the dimensionless groups governing oscillatory flow in a baffled tube. Chemical Engineering Science. 52, 3209–3212.

Ni, X., Mackley, M.R., Harvey, A.P., Stonestreet, P., Baird, M.H.I., Rama Rao, N.V., 2003. Mixing through oscillations and pulsations: A guide to achieving process enhancements in the chemical and process industries. Trans IChemE. 81, 373–383.

Paul, E.L., Atiemo-Obeng, V.A., Kresta, S., 2004. Handbook of industrial mixing: Science and Practice: John Wiley & Sons, Inc., Publication.

Silva, C.S., de Oliveira, O.M., Moreira, I.T., Queiroz, A.F., de Almeida, M., Silva, J.V., da Silva Andrade, I.O., 2015. Potential application of oil-suspended particulate matter aggregates (OSA) on the remediation of reflective beaches impacted by petroleum: a mesocosm simulation. Environ Sci Pollut Res. 1-13.

Simpson, J.H., Lucas, N.S., Powell, B., Maberly, S.C., 2015. Dissipation and mixing during the onset of stratification in a temperate lake, Windermere. Limnology and Oceanography. 1, 29–41.

Shroyer, E.L., 2012. Turbulent kinetic energy dissipation in barrow canyon. Journal of Physical Oceanography. 42, 1012–1021.

Skyllingstad, E.D., Smyth,W.D., Moum, J.N.,Wijesekera, H.,1999. Upper-ocean turbulence during a westerly wind burst: A comparison of Large-eddy simulation results and microstructure measurements. Journal of Physical Oceanography. 29, 5–28.

Spriggs, H.D. 1973. Comments on transition from laminar to turbulent flow. Industrial & Engineering Chemistry Fundamentals. 12, 286–290.

Terray, E.A., Donelan, M.A., Agrawal, Y,C., Drennan, W.M., Kahma, K.K., Williams, A.J., Hwang, P.A., Kitaigorodskii, S.A., 1996. Estimates of kinetic energy dissipation under breaking waves. Journal of Physical Oceanography. 26,792–807.

Thomson, J., Horner-Devine, A. R., Zippel, S., Rusch, C., Geyer, W., 2014. Wave breaking turbulence at the offshore front of the Columbia plume. Geophysical Research Letters. 41, 8987– 8993.

Venosa, A.D., Kaku, V.J., Boufadel, M.C., Lee, K., 2005. Measuring energy dissipation rates in a wave tank. In: Proceedings of 2005 International Oil Spill Conference, Miami, FL. American Petroleum Institute, Washington, DC.

Wuest, A., Piepke, G., Van Seden, D.C., 2000. Turbulent kinetic energy balance as a tool for estimating vertical diffusivity in wind-forced stratified waters. Limnology and Oceanography. 45, 1388-1400.

Zhou, J., Dettman, D.H., Bundred, M., 2015. A comparative analysis of environmental behaviour of diluted bitumen and conventional crudes, in proceedings of the 38th AMOP technical seminar on environmental contamination and response, Environment Canada, Ottawa, ON. 1,495-516.

Appendix B: Standard Operating Procedures

B.1 Mixing Tests using a Rotary Agitator

Objective

This procedure outlines the method of preparing oil-water-sediment samples to be mixed using the rotary agitator. The objective of this test is to monitor the mixing behaviour of oil, water and sediment.

Note: Conduct rotary agitation test early in the week (i.e., on a Monday) so that the mixtures can be monitored daily for the remainder of the work week. Most changes to emulsion thickness occur within two days after mixing. For overnight mixing, an electronic timer switch is used to start the agitation automatically, but caution must be taken to ensure that jars are appropriately sealed and fastened to the agitator to prevent spillage.

Sample information: The samples contain Dilbit/Conventional crude, water and sediment

Each jar contains: 600 ml water, 30 ml oil, 1.2g sediment (for 2000 ppm sediment concentration)

Safety Concerns and Personal Protective Equipment

a) Lab coat, gloves and safety glasses are required

b) Ensure area is marked with pylons when rotary agitator is in use.

c) Refer to MSDS for diluted bitumen and conventional crude (available on Devon Digest link to msdsonline.com)

Apparatus and Materials required

1. 2.2 L jars used for rotary agitator
2. Electronic balance
3. Water (tap, deionized)
4. Oil
5. Sediment
6. Teflon tape
7. Electrical tape to seal jar lids before mixing
8. Disposable pipettes
9. Graduated cylinder/beaker to add water to jar

Procedure: Oil, water and sediment tests (12h overnight mixing)

1. If using the environmental chamber, switch power to ON and set desired mixing temperature.
2. Record run temperature before start of run
3. Set desired mixing speed on agitator and confirm with optical tachometer. Record at least three consistent readings.
4. Adjust speed dial if necessary to achieve set mixing speed and repeat Step 2.
5. Set timer for mixing start and end time.
6. Plug timer into main outlet and plug agitator into timer.
7. Turn agitator power switch to ON.
8. Label jar with the appropriate descriptors (Year, oil type, Jar number).
9. Apply Teflon tape to rim of jar. Ensure to wrap it over the rim to prevent possible leaking.
10. Place jar (without lid) on scale and tare.

11. Add 600 g of water.
12. Record mass of water added.
13. Obtain density of oil at 20 °C, and calculate the mass of oil required for 30 mL of oil.
14. Tare scale again (with water in jar).
15. Add the required mass of oil (equivalent of 30 mL).
16. Record the mass of oil added to the jar.
17. If using sediment, weight 1.2g of sediment (2000 ppm concentration).
18. Record the mass of sediment added.
19. Secure lid on jar.
20. Use electrical tape around lid to prevent spillage during mixing.
21. Record water height (WH), and water+oil (Total height = TH).
22. Allow jars to rest for 4 hours to thermally equilibrate.
23. Mount camera on tripod and confirm camera settings are set to automatically take pictures (see camera instruction manual).
24. Mount jars on rotary agitator.
25. Place pylons to block off area in front of unit while it is running for safety of other lab personnel.
26. After mixing test is complete, remove jars.
27. Allow jars to rest for 1h.
28. Using an optical tachometer, obtain three readings of mixing speed.
29. Average the readings before mixing (Step 3) and after mixing (Step 28) to obtain run mixing speed value.
30. Record post-mixing temperature.
31. Average the readings before mixing (Step 2) and after mixing (Step 30) to obtain run mixing speed value.
32. Record height of water (WH) , and water+oil (Total height = TH) for each jar
33. To monitor emulsion thickness, take daily WH and TH measurements for 7 days (or increase duration depending on test)

34. To separate the oil, water and sediment fractions use a 1L separatory funnel

Clean Up

Note: Do not use an ashing oven to remove oil from jars since any sediment present therein may anneal to the jar's surface causing their transparency to deteriorate.

1. Once all desired oil, water and sediment have been removed from the jar, discard the Teflon tape from around the jar rims.
2. Use toluene to clean jars.
3. Collect all contaminated hydrocarbon waste in an appropriately labelled pail in G131.
4. Using a spatula, remove the Teflon lining and underlying foam piece from the lid, then rinse each of these with toluene until the washings run colourless, followed by methanol and acetone, discarding the washings into an organic waste bottle.
5. Rinse the jar with a small amount of acetone, then dry with a jet of air.
6. Add ~ 20 mL of liquid soap to the jar followed by ~ 1 L of tap water.
7. Cap the jar and agitate well for 1 min.
8. Remove the cap and discard the contents down the drain.
9. Rinse the jar several times with tap water until no more suds are formed.
10. Add 100 mL of deionized water from the carboy in G131to the jar, seal the jar and agitate for 1 min.
11. Remove the cap and discard the contents down the drain.
12. Rinse the jar with acetone and discard the washings into an organic waste bottle.
13. Scrub with paper towel and minimal toluene to remove any persistent stains.
14. Once the jar's lid, Teflon liner and foam piece are dry, reassemble the lid.
15. Place the clean jars on the shelf in the lab with the other jars

Sediment weight calculation:

For 2000 ppm sediment concentration: (which is equal to 2000/1000000=0.002 wt sediment/wt of water), multiply mass of water by 0.002 to get mass of sediment to add to jar (600 g x 0.002 = 1.2 g sediment).

Report: In lab log book keep a record of:

- Tare weights of all jars before addition of oil, water and sediment
- Mass of water added to each jar
- Mass of oil added to each jar
- Mass of sediment added to each jar
- Weights of jars after oil, water and sediment emptied from jar (to calculate losses)
- Record water height (WH) and total height (TH) in lab book and excel file (for emulsion behaviour)
- Before and after mixing temperatures, take average of values to get average run temperature
- Before and after mixing speeds, take average of values to get average run mixing speed

Consumables and Contacts

Product ID	**E-mail/Contact info**	**Phone / Fax**	**Address**
Jars: RA-119 Borosilicate Extraction Bottle 2.2L	David Alff, Environmental Equipment Group	215-343-4490	PO Box 537, Warrington PA 18976
Agitator: 4 Jar: DC-20S/DC 8 Jar: DC-20/DC	David Alff, Environmental Equipment Group	215-343-4490	PO Box 537, Warrington PA 18976

Hazard Assessment and Control Report

Job Title or Occupation evaluated: Rotary agitator jar preparation	**Task:** Oil-water-sediment tests jar preparation	**Completed by**: Hena Farooqi **Date**: August 17, 2015
Location and/or Description of task being evaluated: Lab G131		
Environmental factors, Equipment, Materials, and harmful substances being used: Diluted bitumen, conventional crude	**Potential Hazards:** Spills, inhalation and exposure to hydrocarbons	

Risk Analysis (scale of 1 to 4):

Frequency – 4 Daily, 3 weekly, 2 monthly, 1 occasionally	**3**
Incident Probability – 4 probable, 3 occasional, 2 remote, 1 improbable	**4**
Potential Consequences – 4 Severe, 3 substantial, 2 minor, 1 minimal	**1**
Degree of Risk = Frequency x Probability x Consequences =	**12**
(1 to 9 – low risk, 12 to 27 – medium risk, 32 to 64 – high risk)	

Engineering controls: Fume hood (ventilation)	**Administrative controls:** SOP, trained lab personnel, MSDS	**PPE:** Nitrile gloves, safety glasses, NOMEX lab coats, half mask respirators
Control in place: Yes	Yes	Yes

Worker:__Hena Farooqi_____ Signature:_____

Supervisor:__Heather Dettman____ Signature:_____

Manager:_____ Signature:_____

Date:_____

Definitions:

Frequency of Exposure – How often is the worker exposed to the hazard? This may be each time the worker performs the task. (4. daily, 3. weekly, 2. monthly, 1. occasionally)

Incident Probability – How likely is it that exposure will result in loss, such as injury, illness, property damage, poor work quality or lost production? Consider hazards without existing control measures in the workplace.

4. Probable – May happen at least once a year
3. Occasional – May happen once every 1 – 5 years
2. Remote – Not likely to happen, but possible once every 5 to 10 years
1. Improbable – Not likely to happen

Potential Consequences – How severe will be the loss at the workplace if the exposure is not controlled?

4. Severe – Death, serious injury or illness, permanent disability, extreme property damage

3. Substantial – Lost time injury or illness, temporary disability, substantial property damage

2. Minor – Medical aid injury, minor illness, minor property damage

1. Minimal – First aid injury

Degree of risk= Frequency x Probability x Consequences
Hazard class:

32 to 64 high risk – take immediate action or implement appropriate controls to lower the risk to a level as low as reasonably achievable.

12 to 27 medium risk – take timely action to implement appropriate controls to lower or minimize the degree of risk.

1 to 9 low risk – continued operation is permissible with minimal controls. Monitor the hazard and take action if the degree of risk increases.

Hazard Controls:

Engineering Controls – these are considered first because they are the only control method that can eliminate the hazard. Examples of engineering controls are elimination, substitution, isolation, ventilation and safeguards.

Administrative controls – these are focuses on process, procedure and best practices. Examples include Safe Operation Procedures (SOP), staff rotation, hazard warning sign, training, codes of practice and maintenance programs.

Personal Protective Equipment – this is frequently used in combination with Engineering and Administrative controls. PPE must meet accepted standards in occupational health and safety codes. Examples of PPE are chemical resistant gloves, respirators, hard hats, lab coats, fire retardant coveralls and proper protective eyewear.

B.2 Quantification of Oil-Water-Sediment Interactions

DISCLAIMER

This document and its contents prepared are property of the Government of Canada. This has been prepared for site specific usage only; CanmetENERGY in Devon, Alberta.

1.0 EXPERIMENTAL INFORMATION

Project:	**Fate and Behaviour of Heavy Oils Spilled in Water Environments**
Project Leader:	Heather Dettman
Project Supervisors:	Hena Farooqi
Location:	Lab G131 (main) Lab H106 Lab H102 Lab A161 Lab A163
Chemicals:	Dichloromethane (CH_2Cl_2) Carbon disulphide (CS_2)
Sediments:	Diatomaceous earth Kaolin clay Sand

2.0 HAZARD IDENTIFICATION AND PREVENTION

2.0.1 Personal Protective Equipment (PPE)

Lab coat, closed toed shoes, long pants, and safety glasses are required at all times in the labs.

Gloves must be worn when handling chemicals, samples, or contaminated equipment.

2.0.2 Conduct

Food and Drinks are not allowed in the lab.

Know the locations of first aid kits, eyewashes, safety showers, and other safety equipment.

Keep work area and equipment clean, and return all chemicals and equipment to their proper storage areas after use.

Never directly smell or inhale chemicals. Sample preparation and solvent handling must be done in the fume hood.

Remove gloves before touching door handles, light switches, keypads, and instrument controls.

Do not act in any way that could endanger yourself or others.

2.0.3 Handling of Materials

Before working with any material, understand the associated risks and know the appropriate handling techniques.

1. Volatile organics must be handled in a fume hood with adequate ventilation.
2. If CH_2Cl_2, CS_s, oil, or other solvents spill on your gloves, remove them immediately and don a new pair.
3. If there is a spill, follow the appropriate cleanup procedure outlined in the MSDS.
4. If the chemicals contact your skin or eyes, immediately flush with water and consult with Trevor McHarg.
5. Do not return excess materials to stock bottles.
6. Chemicals must be properly disposed of in the designated areas.
7. Close all chemical containers immediately after use.

2.0.4 Chemical Hazards

CH_2Cl_2 (dichloromethane, DCM, or methylene chloride) is a known cancer hazard and can cause reproductive damage and birth defects. It is an irritant to eyes, skin, and the respiratory tract. It can cause damage to the central nervous system through inhalation and should not be handled outside of a fume hood. Due to its ability to pass through regular laboratory gloves, North Silver Shield gloves are recommended to be worn when handling DCM. Consult the MSDS for further information. DCM contaminated waste water also needs to be disposed of in the proper place (to be discussed)

CS_2 (carbon disulphide) is extremely flammable and should be kept away from ignition sources. It must be stored in a flammables cabinet and should be grounded when working in conditions where static generation is a concern. Due to its vapours, it must not be handled outside of a fume hood. It is an irritant to eyes, skin, and the respiratory tract, and can negatively affect the nervous system, reproductive system, and cardiovascular system. Consult the MSDS for further information.

2.0.5 Physical Hazards

Working in close proximity to a sonicator can cause hearing damage over time. Make sure you are adequately protected or limit your exposure.

Sharps can puncture gloves and skin, so ensure that care is taken when using them. Store them in a way in which they will not present a hazard to others, and dispose of them in the sharps container. If reusing, clean the sharps directly after use.

Dry ice can cause dermal damage when in contact with bare skin. Use insulated gloves when handling dry ice or materials that have been in contact with it. Allow vials and other equipment to warm slightly before touching them with nitrile gloves.

Tripping and ergonomic hazards exist in any workplace. Ensure you are aware of your work environment and how to work safely within it.

3.0 GENERAL DESCRIPTION AND PURPOSE

Many factors influence how oil behaves when spilled in aquatic environments. Sediment, in particular, can influence where the oil resides, how it disperses within the environment, and the rate at which it biodegrades. To better understand how different oils interact with sediment, this study will quantify the interactions between oil and sediment. It will also quantify the interactions between oil and water and look at the amount of oil within the water column during spill conditions.

4.0 EXPERIMENTAL PROCESS

4.0.1 Preparing Sediment Samples

Sediment samples will be collected in 20mL vials and stored in the fridge until they are analyzed

4.0.2 Extracting Oil from Sediment

Materials:

Material	How to label	Location
20 mL vial	*Sample name*, smp s, *date*	"Oil extraction" drawer in G131
20 mL vial	*Sample name, sep s, date*	"Oil extraction" drawer in G131
20 mL vial	*Sample name, dry s, date*	"Oil extraction" drawer in G131
5 mL syringe	*Sample name, s*	"Oil extraction" drawer in G131
0.45 µm filter tip	*Sample name, s*	"Oil extraction" drawer in G131
42 ashless filter circle	N/A	"Oil extraction" drawer in G131
Aluminum cup	Sample name, s	"aluminum foil cap" drawer in blue and yellow fume hood in H106
Metal pick	N/A	Fume hood in G131
Metal tweezers	N/A	Fume hood in G131
Buchner funnel	N/A	"Oil extraction" drawer in G131
Buchner funnel rest	N/A	"Oil extraction" drawer in G131
Vacuum flask	N/A	Glass cabinet by fume hood in G131
Aspirator pump	N/A	Shelf below counter by sink in G131
Stand	N/A	White, open shelf by fumehood
Dry ice holder	N/A	White, open shelf by fumehood
Dry ice	N/A	Freezer in H102
Funnels	N/A	"Oil extraction" drawer in G131
Pipettes	N/A	White, open shelf by fume hood
Flask	DCM	In the fume hood in G131
CS_2/ CH_2Cl_2	N/A	In the fume hood in G131

Purpose:

Quantify the amount of oil in sediment samples and determine the composition of the oil interacting with the sediment. The procedure is for one sample only, but multiple samples can be run at once. From start to finish, including drying, it should take 1-2 days.

Procedure:

1. Using the scale in G131, Record the weights of the “smp” vial and the “sep” vial
2. Add 5 mL of dichloromethane (CH_2Cl_2) to vial “smp”, and weigh and record.
3. Sonicate (operations procedure can be found in section 5.0.1) vial “smp” for 15 minutes. While “smp” is sonicating, bring “dry” vial to A163 and weigh it on the Mettler Toledo XPE105 microbalance. Due to scale sensitivity to static, touch the vial to the metal fume hood plate before weighing. If the scale gives you a static error message, let the “dry” vial sit on the metal plate longer before weighing again. It may also help to load the balance from the top to avoid the static error message.
4. While “smp” is still sonicating, bring the filter circles to H106 and place one in an aluminum cup. Place the filter/aluminum cup in the drying oven (A 104914) for at least 5 minutes. (*The oven in G132 can be used as well if it is not full) Remove the filter/aluminum cup from the oven using gloves and immediately weigh the filter/aluminum cup on the Mettler Toledo AB204 microbalance. The weight will increase rapidly as the filter absorbs atmospheric moisture, so write down the first weight that the balance pauses at.
5. Bring the filter/aluminum cup to A163, collect vials “smp” and “dry”, and bring these to G131.
6. Set up the filter apparatus (see Section 5.0.3) using a Buchner funnel, the Buchner funnel rest, the aspirator pump, a vacuum flask, and a stand. If a large water layer is present in vial “smp,” remove it with a pipette (a small water layer will make later extraction steps easier) and record the amount or water that has been removed (this can be done using the scale).
7. To filter, remove the filter circle from the aluminum cup and place it in the Buchner funnel. Turn on the aspirator pump (operating procedure can be found in section 5.0.4) to create a pressure gradient through the filter. Wet the filter with CH_2Cl_2, so that it seals to the funnel, and immediately pour the liquid portion of the vial on the filter (avoid pouring on the sediment, if possible).

8. Once the liquid portion has filtered through, turn off the aspirator pump and break the vacuum by disconnecting and reconnecting the vacuum hose to the vacuum flask (this will help prevent the filter circle from getting blocked or freezing due to the pressure gradient).
9. Add 2 mL of CH_2Cl_2 to the vial and stir well with a metal pick (or shake vial) to help remove the remaining oil. Turn the aspirator pump back on and pour the liquid portion of the vial onto the filter circle.
10. Repeat steps 8 and 9 until no more oil remains in the vial, and any added solvent stays clear and uncolored.
11. Rinse the filter circle with CH_2Cl_2 until the rinse CH_2Cl_2 becomes clear.
12. Turn off the aspirator pump and disconnect it from the vacuum flask.
13. Pour the contents of the vacuum flask (CH_2Cl_2 filtrate) into the "sep" vial (use a funnel and a stand, to make pouring easier). Rinse the flask with CS_2, pour into the vial, and repeat until the CH_2Cl_2 stays clear and uncolored. Weigh the "CH_2Cl_2-sep" vial and "smp" vial and record the values.
14. Once you have collected the CH_2Cl_2 filtrate you can remove the filter and place it in the aluminum cup.
15. Bring the filter/aluminum cup to H106. Place the filter/aluminum cup in the Fisher Scientific Isotemp drying oven (A104914). (*The oven in G132 can be used as well if it is not full)
16. Bring the dry ice holder to H102 and fill 2/3 full with dry ice (amount will increase if doing multiple samples). Once filled with dry ice, bring it back to G131, and place the vials "sep" inside so that it is surrounded by dry ice that is above the liquid layer. Let freeze for 15 minutes.
17. While the vial is freezing, weigh the 5 mL plastic syringe and 0.45 μm filter tip
18. Remove sample, using metal tweezers or protective gloves, and check that the water layer is frozen. If liquid water is still visible, put the vial back in the dry ice for 5 minutes.

19. Open the vial, and if necessary, use a metal pick to break/move the ice layer aside so that the syringe can access the oil/CS_2 layer.
20. Using the sample syringe, remove the oil/CS_2 layer.
21. With the sample still inside, attach the filter tip to the sample syringe and press the oil/CS_2 layer through the filter tip and into the "dry" vial.
22. If the filter clogs at any point, remove the filter and replace it with a new one (make sure to record the weight of the new filter)
23. If there is still oil/CS_2 left in the vial, repeat steps 19-22 until the entire oil/CS_2 layer has been removed (if water layer has melted during extraction time, place it back in the ice to re-freeze it before repeating steps 19-22).
24. Once all the oil/CS_2 has been removed from the "sep" vial, set the filter and syringe aside to dry. Weigh the "sep" vials and "dry" vials and record the values. Pour the remaining "sep" vial contents into the liquid waste container and dispose of the vial and lid in the contaminated plastic waste and contaminated glass waste, respectively.
25. Bring the "dry" vial containing the **oil/ CH_2Cl_2** mixture to A161 and put it into the nitrogen chamber (operating procedure can be found in section 5.0.2).
26. Once the solvent appears to have dried remove the "dry" vial from the oven and weigh on the microbalance in A163.
27. Calculate the amount of oil present in the 20 mL vial and give this information, and the vial, to analytical (H102).
28. Gather the separatory funnel and glass funnels. Rinse them with solvent then acetone (water if necessary) and allow them to dry overnight
29. The next day, weigh the filter tip(s) and syringe on the scale in G131. Once recorded, the filter and syringe can be disposed of in the "contaminated plastic" disposal Labware should be put back in the proper spots in G131.

4.0.3 Extracting Oil from Water Samples

Materials:

Material	How to label	Location
Separatory funnel	*Sample name, date*	On counter in G131
Separatory funnel stand	*N/A*	On counter in G131
125 mL jar	*Sample name, sep wgw, date*	"Oil extraction" drawer in G131
125 mL jar	*Sample name, dry wgw, date*	"Oil extraction" drawer in G131
10 mL syringe	*Sample name, wgw*	"Oil extraction" drawer in G131
0.45 µm filter tip	*Sample name, wgw*	"Oil extraction" drawer in G131
Metal pick	N/A	Fume hood in G131
Metal tweezers	N/A	Fume hood in G131
Dry ice holder	N/A	White, open shelf by fumehood
Dry ice	N/A	Freezer in H102
Pipettes	N/A	White, open shelf by fume hood
Funnels	N/A	"Oil extraction" drawer in G131
Flask	DCM	Fume hood in G131
CS_2/ CH_2Cl_2	N/A	In the fume hood in G131
Vacuum grease	N/A	"Oil extraction" drawer in G131
Deionized water	N/A	Beside the sink in G131
Rag	N/A	In G131 fume hood, or in rag box by door

Purpose:

Quantify the amount of oil in the water portion of the sample, and determine the composition of the oil. The procedure is for one sample only, but multiple samples can be run at once. From start to finish, including drying, it should take 1-2 days.

Procedure:

1. The water samples are collected in pre-weighed 1L Nalgene bottles and stored in the fridge in G131 until analysis. Weigh and record the weight of the full Nalgene to determine the total weight of the water sample.

2. Using a funnel, carefully pour the contents of the Nalgene bottle into a 1L separatory funnel. Add 10mL of CS_2 to the Nalgene to rinse it out, and then pour the oil/CS2 mixture into the separatory funnel. Repeat this step at least 1 more time, or until the solvent layer is clear.
3. Put a small amount of vacuum grease along the separatory funnel stopper (this prevents it from getting stuck). Close the separatory funnel, hold it tightly closed with a rag, and invert/shake it a few times. Turn the separatory funnel upright and carefully remove the top to vent pressure. Continue shaking and venting until sample is adequately mixed. Caution: Ensure that the sample has been completely vented, to remove built-up pressure, before setting sample down or releasing the stopper. If not properly vented, stopper can pop out and break. Use a large paper clip if necessary to let the sample vent.
4. Let the separatory funnel settle for at least one hour. During this time, take "dry" jar to G131 and weigh it and record the weigh.
5. Weigh the "sep" vial, record the weight, and drain the oil/ CS_2 layer into the "sep" vial. Drain a small portion of the water layer into the vial to ensure that all of the CS_2 and oil was collected. Weigh the "sep" vial and record.
6. If there is still oil present in the separatory funnel, repeat steps 2-5 with CH_2Cl_2 until the entire oil layer has been extracted. If you need to repeat more than once, the oil/solvent layer can be collected in the same "sep" jar to minimize samples
7. Bring the dry ice holder to H102 and fill 2/3 full with dry ice (amount will increase if doing multiple samples). Once filled with dry ice, bring it back to G131, and place jar "sep" inside so that it is surrounded by dry ice that is above the liquid layer. Let freeze for 15 minutes.
8. While the vial is freezing, weigh the syringes and 0.45 µm filters on the scale in G131.
9. Remove sample, using metal tweezers, and check that the water layer is frozen. If liquid water is still visible, put the vial back in the dry ice for 5 minutes.

10. Open the vial and use a metal pick to break/move the ice layer aside so that the syringe can access the oil/ CS_2/ CH_2Cl_2 layer.
11. Using the sample syringe, remove the oil/ CS_2/ CH_2Cl_2 layer.
12. With the sample still inside, attach the filter tip to the sample syringe and press the oil/ CS_2/ CH_2Cl_2 layer through the filter tip and into the "dry" vial.
13. If the filter clogs at any point, remove the filter and replace it with a new one (make sure to record the weight of the new filter)
14. If there is still oil/ CS_2/ CH_2Cl_2 left in the vial, repeat steps 10-13 until the entire oil/ CS_2/CH_2Cl_2 layer has been removed (if water layer has melted during extraction time, place it back in the ice to re-freeze it before repeating)
15. Once all the oil/ CS_2/ CH_2Cl_2 has been removed from the "sep" vial, set the filter and syringe aside to dry. Weigh the "sep" vial and "dry" vial and record the values. Pour the remaining "sep" vial contents into the liquid waste container and dispose of the vial and lid in the contaminated plastic waste and contaminated glass waste, respectively.
16. Bring the "dry" vial containing the **oil/CS_2** mixture to analytical. Let them know that it is CS_2 and that the weight of oil is unknown. Let them know the weight of CS_2 present so that they can calculate the weight of oil.
17. Bring the "dry" vial containing the **oil/ CH_2Cl_2** mixture to A161 and put it into the nitrogen chamber (operating procedure can be found in section 5.0.2).
18. Once the solvent appears to have dried remove the "dry" vial from the oven and weigh on the microbalance in A163.
19. Calculate the amount of oil present in the 20 mL vial and give this information, and the vial, to analytical (H102).
20. Gather the separatory funnel and glass funnels. Rinse them with solvent then acetone (water if necessary) and allow them to dry overnight
21. The next day, weigh the filter tip(s) and syringe on the scale in G131. Once recorded, the filter and syringe can be disposed of in the "contaminated plastic" disposal Lab ware should be put back in the proper spots in G131.

5.0 INSTRUMENTATION PROCESS

5.0.1 Sonicator Operations

This applies to the Fisher Scientific FS30H sonicator

1. Check that the water is clean and free of other materials. If needed, drain the water and refill it with deionized water.
2. If not already in sonicator, place the sample rack in the water bath. Place sample on the sonicator rack (this step can be omitted if sample vials are too small for the sonicator rack).
3. Adjust the water height so that it is approximately ¾ of the height of the sample.
4. If power is not already on, switch it on and check that heat switch is turned on. Turn the dial to desired time.
5. If working in the vicinity of the sonicator, wearing hearing protection is recommended as the sound waves can cause hearing damage over time.
6. Once time is completed, remove sample and dry it.

5.0.2 Nitrogen Chamber Operations

This applies to the Caliper LifeSciences TurboVap LV

1. Arrange the sample(s) so that the nozzles are positioned over the tops of the open vials.
2. Ensure that the lid is closed and turn the power on.
3. Use the buttons to increase/decrease the temperature to 45°C.
4. Use the buttons to set the timer. If wanting it to run without following a timer, set the timer to 00 (recommended).
5. Turn Nitrogen pressure knob till the gauge reads 2.5 psi.

6. Press the button corresponding to the row of nozzles that you would like to turn on (multiple rows can be used at once if there are a large number of samples being dried at once).
7. Press start and check that the pressure of the nitrogen flow is sufficient. Increase/decrease the pressure knob until the surface of the samples appears slightly agitated. This pressure may need to be increased later, once the height of the vial contents has decreased.
8. When removing samples, press stop, turn off the power, and then lift the lid to remove samples.

5.0.3 Aspirator Pump Operations

This applies to the Cole-Parmer Instrument Corporation 7049-00 Aspirator Pump

1. Set the aspirator pump on the counter beside the fume hood.
2. Connect the two shorter tubing ends to two outlets on the face of the aspirator pump. Connect the longest end of the tubing to the vacuum flask.
3. When ready to use, switch the aspirator pump on to start suction.
4. To stop suction, switch off the aspirator pump. Remove the long end of the tubing from the vacuum flask to release the vacuum created within the vial.

Figure 1

6.0 EMERGENCY PROCEDURES

6.0.1 Fire

A pull station is located outside of G131 at the nearest exit door.

Fire extinguishers are located inside G131 (beside the exit door) and in the hall outside G131.

In the event of a fire alarm, immediately leave the building through the nearest exit. Go to the closest muster point and await further instructions.

6.0.2 Injury

Emergency medical response, (9) 911, must be alerted for major injuries.

All injuries should be reported to Trevor McHarg.

A first aid kit is located in the hallway outside G131. Incident forms should be filled out whenever medical supplies are taken from the first aid kit.

6.0.3 Spills

Spill response information can be found in the MSDS of the chemicals being used.

A spill kit is located in the hallway outside of G131.

Alert Trevor McHarg in the event of a spill.

If broken glass is also present, ensure that proper precautions are taken to avoid injury.

6.0.4 Alarms

If a stage 2 alarm sounds, immediately leave the building through the nearest exit. Go to the closest muster point and await further instructions. This indicated that there is an emergency in this area of the site or throughout the site.

If a stage 1 alarm sounds be on alert to evacuate the area. This alarm indicates that there is an emergency in another area of the site.

6.0.5 Eyewash and Safety Shower

An eyewash station is located outside G132 (across from G131). In the event that you need to use it, start flow of water and gently hold eyelid open. Rinse with water for 15 mins and consult Trevor McHarg.

A safety shower is located outside G132 (across from G131). In the event that you need to use it, pull handle and stand underneath the flow of water. Contaminated clothing, unsafe clothing, or clothing that is preventing the affected are from being rinsed, should be removed. Rinse for 15 minutes and consult Trevor McHarg.

6.0.6 Emergency List

Fire Department	(9) 911
RCMP	(9) 911
Ambulance	(9) 911
Government Security	(9) 780-422-3787
Security Desk	8774/8719
Trevor McHarg	8707

7.0 MSDS

MSDS for CS_2, CH_2Cl_2, oils, and other solvents will be provided and made accessible to all G131 workers. It is the worker's responsibility to become familiarized with these documents and to review the hazards, prevention, and emergency measures.

Appendix C: Supplementary data

The change in elemental carbon, hydrogen, nitrogen and sulfur in the +204°C maltenes and asphaltenes fraction of the floating oil from Campaign 1 is shown in tables C-1 to C-4, respectively.

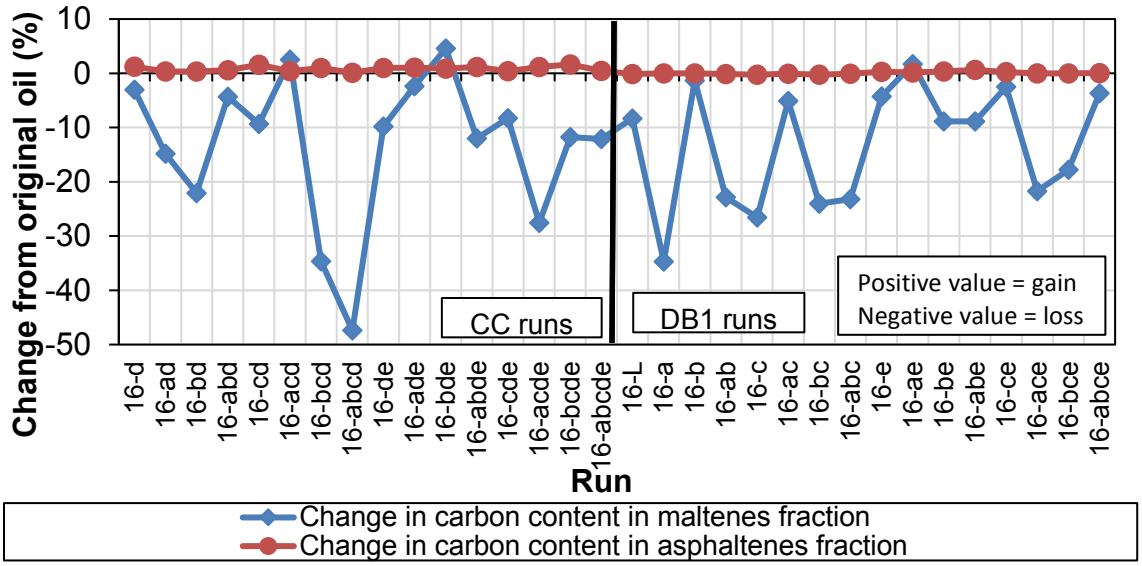

Table C-1: Change in elemental carbon content from original oil for maltenes and asphaltenes fractions

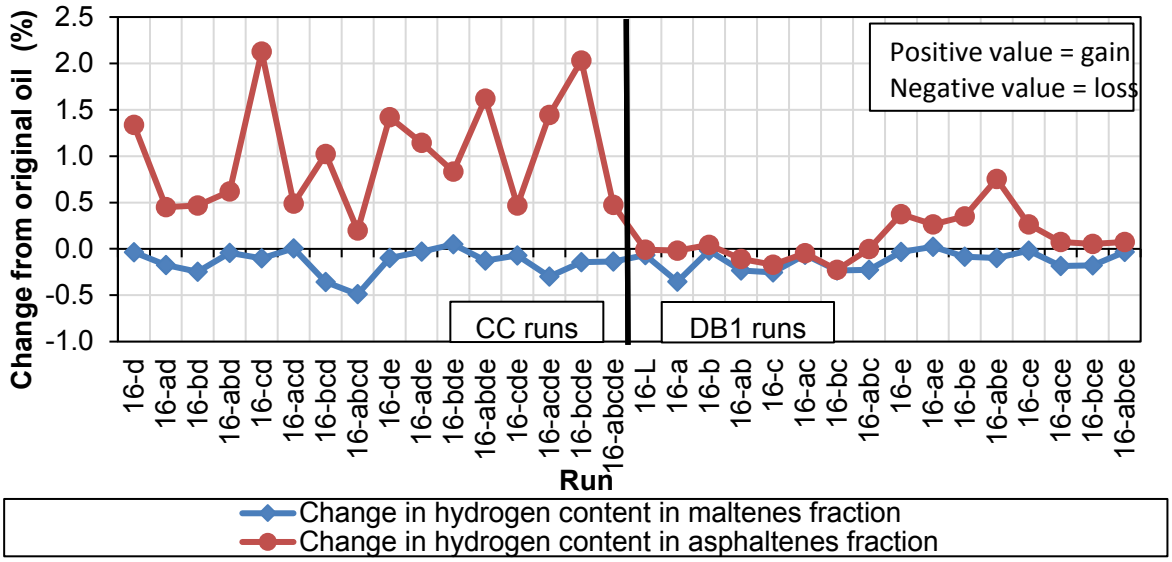

Table C-2: Change in elemental hydrogen content from original oil for maltenes and asphaltenes fractions

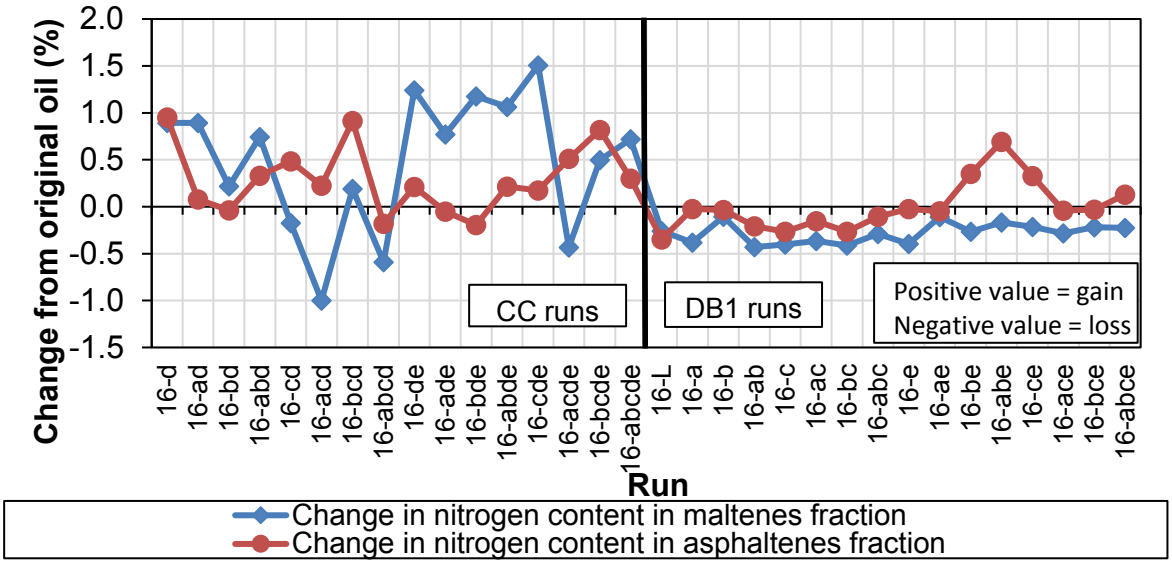

Table C-3: Change in elemental nitrogen content from original oil for maltenes and asphaltenes fractions

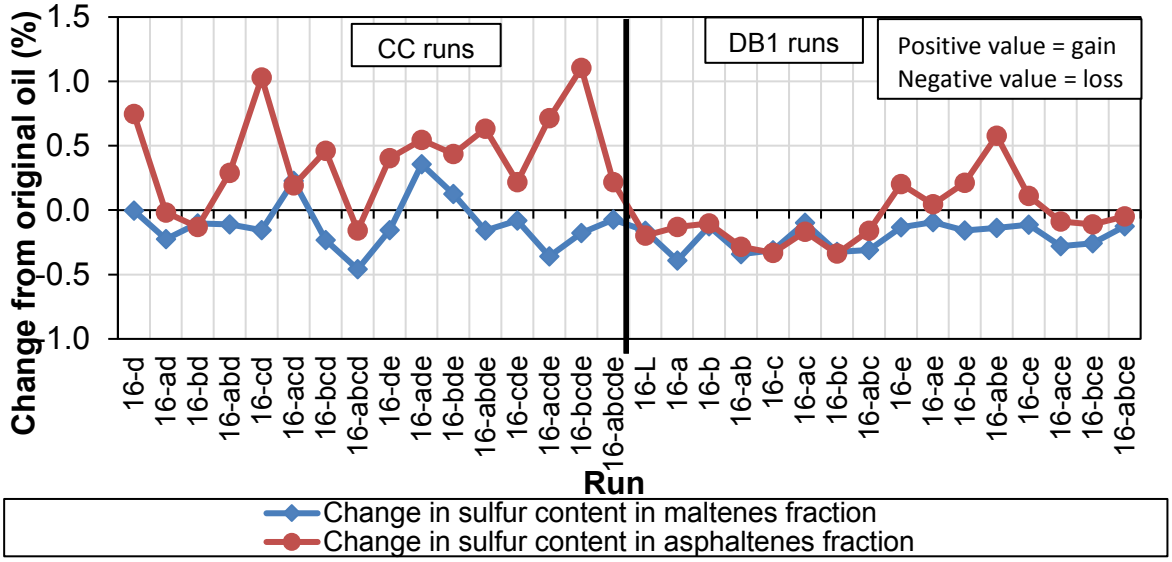

Table C-4: Change in elemental sulfur content from original oil for maltenes and asphaltenes fractions